Triassic macrostratigraphy of the western United States and the ichnology, paleoecology, and paleoenvironments of the Early and Middle Triassic Chugwater Group, Wyoming

By

David M. Lovelace

A dissertation submitted in partial fulfillment of

the requirements for the degree of

Doctor of Philosophy

(Geoscience)

at the

UNIVERSITY OF WISCONSIN–MADISON

2012

Date of final oral examination: 08/24/12

The dissertation is approved by the following members of the Final Oral Committee:

Shanan Peters, Associate Professor, Geoscience
Alan Carroll, Professor, Geoscience
Dana Geary, Professor, Geoscience
Patrick McLaughlin, Associate Professor, Environmental Sciences
Raymond Rogers, Professor, Geology (Macalester College)

DEDICATION

I would like to dedicate this dissertation to my wife Jenn Drake and my son Charley Stephen Drake-Lovelace. Their bright smiles and kind encouragement gave me the strength and motivation required to complete this dissertation. Thanks for your patience and understanding!

ACKNOWLEDGMENTS

I would like to extend my sincerest gratitude to the following individuals who have helped me with this project:

- My advisor Shanan Peters, and my committee members (Alan Carroll, Dana Geary, Patrick McLaughlin, and Raymond Rogers)
- My research group (Eric Williams, Amalia Doebbert, Deb Rook, Noel Heim)
- Collaborators (Scott Hartman, Amalia Doebbert, Tracy Thomson, and Steve Lovelace)
- The UW–Madison Geology Department and UW–Madison Geology Museum for funding and use of facilities, and the Bureau of Land Management for permits to collect on BLM lands
- Special thanks to the Marie Dvorzak, Toby Lathrop, and the Geology Library staff.

TABLE OF CONTENTS

LIST OF FIGURES

Figure

LIST OF APPENDICES

Appendix

ABSTRACT

The Triassic is an extraordinary interval in Earths history. Not only does this interval record biotic recovery from the most devastating extinction of the Phanerozoic, but it also records one of the 'Big Five' mass extinction events at its termination. Triassic continental and marine sediments record the apex of Pangean accretion and the initiation of its break up, a major shift from carbonate dominated to a principally siliciclastic sedimentary record, a Phanerozoic low in the number of sedimentary packages, and the evolutionary origins of the modern fauna (mammals, crocodiles, dinosaurs (birds), lepidosaurs, and turtles). Considering the dynamic history of this time period surprisingly little is known about one of the most conspicuous lithostratigraphic units of the western USA, the Chugwater Group. My research focuses on the stratigraphy and paleontology of the Early–Middle Triassic deposits of the Chugwater Group and provides the first high-resolution quantification of the sedimentary and biological records of the western USA. This dissertation is composed of four principle studies.

In Chapter 2, I quantify the sedimentary record of Triassic deposits in the western USA. The Triassic of the western USA is effectively divided by the Ladinian to late-Carnian hiatus into two major sedimentary suites: Lower Triassic (Griesbachian–Anisian), and Upper Triassic (late-Carnian–Rhaetian). Each of the suites exhibits different rates of sediment accumulation (and volume), degree of sediment heterogeneity, and grain size variability, even though the number of sedimentary packages and their durations are relatively similar. I hypothesize that the differences in deposition are largely related to perturbations in climate during the End-Permian and Early Triassic and by regional tectonics associated with the initiation of Andean-type subduction in the Late Triassic.

In Chapter 3, I quantify the Triassic vertebrate track and body fossil record and compare it to the quantified sedimentary record that resulted from the work of Chapter 2. There is a strong positive correlation between ichnogenus richness (tracks) and both lithology (siltstone) and sediment accumulation rates in the Early Triassic, while genus richness (body fossils) does not exhibit a significant relationship with the sedimentary record. This is not the case for the Late Triassic where genus richness positively correlates with the number of sedimentary packages, but no clear relationships between

ichnogenus richness were observed. This is hypothesized to reflect a prominent taphonomic bias that favors the preservation of tracks in low or waning energy environments. The preservation of body fossils, on the other hand, is low possibly due to the prominence of low energy rapid accumulation environments incapable of concentrating large clasts. A similar bias is seen during the Early Jurassic biotic recovery preserved in dominantly eolian and interdune deposits. Furthermore there is a noticeable lag between the first occurrences of body fossils and the first occurrence of track fossils for nearly all of the major clades. This suggests that addition of ichnological data should be considered when discussing the origins clades, calibrating molecular clocks, or describing the spatiotemporal distribution of clades across the globe (paleobiogeography).

In Chapter 4, I present the first detailed study of the vertebrate and invertebrate track and trace fossil assemblage from the Early Triassic Red Peak Formation as well as their associated sedimentary environments. I describe a previously unrecognized paleoecology that represents almost all trophic levels. The dominantly hygrophilic invertebrate ichnofauna is suggestive of a water table near, at, or above the surface for much of the year. Vertebrate tracks indicate the presence of small archosauromorphs, small to medium sized dinosauromorphs, and large bodied archosaurs. In addition, the presence of the ichnogenus *Chelonipus* (turtle tracks) marks the oldest record of turtles in North America, extending their temporal range on this continent by more than 30 million years.

In Chapter 5, I investigate the depositional history of the Alcova Limestone. This limestone is one of the most readily recognized lithostratigraphic units in the Chugwater Group. Its origins, however, have been contentious, and reconstructions of its depositional enironment range from lacustrine to marine. The $^{87}Sr/^{86}Sr$ system was chosen to test these origin hypotheses because the ratio of $^{87}Sr/^{86}Sr$ in Early Triassic seawater demonstrates a monotonic increase before rapidly decreasing just across the Early-Middle Triassic boundary. The marine strontium curve provides a signal with which to compare $^{87}Sr/^{86}Sr$ ratios measured in seven samples of Alcova Limestone; results of the $^{87}Sr/^{86}Sr$ analysis are consistent with a marine origin. Furthermore, these data are strongly suggestive of a mid-late Spathian (Early Triassic) age range for the deposition of the Alcova Limestone. This

provides the first reliable age constraint for the underlying vertebrate and invertebrate ichnocoenoses. These data also reject the hypothesized lacustrine origin for the Alcova Limestone.

CHAPTER 1

INTRODUCTION

1.1 Motivation

The Triassic is a unique period in earth's history that includes the first 50 million years of the Mesozoic (252.6 to 202 Ma) (for currently defined boundaries see Yin et al., 2001; Muttoni et al., 2010; for review see Preto et al., 2010). For example, the Triassic experienced the lowest percent of continental flooding outside of the Neogene (Ronov et al., 1980; Peters, 2008), recorded the zenith of Pangean accretion (Parish, 1993; Veveers, 1994; Columbi and Parish, 2008), and is bounded by two of the five major mass extinctions (Raup and Sepkoski, 1982; Twitchert, 2006). The Triassic also records the origination of many new clades of terrestrial vertebrates often called the "modern fauna," which includes turtles, lepidosaurs, archosaurs (crocodiles, dinosaurs, and birds), and mammals (Sereno, 1997; Rieppel and Reisz, 2003; Twitchert, 2006; Muttoni et al., 2010). Given the eventful history of the Triassic Period and the paleontological significance, relative to the boundary intervals, few detailed paleoenvironmental studies have focused on the period of time between the end-Permian and Triassic-Jurassic extinctions (e.g., Smithian-Carnian; Preto et al., 2010). More specifically, few attempts have been made to quantify the sedimentary record of the Triassic in the western USA (Peters, 2006), and only a limited number have focused on the paleontology and sedimentology of the Spathian–Carnian interval (Lucas et al., 2002) in the northern Rocky Mountain west (i.e., Wyoming).

Sediments that span the intervening late-Early Triassic through early-Late Triassic (Spathian–Carnian) are often used to test hypotheses regarding the timing and evolutionary history of terrestrial fauna including turtles, mammals, and archosaurs (Demathieu, 1989; Rogers et al., 1993; Sereno, 1999; King and Benton, 1996; Langer et al., 2009). The preservation of body and trace fossils provides necessary evidence to observe change in paleoenvironmental and paleoecological composition over time. These data in conjunction with observations of paleoclimate proxies (paleosols), sedimentology, and geochemistry, can be used to advance paleoenvironmental reconstructions of multiple terrestrial depositional environments (Jennings and Hasiotis, 2006; Prochnow et al., 2006; Jennings and Lovelace, 2008; Cleveland et al., 2008; Jennings et al., 2011). Paleobiogeographic and macrostratigraphic studies intent on understanding the spatiotemporal distribution of sediments, paleoenvironments, and floral and faunal diversity have demonstrated a need for further investigation of Triassic units at regional scales (Lockley et al., 1994; Avenzini et al., 2004; Hunt and Lucas, 2007a; Peters, 2008; Langer et al., 2009).

In order to understand the spatiotemporal distribution of sedimentary deposits across the Triassic of the western USA a relational database was created to quantify the rock record across this interval. A quantitative record of depositional characters such as volume of sediment, rates of accumulation, lithology, and the number of sedimentary packages, can facilitate comparisons between Lower and Upper Triassic lithostratigraphic units which record differential affects of tectonic, climatic and biological influences (Welles, 1947; Peabody, 1948; McKee, 1954; Parish, 1993; Dubiel, 1994; Heller et al., 2003). For instance the Early Triassic records the initiation of the delayed end-Permian

biotic recovery and extreme carbon isotope excursions until the Middle Triassic boundary (Benton, 2010; Payne et al., 2004; Payne and Kump, 2007). While the Late Triassic exhibits a relatively stable carbon record until the end-Triassic extinction event at the Triassic-Jurassic boundary (Sephton et al., 2002; Schoene et al., 2010). The missing upper-Middle Triassic and lower-Upper Triassic strata has been previously noted (Dubiel, 1994), but no hypotheses have been generated regarding its absence. It is thought that a macrostratigraphic analysis of the western USA will address this deficit and provide an opportunity to quantitatively test differences between Lower and Upper Triassic deposits.

1.2 Geologic Setting

The Triassic of the western USA (Fig. 1.1.) is often expressed at the surface in extraordinary exposures of marine and terrestrial rocks that collectively span the first 50 million years of the Mesozoic; however, few locations offer an uninterrupted sequence of Triassic rocks in the western US. One of the more complete sequences of rocks of this age can be found in the Chugwater Group of Wyoming (Fig. 1.2). The Chugwater Group was the focus of a small group in the mid-1960s (Picard and High, 1964; Picard, 1967; High and Picard, 1967; Picard and High, 1968; High and Picard, 1969; Picard et al., 1969; Picard, 1978, for review); although, the Chugwater Group has not received much attention since (see Irmen and Vondra, 2000 for review). Within the Chugwater Group the earliest Triassic (Griesbachian; conodont biochrons) is represented by the shale and dolomitic-mudstone rich Dinwoody/Goose Egg Formation (Paull and Paull, 1983; 1990; 1994), which in turn is conformably overlain by the fine-grained red beds of the Red Peak Formation (Picard, 1967). The stromatolitic Alcova Limestone is either Early

Triassic (Spathian?, [paleomag] Steiner et al., 1993) or earliest Middle Triassic (early-Anisian? [estimated from vertebrate paleontology] Storrs, 1991).

The early-Middle Triassic (Anisian) is represented by foreshore and eolian sandstones of the Crow Mountain Formation (Johnson, 1990; Irmen and Vondra, 2000), the fluvial/floodplain dominated 'unnamed redbeds', and (in part) the course-grained fluvial Jelm Formation of southern Wyoming (Reeside, et. al., 1957). It is likely that no Ladinian aged rocks exist within the Chugwater Group; this is consistent with missing Ladinian aged rocks in the remainder of the Rocky Mountain region (Dubiel, 1994).

The Popo Agie Formation and the upper Jelm Fm comprise the only Late Triassic strata in the study area (Carnian-Norian; [vertebrate biochrons] Lucas et al., 2002; Jensen and Kowallis, 2005; Zeigler et al., 2008). The Bell Springs Formation (basal member of the Nugget Sandstone) is thought to be Late Triassic (Norian-Rhaetian?); however, this designation is based on isolated theropod dinosaur traces (Hunt and Lucas, 2007b) and needs further refinement. There are two potentially large unconformities within the succession at the Crow Mountain—Popo Agie contact and along the Popo Agie—Bell Springs contact (Pipiringos and O'Sullivan, 1978). The amount of missing time represented by the unconformable surfaces is not well constrained. The lack of paleontological remains and low volcanic activity along this passive margin setting make constraining the age of these deposits difficult. Each of the units above will be discussed in more detail within the context the following four chapters.

Most studies of terrestrial units within the Triassic of the western USA have focused on the Early–Middle Triassic (i.e. Moenkopi Formation) and the Late Triassic, such as the Dockum Group, the Chinle Group, and the Delores Formation of the desert

southwest (Utah, Arizona, Colorado, New Mexico, and Texas; Blakey and Gubitoza, 1983; Lucas and Hunt, 1993; Lehman and Chatterjee, 2005; Zeigler et al., 2008; Dickenson and Gehrels, 2009).

1.3 Chapters

Answering questions that relate to biotic change (macroevolutionary patterns), climate, or paleoenvironment, rely on the collective focus of a variety of studies at a variety of scales, from global modeling of climate (Parrish, 1993; Pollard and Schulz, 1994), continental scale meta-analyses (Peters, 2006; Peters and Heim, 2010), to detailed local observation (Prochnow, et al., 2006; Cleveland, et al., 2008). Research presented in this dissertation is divided into four chapters; each focuses on a different scale, ranging from local (central Wyoming), to broadly regional (western USA). The four chapters address the following principal goals of the dissertation:

Chapter 2) *Triassic macrostratigraphy of the western USA*. This chapter quantifies the spatiotemporal distribution of sedimentary packages and their associated attributes and provides a foundation upon which hypotheses of tectonic, climatic, and biologic influences on the structure of the geological record can be tested.

Chapter 3) *Tracking Triassic vertebrate diversity: variability of vertebrate trace and body fossils in the Triassic of the western USA*. This chapter investigates the relationship between the biologic and stratigraphic records to test the influence of governing agents (as introduced in Chapter 2) on the preservation of trace and body fossils and how those influences might affect our understanding of biologic diversification during the terrestrial biotic recovery, and the origination of the modern fauna.

Chapter 4) *Paleoenvironments and paleoecology of an early Triassic invertebrate and vertebrate ichnoassemblage from the Red Peak Formation (Chugwater Group), central Wyoming*. This chapter describes a previously unknown vertebrate ichnocoenoses from the Early Triassic of the Rocky Mountain west, and the environmental context in which they are preserved.

Chapter 5) *A new age constraint for the Spathian (Early Triassic) marine Alcova Limestone (Chugwater Group), Wyoming*. This chapter uses $^{87}Sr/^{86}Sr$ ratios of the Alcova Limestone to test hypotheses regarding the nature of its deposition and its age.

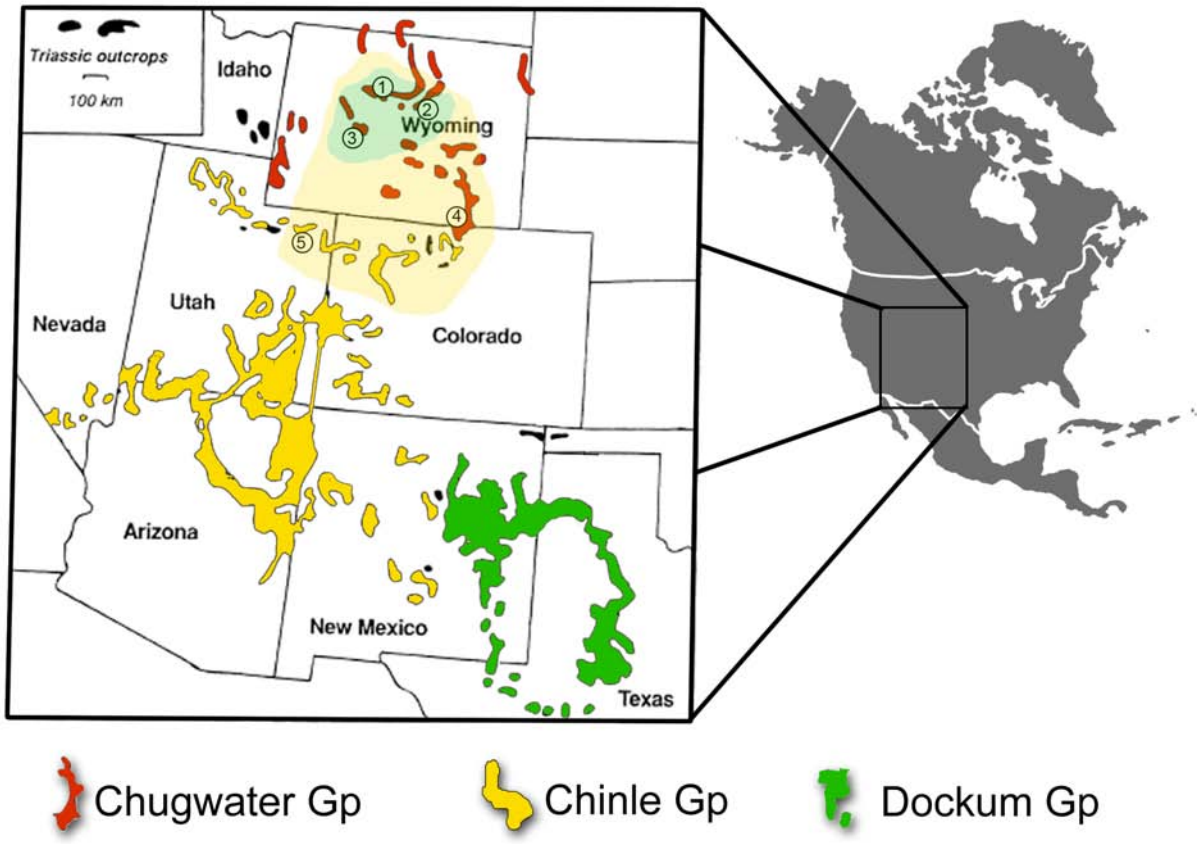

FIGURE 1.1—Surface exposures of the Triassic rocks throughout the Rocky Mountain west (inset; modified after Lucas and Hunt, 2007a). The inset outlines the large-scale regional study area to be included in the meta-analysis using a high-resolution Macrostrat style database and The Paleobiology Database. The light green area within Wyoming indicates outcrop containing significant evidence of increased biological diversity in the late-Early Triassic (local scale; Chapter 2). Outlined area (peach) designates the regional study area where Middle and early-Late Triassic strata were studied. Numbered circles represent field areas where stratigraphic sections were measured. The inset outlines the large-scale regional study area to be included in the meta-analysis using the Macrostrat and The Paleobiology Databases.

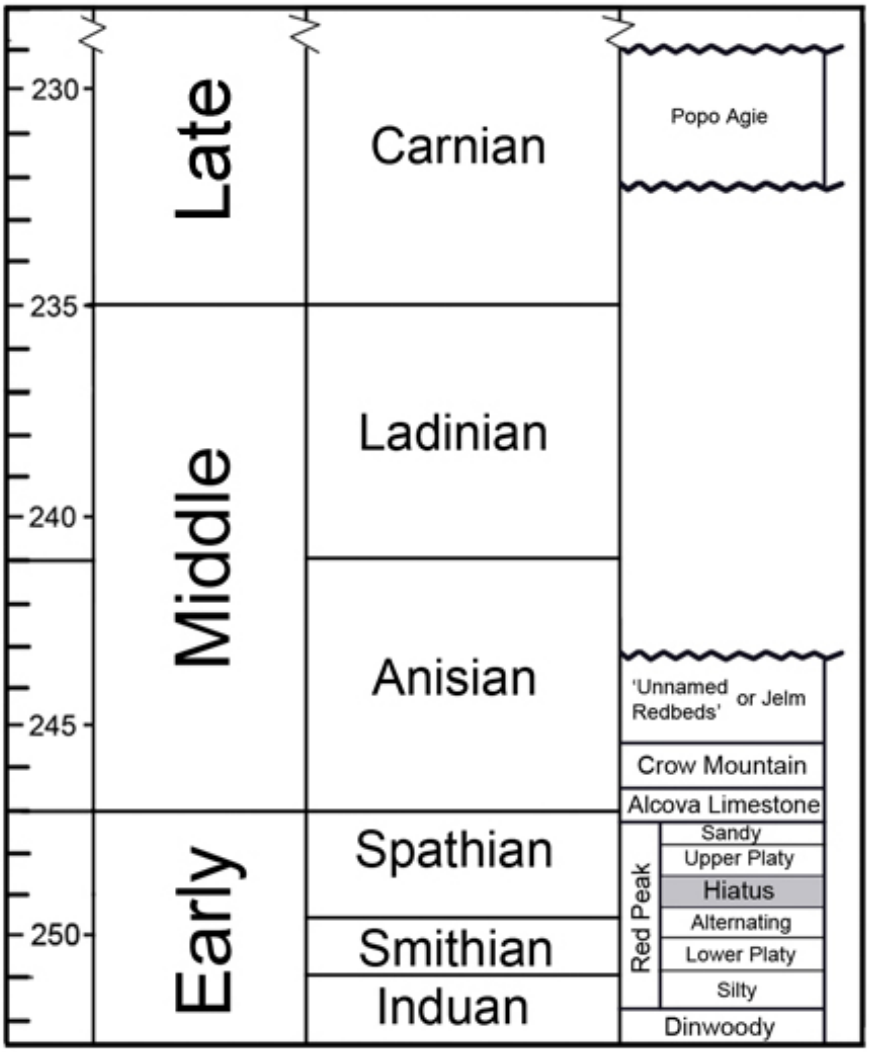

FIGURE 1.2—Temporal relationships of stratigraphic units within the Chugwater Group (excluding the Griesbachian aged Dinwoody Formation). Time scale after Mundil et al. (2010).

CHAPTER 2

Triassic Macrostratigraphy of the Western United States

ABSTRACT

Quantification of the sedimentary record makes it possible to more fully interrogate the geologic histories of strata across a specified temporal range. The Triassic is an extraordinary time interval that experienced profound biologic and geologic events. Macrostratigraphy of the continental margin of western Pangea in what is now the western USA provides an opportunity to test the congruence of quantified results with hypotheses that relate possible climate and tectonic influences on the formation of the sedimentary record across this interval. This study describes the spatiotemporal distribution of sedimentary packages (and their lithological attributes) in the western USA, which preserves the most complete continental Triassic record in North America.

Results demonstrate a significant climatic control on Early Triassic sediment accumulation, which is up to 4.5 times greater than accumulation rates seen in the Late Triassic. It is suggested that global perturbations in $\delta^{13}C_{carb}$ closely match sedimentation rates, rock volume, and lithologic variability in the Early Triassic. It is also during this interval that the highest turnover rate of sedimentary packages occurs. In contrast, the Late Triassic has much lower rates of sediment accumulation but greater lithologic heterogeneity, including several coarse-grained intervals linked to broad scale tectonic events along the cordilleran margin. Further results show the distribution of sedimentary package duration throughout the Triassic interval is nearly identical to that reported for the entire Phanerozoic. This suggests tectonic processes that govern package longevity

are similar in the Triassic of the western US to those that govern larger scale patterns across the continent. Quantification of the spatiotemporal distributions of Triassic sediments has provided a framework for comparing the structure of the sedimentary record across this dynamic interval. It is anticipated that this study will be the starting point for further investigations of attributes integral to the Triassic system, including improved studies of mass balance, interrogations of the Middle Triassic problem (i.e., the absence of middle Triassic deposits on proximal shelf and continental environments), and the preservation and distribution of body and trace fossils essential to understanding biotic recovery, the origins of the modern fauna, and the end-Triassic extinction.

2.1 INTRODUCTION

Sedimentary rocks preserve evidence that is central to understanding the history of life and environment. The distribution of sedimentary rocks in time and space is influenced by processes that govern the formation and destruction of sediment accommodation space (Wyld, 1991; Lawton, 1994; Heller et. al., 2003). The characteristics of preserved sediments in that space are a function of climate, environment, and biologic properties of the depositional system (Parish, 1993; Hay and Wold, 1998; Knoll, 2003; Ziegler et al., 2003; Pruss et al., 2006; Preto et al., 2010).

The Triassic of the American west (Wyoming, Colorado Plateau, eastern New Mexico and west Texas) preserves an iconic body of rock that records evidence of tectonic, climatic, environmental, and biological events that occurred during an extraordinary period in earth's history (Parish, 1993; Blakey, 1973, 1988; Blakey et al., 1993; Irmis et al., 2007; Dickinson et al., 2010). The onset of this period is marked by

dramatic shifts in global atmospheric carbon (Payne et al., 2004; Galfetti et al., 2007; Payne and Kump, 2007), biotic recovery from the end-Permian mass extinction (Pruss et al., 2005), a global reef (Fagerstrom, 1987) and coal gap (Bestougeff, 1980; Retallack et al., 1996; Berner, 2005), and the culmination of the Sonoma Orogeny (Speed, 1979; Wyld, 1991). There have been numerous studies investigating the paleogeography, sedimentology and paleontology of this interval (e.g., Welles, 1947; McKee, 1954; Blakey, 1973; Stewart et al., 1972a, 1972b; Blakey and Gubitosa, 1984; Lucas et al., 2001; Zeigler et al., 2008; Martz and Parker, 2010).

Early Triassic rocks are absent in the Late Triassic rift basins of the east coast (Olsen et al., 1996). However, Early and Late Triassic continental, coastal, and marginal to deep marine systems are all represented by sedimentary rock bodies in the Rocky Mountain west making this region ideal for testing hypotheses that encompass the entire Triassic. Early Triassic formations of the western US, including such well-known units as the Moenkopi, Virgin Limestone, Thaynes, and Red Peak formations all demonstrate a dominantly fine-grained composition and an overall basinward thickening that in places exceeds 1500 meters (Clark, 1957; Picard, 1967; Blakey, 1973; Paull and Paull, 1994). Unfortunately, these same units contain a meager fossil record compared to their Middle and Upper Triassic counterparts. Middle Triassic units are poorly represented and dominantly restricted to the Anisian (Morales, 1987; Dubiel, 1994; Nesbitt and Angielczyk, 2002), and no definitive Ladinian or early-Carnian aged rocks of terrestrial origin exist in the region. In contrast, the Upper Triassic Chinle (Lucas, 1991; Nesbitt; 2010) and Dockum (Lehman and Chatterjee, 2005) groups appear to display more

lithologic heterogeneity and a much more diverse fossil record, but they do not achieve near the same thicknesses as their older counterparts in the Early Triassic.

Because of the relative completeness, the Triassic of the Rocky Mountain west is an ideal region to compare Triassic histories in order to test hypotheses of tectonic influence as well as environmental and biological evolution. However, in order to understand how Triassic tectonic, environmental, biological, and depositional systems evolved it is crucial to understand the spatiotemporal distribution of sedimentary packages that record the geologic history of this region. Here I present results of a macrostratigraphic analysis (Peters, 2006a; Hannisdal and Peters, 2010) of the Triassic of the Western US. Quantification of sedimentary packages and their associated properties—lithology, volume, and package distribution and duration, as well as rates of accumulation, package initiation, and package truncation—provides a means to interrogate these intervals. This will forward our understanding of local and system wide factors that led to the discrete characteristics preserved within the sedimentary record and address three key questions: 1) What does the spatiotemporal distribution of sediment look like? 2) How do the effects of principal governing forces change through time? 3) How do the end-Permian extinction, atmospheric carbon perturbations, and the evolving cordillera influence the accumulation and preservation of sedimentary packages?

2.1.1 Macrostratigraphy primer

The spatial distribution of sedimentation is controlled by many geological processes including tectonics (Worsley, 1986; Fielding, 2011), climate (Parish, 1993; Preto, 2010), and eustatic sea level (Haq et al., 1987; Hallam, 1992;). There have been

several major studies that have impacted our understanding of the temporal and spatial architecture of the geologic record based largely on outcrop area measured from geological maps (Gregor, 1985; Sloss, 1976; Ronov et al., 1980). The resolution of these studies was on the order of several 10's of million years (e.g., epochs and periods). More recently Peters (2005) and Peters and Heim (2010) compiled an improved data set for North America based principally on the American Association of Petroleum Geologists Correlation of Stratigraphic Units of North America (COSUNA) charts (Childs, 1985) and a similar compilation assembled by the Geological Survey of Canada. This data set (formalized into the Macrostrat Database) has facilitated numerous interrogations (i.e., Peters, 2006a, 2006b, 2008; Hannisdal and Peters, 2010; Heim and Peters, 2011; Peters and Gaines, 2012) of hypotheses related to the composition of the geologic record at a higher temporal resolution than previous studies (e.g., 1-3 million years). Although most of Peters (2006a) analyses were on the order of stage (in the Paleozoic and Mesozoic) or subepochs (Cenozoic), higher resolution studies are possible. This is in part because the COSUNA charts were compiled in the mid-1980s and represent the knowledge of the geologic record at the time. While the COSUNA charts have proven to be a valuable data set the state of understanding has improved since its completion, and in many cases the original data set does not adequately reflect resolvable stratigraphic units necessary for higher resolution temporal studies (Fig. 2.1). In addition, more recent geochronological constraints have been attained for certain intervals such as the Late Triassic of the western US, which provide better temporal resolution than previously reported (Irmis et al., 2011; Ramezani et al., 2011; Zeigler et al., 2011; Lucas et al., 2012). Thus, the dynamic nature of the Macrostrat Database and studies such as this aid

in enhancing the resolution of the data set while addressing specific questions regarding the structure of the geologic record.

Peters (2006) presented five fundamental aspects necessary to summarize the temporal and spatial structure of the geologic record (macrostratigraphy): 1) rock quantity, 2) rock type, 3) the spatial distribution of rock, 4) rock emplacement setting, and 5) temporal continuity of the rock record. Temporal continuity (sensu Peters, 2006a) refers to the duration of uninterrupted rock formation at a given scale of temporal resolution at a given location. It was further demonstrated that the temporal distribution of sediment packages and hiatuses that bound them (e.g., gap-bound packages) could be treated in much the same way as paleontologists treat the temporal span of a genus or species (Foote, 2000). For instance a gap-bound package can span the entire bin (both boundaries crossed), cross only the bottom boundary and then terminate in a bin (last occurrence), initiate in a bin then cross only the top boundary (first occurrence), or remain confined to the bin (first and last occurrence). This provides a means of measuring parameters such as geologic "diversity" (which is related to rock quantity), geologic rates of initiation and truncation (reflecting rates of expansion in the area of rock formation and contraction/erosion, respectively). Here, I apply the principles of macrostratigraphy to quantify the spatiotemporal distribution of sediments across the Triassic of the western USA.

2.2 Methods

Hannisdal and Peters (2010) demonstrated the efficacy of compiling gap-bound packages of sediment from multiple geographic locations as a means to quantify temporal

variation in the factors that govern sedimentation, including tectonic subsidence, sediment supply, and base level change. Although their analyses focused on model-generated results for a siliciclastic passive margin-type setting, macrostratigraphy has also been successfully applied at high resolution in non-marine basins by Aswasereelert et al. (in press). Their approach to the macrostratigraphy of the Green River Formation was founded on temporally well-constrained (radiometric dates from tuff deposits) detailed stratigraphic sections that have a 10 cm resolution from field and core data compiled from the literature. Calculations of lithological attributes (i.e., facies associations) produced macrostratigraphic time series that demonstrated stratigraphic architecture of lacustrine contraction and expansion (e.g., the stratigraphic signal of external forcing mechanisms). They conclude that the incorporation of spatiotemporal variability provides an outstanding quantitative framework for basin-scale analyses. A similar methodology is followed here to produce a quantitative analysis of the temporal and spatial distribution of sedimentary rocks across the Triassic system of the western USA.

2.2.1 Triassic Database

In order to quantify the structure of the geologic record of the study area a relational database (TDB: Triassic database) was created by integrating stratigraphic descriptions from the primary literature that ranged across a large region (western USA) spanning 10 myr before (262 ma) and 10 myr after (190 ma) the Triassic Period. Data deriving from original fieldwork in the Chugwater Group of Wyoming were also included (Lovelace and Lovelace, in press). Thirty-five geographical locations were chosen, within which a synthetic stratigraphic column representative of the stratigraphy

of each bounded area in the backarc depositional system. Five additional geographical locations (AT1–AT5; Appendix 1) were selected to represent the limited stratigraphic data in the arc, basinal and shelf terranes (*sensu* Speed, 1978). These additional data are excluded from most analyses because they are limited in spatial and temporal resolution and because few of the original sedimentary rocks remain after post-depositional alteration (metasedimentary to metamorphic grade rocks), making lithological and environmental attributes difficult to consistently identify. However, these data may provide a starting point for interrogating the structure of the sedimentary record along the active margin during the Triassic.

2.2.2 Columns

Synthetic column locations were based on gross outcrop area, regional and local stratigraphic study availability, and similarity of lithologic characteristics and boundaries. Column locations were broadly grouped by depositional area into four zones (Fig. 2.2): 1) Wyoming (Chugwater Group), 2) Nevada (Thaynes/Virgin Fm), 3) Four Corners (Moenkopi/Chinle Group), and 4) Dockum (Dockum Group).

Each synthetic column was created through the compilation of multiple sources to create a representative composite stratigraphic section that is vertically scaled to time not thickness (Fig. 2.3). Attributes for each lithostratigraphic unit (e.g., unit, member or formation) were manually entered into the TDB. These data include: rank, age (top/bottom), thickness (min/max), area (of column location), lithology (primary, secondary, and tertiary); and depositional environment(s). Errors potentially occurred at several key phases during the creation of the database (constructing the temporal

boundaries of lithostratigraphic units, interpreting nomenclatural differences across publications, data entry, and construction of synthetic columns). The largest source of error is likely to be the assignment of temporal boundaries and correlation of stratigraphic units between colums. The age boundaries of Triassic stages used in this study follow those outlined by Mundil et al. (2010), although the placement of the Norian–Carnian boundary remains contentious (Mundil et al., 2010; Zeigler et al., 2011; Lucas et al., in press 2012). The paucity of absolute age dates and absence of marine ammonite and conodont zones in most of the Triassic of the western US makes defining the absolute age of continental lithostratigraphic units difficult. The problem is exacerbated by contradictory age assignments based on vertebrate remains (Lucas et al., 2001; Lucas et al., 2002; Klein and Lucas, 2010; Lucas, 2010), recent paleomagnetic studies (Zeigler et al. 2011), and recent U-Pb dates from detrital zircons from sandstones within several lithostratigraphic units of the Chinle and Dockum Groups (Riggs et al., 2003; Dickinson and Gehrels, 2008; Heckert et al., 2009; Irmis et al., 2011; Ramezani et al., 2011). Because of this the TDB is considered a dynamic tool that will, like the Macrostrat Database, evolve over time as greater consensus is reached regarding temporal ranges and regional correlation of lithostratigraphic units and temporal distribution of lithological units within them.

2.2.3 Time-series Analyses

A hiatus-recognition threshold of 1 million years was applied for macrostratigraphic analyses, yielding 93 total sedimentary packages (inclusive of all four classes of gap-bound packages). Shorter bin durations for non-marine deposits are not feasible until a more accurate temporal resolution can be attained for each

lithostratigraphic unit. To quantify the structure of the geologic record across the Triassic (including 10 million year tails that proceed past the Permian and Jurassic Period boundaries to account for edge effects) time series were produced for each bin by tallying the number of packages that contained the attribute in question.

2.3 RESULTS

A total of 233 lithostratigraphic units were entered into the relational database. The dominant lithofacies of these lithostratigraphic units are principally represented by mudstone (52 lithostratigraphic units), siltstone (65 lithostratigraphic units) and sandstone (91 lithostratigraphic units); the data set is composed mostly of continental units (~84%).

2.3.1 Sediment Packages (Fig. 2.5–2.6)

A time-series of the total number of sedimentary packages in both the backarc (the study area outlined in Fig. 2.2) and the arc, basinal and shelf terranes depositional systems exhibits two distinct patterns. In the arc, basinal and shelf terrane depositional systems there is a gradual increase from 1 to 5 packages across the Early and Middle Triassic, then a relatively constant number of packages throughout the Late Triassic. The backarc depositional system, however, has an absence of preserved sediments spanning roughly 10 million years around the Middle-Late Triassic boundary (Dubiel, 1994), which is bracketed by two distinct pulses of sediment accumulation (Note: the use of "sediment accumulation" throughout this chapter refers to a measurement of rock accumulation that does not compensate for compaction during lithifaction [Fig. 2.5]). Because of this apparent structure, the time-series are effectively divided into two distinct intervals, hereafter referred to as the Early–early-Middle Triassic (ET) suite and the Late

Triassic (LT) suite. Although the exact ages of ET termination and initiation of LT sediment accumulation is unknown and may change with the addition of new information, the lateral relationships of the units are well established by physical correlation on the outcrop (e.g., Woody, 2006; Zeigler et al., 2008; Martz and Parker, 2010). This suggests the overall patterns documented here will remain relatively stable, despite future changes in the timescale (e.g. they may accordion to younger or older dates as new age data are generated; i.e., Irmis et al., 2010; Ramezani et al., 2011).

Permian packages decline rapidly during the latest Capitanian until a plateau of 6 packages is attained for the remainder of the period. The overall pattern of the ET suite reflects a rapid increase in the extent of sedimentation just after the Permian-Triassic boundary; this increase reaches an apex at the end of the Spathian, decreases by approximately half at the Spathian–Anisian boundary, and then declines rapidly to zero by the early Ladinian. Sediment accumulation does not resume until around 228-225 Ma.

Initiation of sediment accumulation in the LT suite is rapid and the greatest quantity of packages (22) is attained almost immediately. There is a notable decline in the number of packages (14) around 218 Ma, reaching a plateau around 19 packages for the remainder of the Norian. At the Norian-Rhaetian boundary there is a gradual decrease across the Rhaetian to 3 packages before increasing to around 10 packages in the Hettangian and Sinumurian (Early Jurassic).

There is a rough similarity in the overall ET and LT suites patterns, namely that there is a relatively rapid rise in the number of packages (and thus sediment volume) and then a gradual decreases after a period of stabilization (much shorter in the ET). The duration of the rapid rise (2–3 million years) and gradual decline (8–9 million years) is

the same for both intervals, but the period of stabilization is 4 times greater in the LT (12 million years).

Marine to non-marine packages were compared across the same interval (Fig. 2.6), and several notable patterns were identified. The first is that marine sedimentation is most prominent at the initiation of each suite; the relative abundance of marine to non-marine sediments is comparatively equitable during the ET, but disparate in the LT. However, there is a notable inverse relationship between number of marine packages and non-marine packages in the ET. As marine packages increase, non-marine packages decrease, although it is not a 1:1 relationship. There are three possible states for any given time bin: marine, non-marine, or hiatus (unless the bin is shared by two conditions). If it were a 1:1 relationship, this would imply a simple turnover from non-marine to marine environments, or the reverse. However, the rate of increase in the number of marine packages is greater than the rate of decrease in non-marine packages. This demonstrates an initiation of sediment accumulation in columns that in previous time intervals had no sediment accumulation (e.g. an initiation of more landward sediment accumulation). In the reverse scenario, as the number of marine packages decreases there is an increase in non-marine packages that appears to be coupled (e.g., a roughly 1:1 relationship) until the Spathian–Anisian boundary where the two systems decouple and non-marine packages increases as marine packages declines to zero.

There are far fewer marine packages in the LT, and the pattern may not be significant. There is also a distinct decline in non-marine sediment packages coincident with the initiation and truncation of a brief period of marine sediment accumulation around 218 Ma.

2.3.2 Volume (Fig, 2.7–2.8)

The area represented by the 35 geographical locations is relatively evenly distributed spatially (see Fig. 2.2), comprising roughly 50% of the total depositional area. Volume calculations were conducted using these assumptions: 1) the average of recorded maximum and minimum thickness for each column is assumed to apply over the entire area represented by that column, 2) the intervening space between areas represented by columns can be assumed to have a volume that is an average of the columns that bound it (although only column volumes are reported), 3) sedimentation within each package is continuous and uniform in rate of accumulation.

The volume of sedimentary rock for the Triassic interval of the study area is divided into two suites, the ET and LT, as defined above (Fig. 2.7). The most striking pattern is the similarity between the number of packages and the total volume (scaled) with the distinct exception of the entire Early Triassic where the total volume exceeds the number of packages by a factor of 3. Of the entire Triassic interval 73% of the total volume is represented in the first 12-14 million years, although, the ET only comprises 40% of the total Triassic sedimentary packages. The remaining 27% represents the last 25-28 million years and 60% of the total sedimentary packages. When the volume is age weighted (e.g., volume/million year), the average ET volume is 4.5 times greater than in the LT.

The non-marine component comprises 97% of the LT volume (non-marine = 1.2E+5 km^3), while the non-marine component of the ET represents 72% of its volume (non-marine = 3.2E+6 km^3). The most notable quantity of marine sediment accumulation

is in the Early Triassic from the Smithian to the earliest Anisian. During this interval the volume of marine sediment accumulation exceeds that of the non-marine. This is coincident with a deceleration in sediment accumulation in the non-marine (almost a factor of 2), although there is an overall increase in non-marine sediment packages (Fig. 2.6) at this time. The remainder of the Triassic does not preserve marine deposits within the study area.

2.3.3 Lithofacies and grain size distribution (Figs. 2.9 and 2.10)

For each lithostratigraphic unit a dominant lithology was determined based on the most representative of six rock types (carbonate, shale, mudstone, siltstone, sandstone, and conglomerate). The carbonate attribute (n = 14) refers mostly to limestone (n = 13), but also includes the single dolomitic interval within the study area. Conglomerates are relatively rare as a dominant lithology as they often only make up small (but readily recognizable) portion of a given lithostratigraphic unit, even those that are often labeled conglomerate, such as the Shinarump Conglomerate, are dominantly sandstone with conglomeratic intervals (McCormick and Picard, 1969; Stewart et al., 1972b; Chan, 1999; Heller et al., 2003).

Time-series displayed in Figure 2.9 show absolute and relative distributions of dominant lithology across the Triassic. The Early Triassic has previously been suggested to have a dominant fine-grained lithology and little variability in siliciclastic composition, while the Late Triassic was shown to exhibit a pulse of coarser sediments across the T-J boundary (Peters, 2006a). This argument is supported by the current results, which demonstrate that close to 50% of the lithologic abundance is siltstone, with a minority of

mudstone and finer sediments in the Early Triassic; sandstone is not strongly expressed until the end of the Early Triassic and into the Middle Triassic where it rapidly becomes the dominant lithology. Although principally fine grained in nature, the ET shows a distinct coarsening trend until the Middle Triassic hiatus (Fig. 2.10). The LT demonstrates a greater degree of lithologic variability. There are two rather marked coarse-grained, conglomeratic pulses of fluvial sandstone accumulation bound by older and younger floodplain and interfluve mudstone on either side; one in the late Carnian, the second in the mid-Norian. The late Norian through the early Jurassic demonstrates a gradual increase in grain size, as sandstone once again becomes the principal lithology.

2.3.4 Accumulation rates-totals (Fig. 2.11)

The rate of sediment accumulation was calculated by the average thickness of a given unit (*n* meters) divided by the duration (*n* million years) to give a per-bin rate of accumulation. This yields an approximate minimum rate of average sediment accumulation across the interval; compensation for sediment compaction variability was not accounted for in these calculations. Most non-marine sedimentary volumes were not deposited evenly over time; rather they are the cumulative result of periodic rapid depositional events. Moreover, there are numerous time surfaces that record durations large enough (10^4 –10^6 yr) to impact averaged rates of accumulation (i.e., well-developed paleosols) that are unaccounted for in this data set (e.g., Jenny, 1941; Cleveland and Atchley, 2007; Prochnow et al., 2006). However, the calculated rates provide a reasonable tool for comparing relative rates across the spatiotemporal range of the study area even though they are biased towards a lower sedimentation rate. The long-term accumulation rates (e.g., mean = 13.5 m/my and median = 15.1 m/my) across the study

interval are comparable to minimum values calculated for long-term accumulation averages across continental scales (Ronov et al., 1980; Sadler, 1981; Peters, 2006a). Future work quantifying the spatiotemporal distribution of time averages surfaces (e.g., number of preserved paleosols and their minimum estimated time for formation) would provide a better understanding of their impact on accumulation rates averaged over larger temporal ranges.

2.3.5 Accumulation rates-Marine vs. Non-Marine (Fig. 2.12)

Because the ET is represented by a much higher percentage of marine rock (28%) than the LT (2%); Figs. 2.6 and 2.8) it was hypothesized that the marine contribution to the total accumulation rates may have overwhelmed the coeval non-marine component. The marine and non-marine rates of sediment accumulation were separated (Fig. 2.12) to test this hypothesis. Figure 2.12 demonstrates that the marine system has a higher rate of accumulation than the non-marine in both the Early and Late Triassic. However, the ET non-marine still appears to have an increased average rate of accumulation relative to the LT (mean = >25% higher). Two peaks, one in the Dienerian, the other in the Spathian are nearly double the LT average. These higher rates of sedimentation may be coupled to increase subsidence as the terrestrial system rapidly prograded basinward during the Dienerian and early Spathian regressions (Blakey, 1973, 1977: Haq et al., 1987; Embry, 1988, Hallum, 1992, Paull and Paull, 1994).

There is a notable decrease in the rate of non-marine accumulation coincident with the peak rate of marine accumulation in both the ET and LT. This deceleration in non-marine accumulation may be related to increased bypass, gradient shallowing, or

possibly unidentified hiatal surfaces. When the volume of marine and non-marine packages are considered (e.g., Fig. 2.8) there is a substantial increase in non-marine volume during the Dienerian regression compared to the early Spathian regression suggesting different modes of creating accommodation or sediment supply for each event. The most striking lithologic difference, demonstrated in Figure 2.9, is the abundance of carbonate during the Smithian transgression relative to the overwhelming contribution of silt during the Griesbachian transgression (Paull and Paull, 1990; 1994). This observation is suggestive of a decreased siliciclastic supply to the whole system during the Smithian event, not just sediment bypass of the non-marine. This may be linked to the proposed cooling event and reestablishment of more diverse primary producers decreasing the rate of continental weathering (Knoll et al., 1996; Berner, 2005; see section *ET suite and* ™C^{13}_{carb} for further discussion). However, increased spatiotemporal resolution in the marine system is needed to quantify differences in carbonate and siliciclastic deposits, specifically with respect to mixed carbonate-siliciclastic rock bodies.

2.3.6 Fundamental packages (Fig. 2.13)

Decline in the number of through ranging packages (bt) highlight the disruption of the temporal continuity at the Early–Middle Triassic boundary, and three intervals within the Late Triassic (Fig. 2.13). The Early–Middle Triassic break marks a significant shift from the siltstone dominated lithostratigraphic units to those dominated by sandstone. This interval also correlates with the termination of marine accumulation possibly indicating a tectonic control imparting its effect on the sedimentary record. The cause of the late-Middle Triassic absence in the rock record (few, if any Ladinian sediments likely

exist in the Rocky Mountain west) has yet to be identified. Through-going packages in the LT correlate with lithostratigraphic units that maintain a relatively stable (consistent) distribution of environments and lithologies (dominantly floodplain deposits).

The time-series of initiation followed by persistence (Ft) portrays a consistent decay after an initial peak at the onset of both the ET and LT. While this pattern mirrors the overall number of sedimentary packages in the ET (e.g., relative rates of first occurrence are consistent throughout the ET), there is a distinct divergence in the LT. This may be the result of an increased number of through-going packages in the mid-LT.

Truncations of packages that initiated prior to the interval (bT) show two spikes in the ET that correspond to termination of marine sedimentary packages during the Dienerian and early-Spathian regressions. Sedimentary packages that both start and stop within a given interval display a distinct pattern that reflects a few widespread, but temporally limited formations, namely the Griesbachian aged Dinwoody Fm (first peak in ET), the Spathian aged Alcova Limestone (second peak in ET), and the Shinarump/Santa Rosa Formation (first peak in LT).

From the fundamental sedimentary packages (above) initiation (FL + Ft) and truncation (FL + bL) rates were calculated using equations derived by Foote (2000). The most notable observation in initiation and truncation rates is the difference in pattern between the ET and the LT (Fig. 2.13). The ET displays relatively high turnover rates at any given interval, whereas the LT experiences discrete pulses of turnover (higher frequency of turnover). The extreme rate of initiation and truncation at the onset of the LT is again representative of the Shinarump/Santa Rosa Formations, which are broad

ranging spatially, but temporally limited. The high turnover rate in the ET is expected given that the ET experiences two incursions of marine sedimentation. This is largely due to the environmental and lithological variability associated with relative (or global) sea level rise and fall at any given location (e.g. sharp lithologic boundaries associated with surfaces of erosion, for instance, sequence boundaries).

2.3.7 Duration (Fig. 2.14)

The distribution of package durations approximates an exponential distribution ([number of packages] = $23.85e^{-0.03t}$; $r^2 = 0.931$). Peters (2006) described the distribution of package duration for North America as also expressing a roughly exponential distribution with a decay constant of -0.03*t*, and a decay constant of -0.04*t* when an excess number of long-duration packages (0.58%) were excluded. The similarity between these two studies (at different scales) suggests that the underlying tectonic processes that controlled package duration for the Phanerozoic of North America (Wilkinson et al., 1991; Peters, 2006a) are similar to those that controlled package duration of Triassic sediments in the western US. These observations are also consistent with previous calculations of basin longevity (Woodcock, 2004).

2.4 DISCUSSION

The Early Triassic can be differentiated from the Late Triassic in many respects: spatiotemporal distribution of lithology, rate of sediment accumulation, grain size distribution, patterns of sedimentary package truncation and initiation rates, and volume of preserved rock. All of these quantifiable states result from the interaction of multiple geological processes that can be difficult to separate (namely climate and tectonics).

However, results from the quantifiable states above yield new information on the evolution of the Triassic in this region. By interrogating these quantitative results, it is possible to provide additional constraints on the processes that may have been responsible for the observed patterns of sediment distribution within the Triassic of the Rocky Mountain west.

The potential of error in this study principally lie in the time domain. However, extensive outcrops allow for relatively strong correlative control preserving the fidelity of lateral associations and confine the majority of error to the temporal distribution of those relationships. Recent efforts in U-Pb dating of detrital zircons (see Lucas et al., in press for review) in the well-studied Chinle Group have reduced the temporal error within much of the Late Triassic interval. Biostratigraphic controls provided by intermittent marine limestone helped constrain temporal ranges of Early Triassic units (Solien, 1979; Goodspeed and Lucas, 2007; Lucas et al., 2007; Chapter 4).

Radiometric dates attained from the Petrified Forest Member (Ramenzani et al., 2011) also allow for a more rigorous estimate of accumulation rates than the method outlined above. These calculated accumulation rates (24 to 28 m/my; Ramenzani et al., 2011) are similar to the results produced in this analysis for the same lithostratigraphic unit (Columns 24-28; mean = 30 m/my, median = 25 m/my) in this study.

The Early Triassic demonstrates a strong increase in the average rate of sediment accumulation relative to the Late Permian and Middle and Late Triassic rates. The ET displays more voluminous sedimentary packages (up to 3–4 times maximum LT volumes), and a higher average sedimentation rate (2–3 times maximum LT rate). This

may be due to a larger number of short duration hiatuses in the Middle and Late Triassic. These hiatuses are likely tied up in a large number of time surfaces represented by well-developed paleosols (Cleveland and Atchley, 2007; Prochnow et al., 2006), erosional surfaces along sequence boundaries (Beer, 2005; Cleveland et al., 2008), or overestimated lithostratigraphic unit temporal durations.

Comparisons of Early and Late Triassic depositional suites demonstrate a similarity in the number of packages represented in each system, although many of their associated lithologic attributes differ significantly. For instance, the longer-lived LT exhibits greater lithologic heterogeneity and greater variance in the distribution of dominant grain size. One noticeable trend is the double pulse of coarse clastics in the late Triassic. The first occurs at the onset of LT sediment accumulation and represents the widespread Shinarump, Gartra Grit, and Santa Rosa formations. This widespread, coarse grained deposit, is thought to reflect a broad but gentle uplift resulting from the initiation of Andean style subduction along the western margin of the continent (Armstrong and Ward, 1993; Dickinson and Gehrels, 2000; Heller et al., 2003). This initial rapid pulse of coarse-grained sediment is followed by a brief decrease in sedimentary packages and grain size. Another pulse of sandstone (Moss Black–Sonsela formations) then occurs with a concomitant increase in sedimentary packages that transition into the mudstone-dominant late Norian. It is possible that these pulses represent episodic events during the initial subduction of the underthrusted slab, which would create similar conditions proposed for the deposition of the Shinarump Formation (Heller et al., 2003).

It has also been suggested that the coarsening trend across the Triassic–Jurassic boundary may be the result of extensive regressions (Hallam and Wignall, 1999; Peters,

2006a). Sandstones of Late Triassic and Early Jurassic age in the study area are primarily eolian in origin. The development of widespread ergs across the study area in the Early Jurassic (e.g. Glen Canyon Group, Wingate, Nugget Formation) may be climatically driven rather than controlled relative or eustatic sea-level fall (Parish, 1993, Lucas, 1999; Tanner and Lucas, 2007). It is noteworthy that the coarsening trend in the ET is coincident with what has been interpreted as a regional regression (Paull and Paull, 1994). The differences in lithologic attributes seen in the ET and LT suites are suggested to be the result of different tectonic and climatic conditions during each interval.

2.4.1 Tectonics

Comparisons of the distribution of package duration is nearly identical to that calculated for the Phanerozoic of North America (Wilkinson, 1991; Peters, 2006a), which suggests that, even at the continental, regional, and basin scale, there are similar underlying tectonic controls that affect sediment accumulation and truncation (Woodcock, 2004). It appears that the majority of tectonic controls are related to regional extension along the cordillera with an initiation or shortening at the end of the Triassic.

2.4.1.1 Early Triassic

The Early Triassic is a considerably dynamic time that records a delayed end-Permian biotic recovery that is linked to perturbations in global climate (for instance, extreme carbon isotope excursions [CIE]) and inhospitable marine conditions (Payne et al., 2004; Pruss et al., 2005; Pruss et al., 2006). Tectonically, the ET suite may have experienced far-field effects during the termination of the Sonoma Orogeny, such as variable subsidence (local accommodation) associated with extension in the basinal

terrane of the backarc (Speed, 1978; Wyld, 1991). Increased rates of sedimentation are likely linked to both tectonic and climatic influences associated with increased aridity and continental weathering throughout the continental interior as Pangean accretion neared its zenith. There also may be a significant link between CIE's and carbonate and black shale production during this interval as well.

2.4.1.2 Middle Triassic

The most recognizable feature of the spatiotemporal distribution of sedimentary packages and their associated lithologic attributes is the 10 million years absence at the Middle and Late Triassic boundary, which effectively breaks the Triassic of the Rocky Mountain west into two depositional suites. However, poor temporal control of the termination of sediment accumulation in the Middle Triassic, timing of the resumption of sedimentation in the Late Triassic, and the issue of the missing Middle Triassic siliciclastic contribution to the system as a whole remain problematic.

The Middle Triassic Problem: The absence of Middle Triassic deposits has long been identified (Reeside et al., 1957; Dubiel, 1994), although an explanation of its absence is wanting. In the eastern US the initiation of Triassic sedimentation is concomitant with the formation of extensional basins during the rifting of the super continent Pangea where Triassic sediments overlie Precambrian to early Paleozoic rocks (Reeside et al., 1957; Olsen et al., 1996). However, unlike the east coast, Triassic sediments of the western US were largely deposited on a low-gradient passive margin (Marzolf, 1994). A carbonate rich platform is found in western Utah, and eastern Nevada during the Spathian (e.g. Virgin and Thaynes Fms; Solien, 1979; Pruss and Bottjer, 2004;

Pruss et al., 2005). During mid-Anisian through earliest Carnian platform carbonates are only found further basinward in western Nevada on the shelf terrane (Speed, 1978); all clastic material of the shelf terrane is considered locally derived from block faulting associated with continued regional extension (Silberling and Wallace, 1969; Nichols and Silberling, 1977; Wyld, 2000), and are no longer present in eastern Nevada–western Utah. This shift towards more westward deposition of carbonates is consistent with the Spathian–Anisian regression, possibly associated with increased extensional accommodation near the Triassic volcanic arc (Paull and Paull, 1994; Wyld, 2000).

Terrestrial sedimentation is recorded, at minimum, during the earliest Anisian, but temporal controls for the duration of Middle Triassic deposition are also lacking. Most authors believe that sedimentation ends by the mid– to late–Anisian (Morales, 1987; Hunt et al., 1993; Marzolf, 1994; Lucas, 1998; Nesbitt and Whatley, 2004). The duration of the Middle Triassic Jelm Formation is unknown, but thought to be at least Anisian and possibly earliest Ladinian in age (Pipiringos, 1963). It is likely that terrestrial deposits of Middle Triassic age are only represented by strata of Anisian age; however the age Jelm still remains to be adequately defined.

The termination of siliciclastic preservation in latest Early Triassic through early-Late Triassic either indicates cessation of deposition, or subsequent erosion and transportation immediately prior to the initiation of Late Triassic sedimentation. However, the presence of widespread paleosols such as the Mottled Strata and Palo Duro geosol (Kanhalangsy, 1997; Beer, 2005) that developed on the upper surface of the Moenkopi Formation (or older Permian units in the case of the Palo Duro) suggests a regional exposure surface during, at minimum, the early–mid Carnian prior to the

deposition of the Shinarump–Santa Rosa sandstone units. Chan (1999) described loessite deposits in northern Utah at a similar level and suggested that this loess deposit took a significant amount of time to form on a subaerially exposed dry interfluve. Loess deposition was followed by incipient paleosol formation and subsequent deposition of the overlying Gartra Grit (Shinarump equivalent conglomeratic sandstone). Further investigations of these time-surfaces may help determine their temporal duration.

Syntectonic deposition of shallow-marine platform carbonates associated with regional subsidence-created accommodation occurred during regional extension throughout much of the shelf terrane. This implies a significant decrease in terrigenous sediment supply given that terrigenous sediments did not reach the marine basin during the Middle Triassic and did not start accumulating again until the Late Carnian (Burke and Silberling, 1973; Nichols and Silberling, 1977; Wyld, 2000).

Once terrigenous sediments again reached the marine system (late Carnian; Wyld, 2000) they quickly overwhelmed carbonate production. This indicates that there is either an outstanding volume of rock unaccounted for due to erosion, a lack of sediment supply (insufficient sediment creation?), or possibly transient sediment storage in the highlands or unidentified basins. Further quantification of the rock record in the shelf and basinal terranes is needed to more adequately address the Middle Triassic problem.

2.4.1.3 Late Triassic

Although the LT suite also experienced far-field effects from variable rates of subsidence and uplift along the continental margin due to extension associated with the Triassic arc (Wyld, 1991, 2000), it also experienced broad-scale shallow uplift related to

the initiation of Andean-type slab subduction (Heller et al., 2003). The transition to Andean-type subduction is linked to the commencement of Late Triassic sedimentation, most notably, the widespread coarse-grained and conglomerate rich fluvial pulses (Shinarump–Santa Rosa–Gartra Grit formations). An additional regional pulse of coarse-grained fluvial sedimentation (Moss Black–Sonsela formations), which occurred in the mid-Norian, is suggested to be linked to this event as well.

2.4.1.4 *Early Triassic suite and global $\delta^{13}C_{carb}$ (Fig.2.15)*

It has been well established that the Early Triassic experienced a highly unstable $\delta^{13}C$ record with three prominent excursions that ranged from +7 to -2 per mil (Payne et al., 2004; Korte et al., 2005, Galfetti et al., 2007 Horacek et al., 2007; Payne et al., 2007; Preto et al., 2010). In addition, the marine record of $^{87}Sr/^{86}Sr$ exhibits a large monotonic increase across the Early Triassic and a sharp decline after reaching an apex at the Spathian–Anisian boundary (Korte et al., 2003; Tanner, 2010). It is hypothesized that the prominent shift from siliciclastic to carbonate deposition in the Smithian–Spathian reflects a climatic signal rather than one dominantly controlled by end-Sonoma or regional tectonics, although the effects of tectonics are not absent since increased accommodation was likely gained through regional subsidence caused by sediment loading (Blakey, 1977; Lawton, 1994).

Galfetti et al. (2007) suggested that the onset of carbonate precipitation at the Smithian–Spathian boundary in India and China initiated after the peak of a rapid positive $\delta^{13}C$ excursion (CIE). It has been suggested that this interval also experienced an increase in ocean oxygenation and a significant decrease in siliciclastic deposition

possibly tied to a global cooling event as atmospheric CO_2 was drawn down by increased organic carbon burial (Knoll et al., 1996; Berner, 2005). This cooling is thought to have temporarily reduced the affect of monsoonal precipitation and decreased the supply of siliciclastics to the oceans. Ocean waters at the earlier CIE (seen at the Dienerian–Smithian boundary) are thought to have experienced low oxygenation (anoxia/hypercapnia; Twitchert and Wignall, 1996; Wignall and Twitchert, 2002) coupled with increased organic carbon burial and greater siliciclastic input (Galfetti et al., 2007).

The first major positive CIE occurs at the Dienerian–Smithain boundary (ca. 251 Ma), the second at the Smithian–Spathian boundary ca. (249 Ma), and the third at the Spathian–Anisian boundary (ca. 247 Ma); comparable $\delta^{13}C_{carb}$ results are seen globally (Payne et al., 2004; Corsetti et al., 2005; Korte et al., 2005; Galfetti et al., 2007; Horacek et al., 2007).

When time-series of lithofacies, marine, and non-marine volumes from the study area are compared with $\delta^{13}C_{carb}$ several patterns emerge (Fig. 2.15). The first positive Early Triassic CIE is seen at the Dienerian–Smithian boundary. Prior to this boundary it is notable that the principal marine lithofacies in the study area are voluminous fine-grained siliciclastics (e.g., Dinwoody Formation; Paull and Paull, 1993). Positive CIE is linked to increased organic carbon burial (Tanner, 2010); organic carbon rich sediments are evident in the black shaley-siltstones of the Dinwoody and Black Dragon formations that lead up to the CIE peak (Paull and Paull, 1993; Lucas et al., 2007). The first widespread limestones in the Early Triassic are found during the mid-to-late Smithian (Timpoweap–Sinbad Limestone, and lower beds of the Thanyes Formation; Lucas et al.,

2007). Peak limestone deposition occurs at both the first and second negative ™ ^{13}C excursions, each is marked by unusual facies such as subtidal microbialites, carbonate sea-floor precipitates, and microbial patch reefs (Pruss et al., 2006).

At the Smithian–Spathian boundary the second CIE coincides with peak deposition of black shales, dominantly in the Thaynes Formation of Idaho, Nevada, and Utah; these are the thickest deposits of any locality within the entire study area. There is a short-lived decrease in the volume of limestone across this boundary, although this is likely a result an early-Spathian regression (Paull and Paull, 1993; Paull and Paull, 1994). Limestone precipitation increases until mid-Spathian and begins to decrease gradually until a shoulder is reached at the third and final CIE.

The final CIE occurs at the Spathian–Anisian boundary were carbonate production abruptly ceases. It is important to note that this is also the point at which almost all marine rocks disappear from the stratigraphic record in the study area; however, carbonates are prominent in the shelf terrane as reefs began reestablishment throughout the Middle Triassic (Wyld, 2000; Pruss and Bottjer, 2004). The cessation of marine deposits is in part due to relative (or global?) sea level fall and initiation of non-marine fluvial and eolian deposition (Irmen and Vondra, 2000), and in part from erosional truncation of Triassic rocks in the westernmost study area.

The change from siliciclastic dominated marine lithofacies in the early-Early Triassic to the carbonate dominated late-Early Triassic is consistent with hypotheses that suggest increased atmospheric pCO_2 decreased the pH of ocean waters, coupled with decreased ocean circulation led to a carbonate crisis, hence the heavy loss of specific

organisms (e.g., brachiopods, tabulate and rugose corals, radiolarians; Pruss et al., 2006). This lead to the Early Triassic reef and chert gaps (Fagerstrom, 1987; Racki, 1999), and produced conditions on land that impacted terrestrial primary production of plants leading to the coal gap (Bestougeff, 1980; Retallack et al., 1996; Berner, 2005). The relatively dramatic shift from siliciclastic to carbonate marine deposition in the late-Early Triassic has been speculated to be a result of decreased supply terrigenous sediments. However, the $^{87}Sr/^{86}Sr$ ratio in marine water exhibits a sharp monotonic increase across the Early Triassic and rapid decrease at the Early–Middle Triassic boundary.

The $^{87}Sr/^{86}Sr$ ratio in seawater has a long residence time (~10^6 yr) relative to oceanic mixing times (10^3 yr) such that it takes timescales greater than 10^4 years to affect ocean $^{87}Sr/^{86}Sr$ levels (McArthur, 2007). This suggests a continual terrestrial contribution throughout the Early Triassic, possibly sourced from increased weathering of elevated basement rock due to higher pCO_2 (Berner, 2005), loss of diverse flora (Veevers et al., 1996; Visscher et al., 1996; Ward, 2000; Michaelsen, 2002), or a combination of these factors (Korte et al., 2003). Alternately, increased weathering associated with aridification of the continental interior during Pangean accretion would produce a similar effect. This is consistent with the observation of an unusually high rate of accumulation of siliciclastic sediments for the early-Early Triassic, but it does not resolve the issue of decreased siliclastic deposition in the late-Early Triassic. In order to test this hypothesis further work is warranted to quantify the variance in siliciclastic sedimentation rate and volume for the Early Triassic in the western US. Higher resolution quantitative analyses are possible in the marine sections of this time interval

because of well-constrained biostratigraphic horizons (chiefly conodont and ammonite biozones).

2.5 CONCLUSIONS

The quantification of the sedimentary record provides a way to measure and compare changes in a dynamic system. Given the extraordinary history of the Triassic it is essential to apply quantitative methods to further interrogate the rock record. This work represents the first effort to quantify the sedimentary record of the Triassic of the western USA.

Rapid positive carbon isotope excursions reflect the high rate of $\delta^{13}C_{org}$ burial, which is expressed by deposition of organic rich black shales of the Thaynes, Dinwoody, and Black Dragon formations. The two negative excursions are each associated with increased carbonate precipitation in the Smithian and Spathian, namely in the Sinbad–Timpoweap and Thaynes–Virgin limestone formations. The higher rates of sediment accumulation result in the obvious difference in sedimentary volume between the ET and LT suites. It is suggested that the dominance of fine-grained siliciclastics may be related to higher rates of weathering due to increased humidity coupled with the end-Permian loss of floral diversity and increased atmospheric pCO^2. The quantitative results suggest that climate and low biological diversity (e.g., increased organic burial, decreased reef production, reduced influence of floral stabilization) played a strong role in the Early Triassic deposition.

Although the LT suite also experienced far-field effects from variable rates of subsidence and uplift along the continental margin due to extension associated with the

Triassic arc, it also experienced broad-scale shallow uplift related to the initiation of Andean-type slab subduction and regional shortening. The transition to Andean-type subduction is linked to the commencement of Late Triassic sedimentation, most notably, the widespread coarse-grained and conglomerate rich fluvial pulses (Shinarump–Santa Rosa–Gartra Grit formations). An additional regional pulse of coarse-grained fluvial sedimentation (Moss Black–Sonsela formations) is suggested to be linked to this event as well.

Comparisons of the distribution of package duration are nearly identical to those calculated for the Phanerozoic of North America, which suggests there are similar underlying tectonic controls that affect sediment accumulation and truncation at both the local and regional scale. Further studies that improve the temporal and spatial resolution, extend the temporal range, refine associated attributes (i.e., thickness, environments of deposition, lithologic variability), and exogenous factors (such as stable isotope variability, precipitation, and temperature) will contribute to our understanding of the evolution of the sedimentary record and attributes inherent to it.

ACKNOWLEDGEMENTS

I would like to than Shanan Peters, Noel Heim, and Debra Rook for their conversations and help with all things Macrostratigraphy and with the use of the Paleobiology Database. Without their help and patient tutelage, this project would not have been possible.

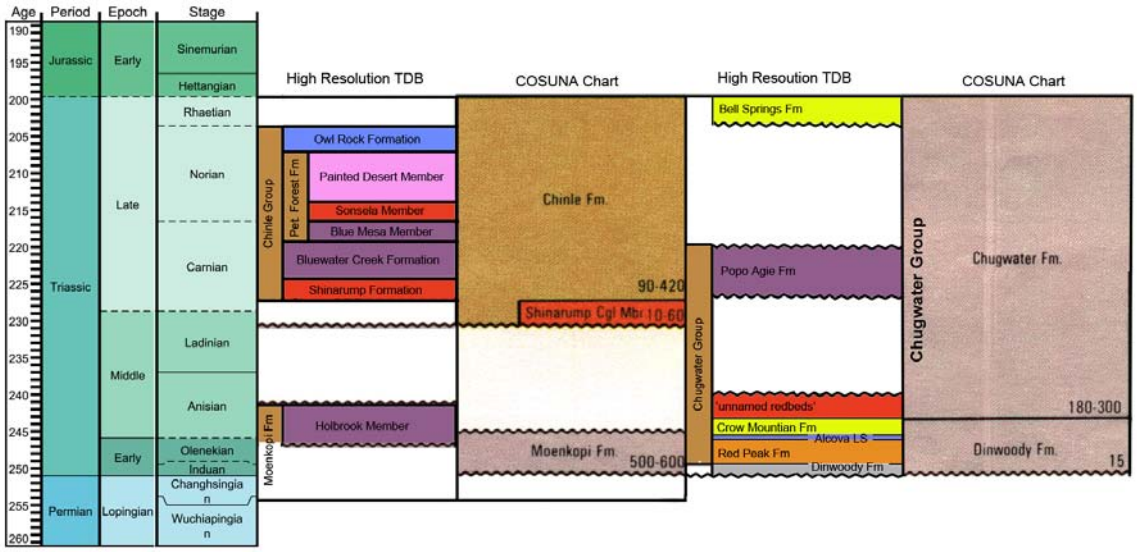

Figure 2.1—Comparison of temporal and stratigraphic entity resolution between the original Macrostratigraphy Database (MDB) and the high resolution Triassic Database (TDB; this study). The inclusion of members (where appropriate) and formations allows for more detailed analyses of quantifiable characteristics (e.g., lithology, thickness, volume, environment, etc.).

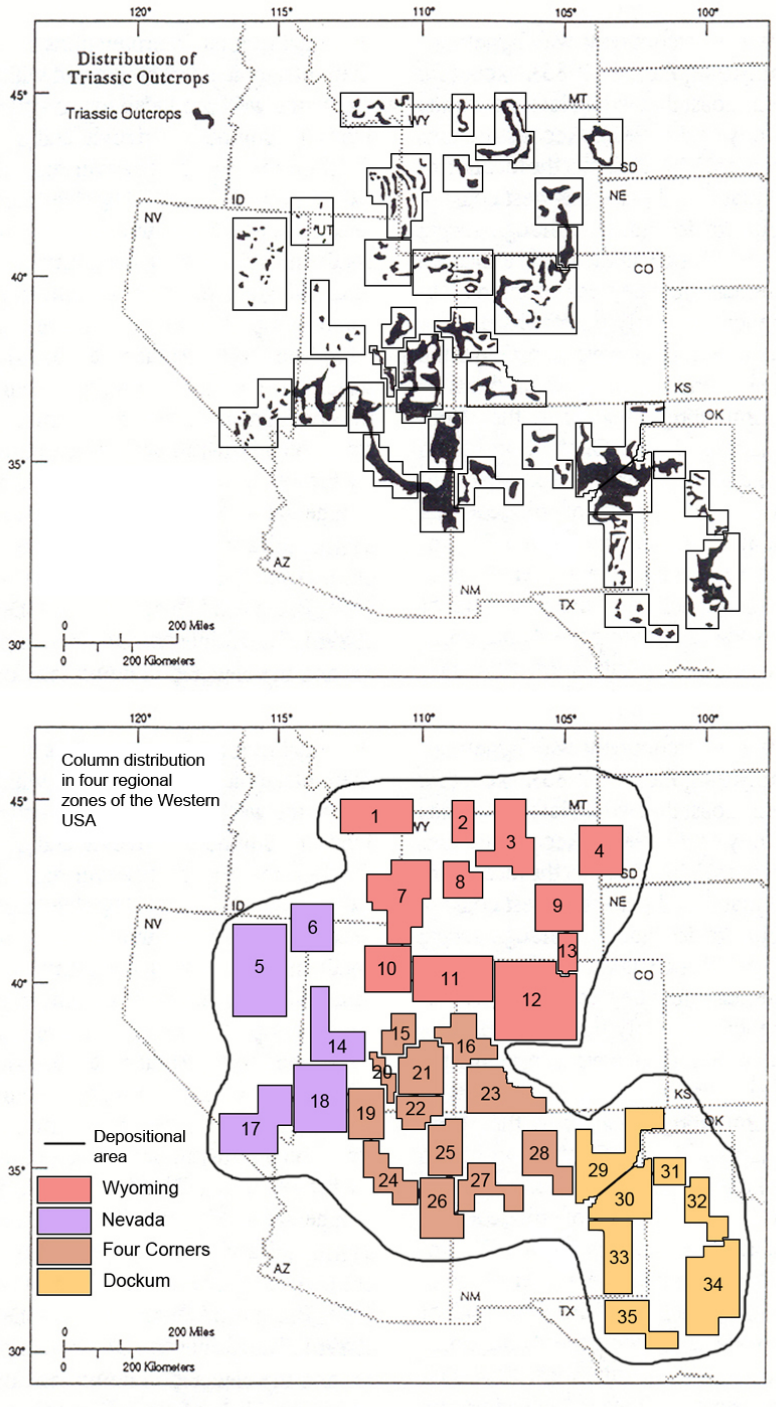

Figure 2.2—Outcrop areas (upper) and bounding areas of the 35 synthetic columns across the western USA. The surface area of the 35 columns represents roughly 50% of the total depositional area (black solid line). Base map and outcrop locations modified after Lucas and Hunt, 2007a.

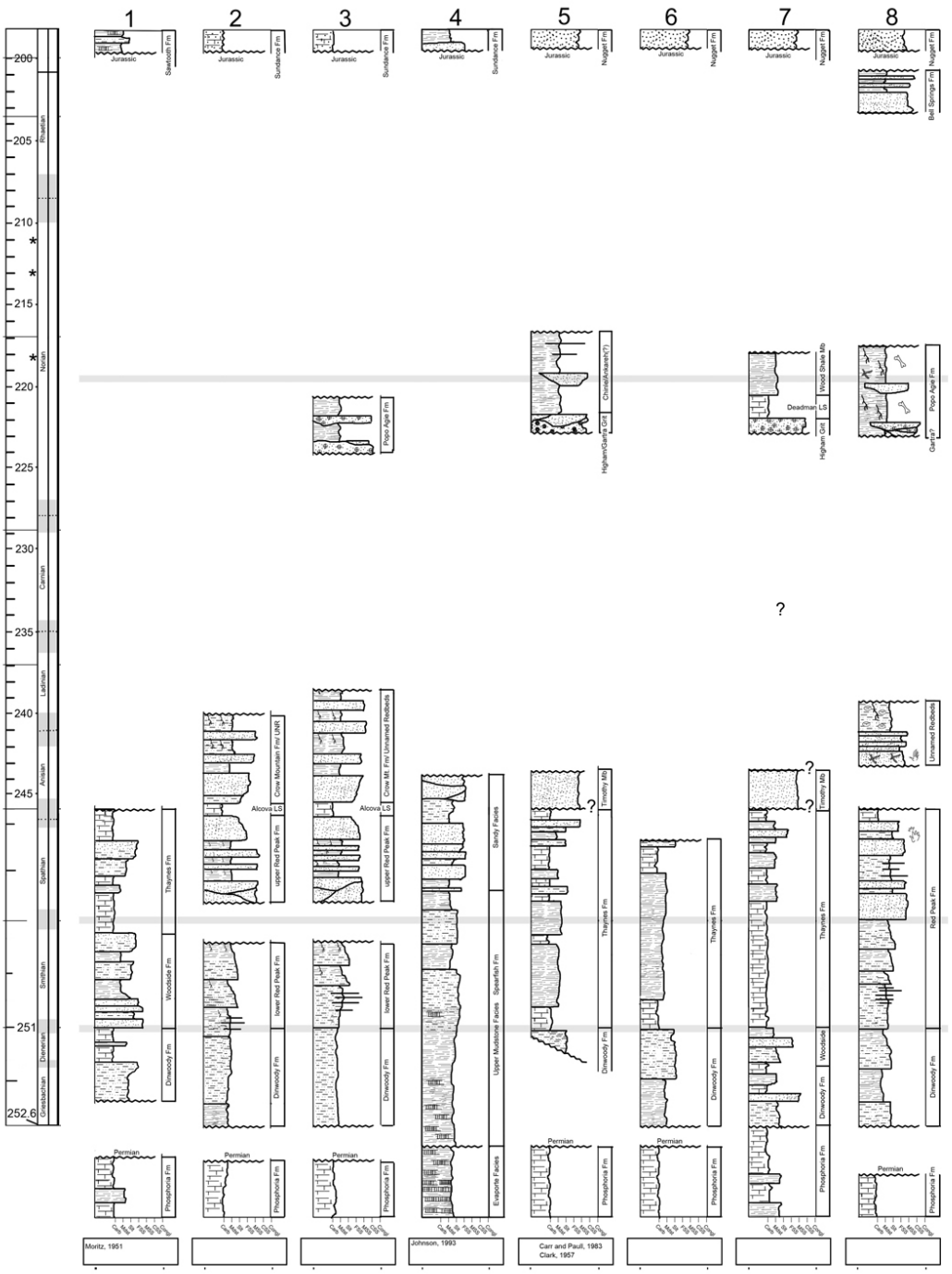

Figure 2.3—Example of synthetic columns 1-8 (see Appendix 1 for complete full resolution image). Note: scale for the early Triassic is different than the Middle and Late Triassic for easier viewing of short-lived, but abundant lithostratigraphic units.

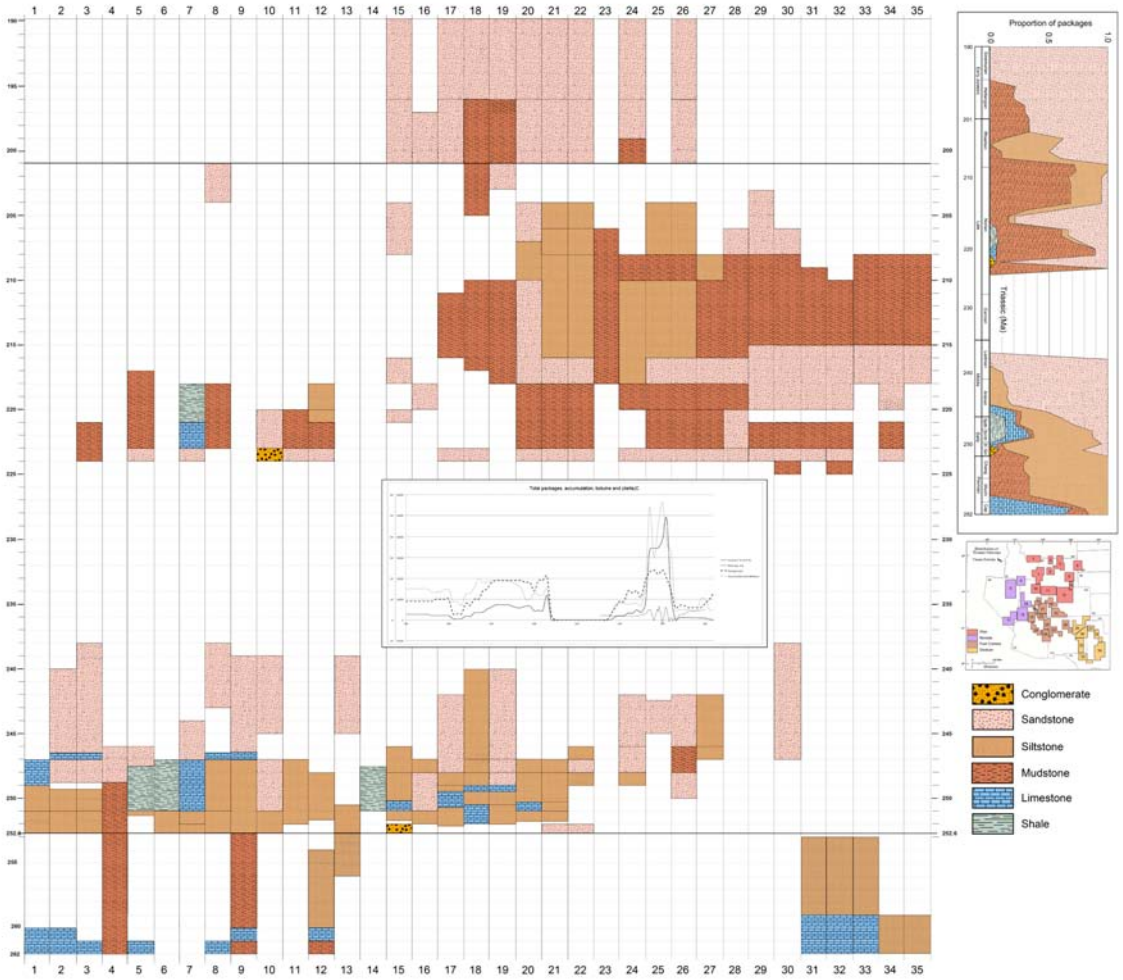

Figure 2.4—Distribution of dominant lithology from 262 Ma to 190 Ma (see Appendix 2 for full resolution image).

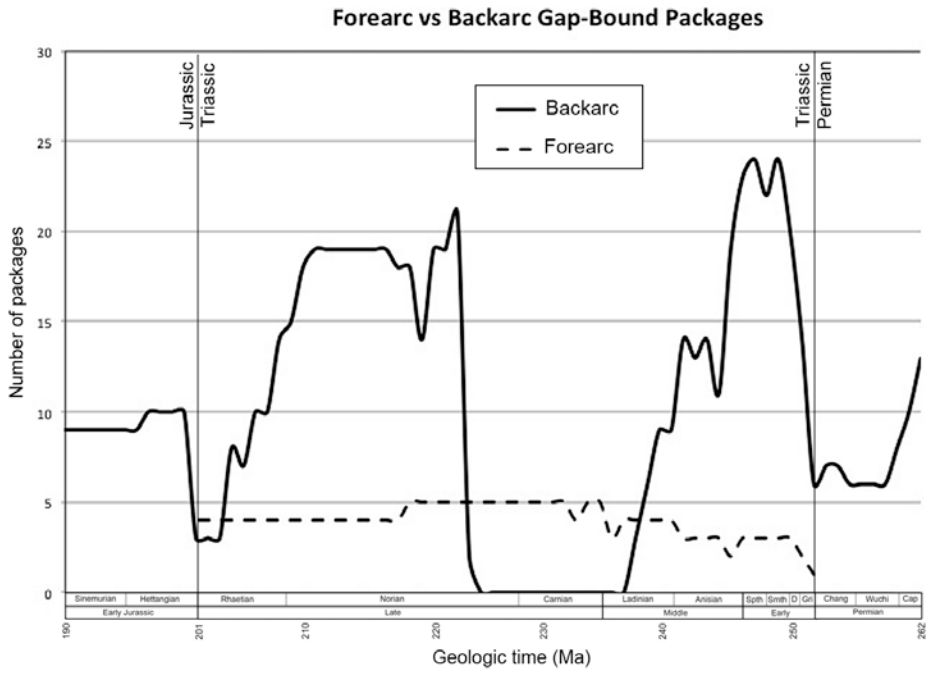

Figure 2.5—Time series of the total number of packages irrespective of rock type or environment of deposition. Backarc data (solid line) represents the 35 columns (columns 1–35 of Appendix 1) from the study area. Basinal and shelf terrane data (dashed line) is based on 5 columns (AT1–AT5 of Appendix 1); this data is not used in the remaining studies. The total number of packages in each 1 million year time interval is a measure of rock quantity; this measure demonstrates a clear decline in the mid-Middle Triassic culminating in an absence of rock through the last part of the Middle Triassic and throughout much of the Carnian (separation of the two principal periods of sedimentation). A rapid increase in packages occurs at the beginning of the Early Triassic and as package accumulation resumes around 225 Ma, package number gradually declines toward the end the mid-Middle Triassic and the Late Triassic. Note: the Carnian-Norian boundary follows Mundil et al. (2010). Data are plotted at age of each interval base.

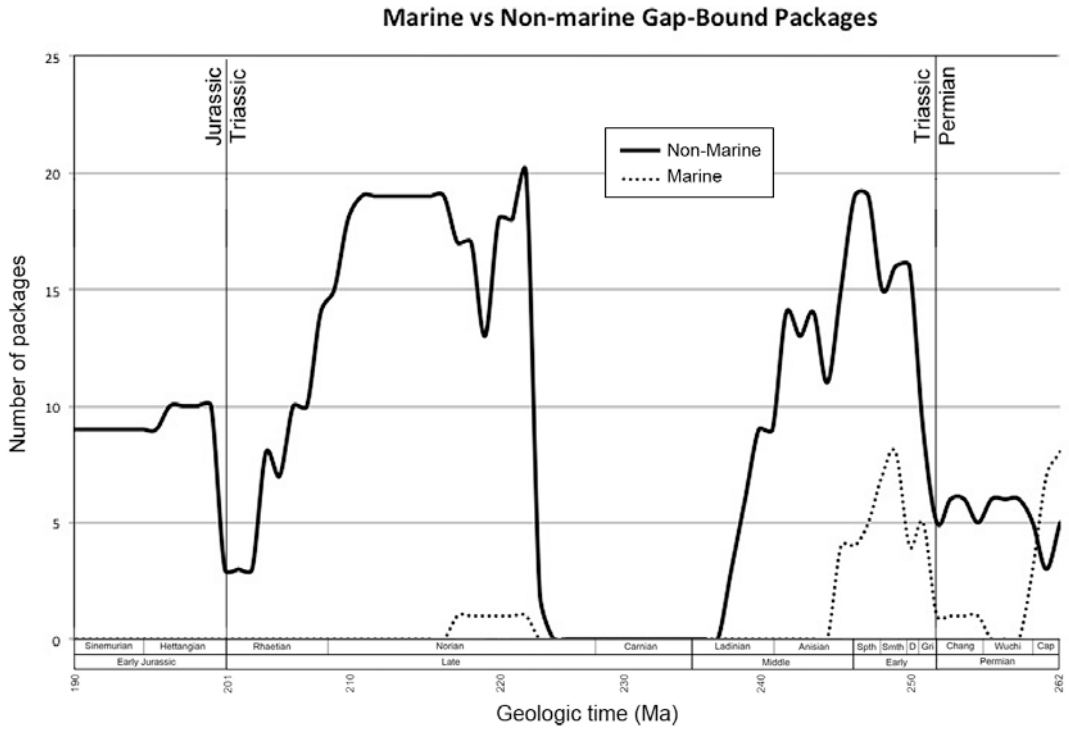

Figure 2.6—Time series of total number of marine and non-marine packages gap-bound packages irrespective of rock type. Note the inverse relationship to the peaks of marine packages (dashed line) in both the Early and Late Triassic and their corresponding troughs in non-marine packages (solid line). The oldest Permian packages (ca. 262 Ma) begin to decrease rapidly (younging) displaying the regional unconformity between Permian marine and Triassic strata. Data are plotted at age of each interval base.

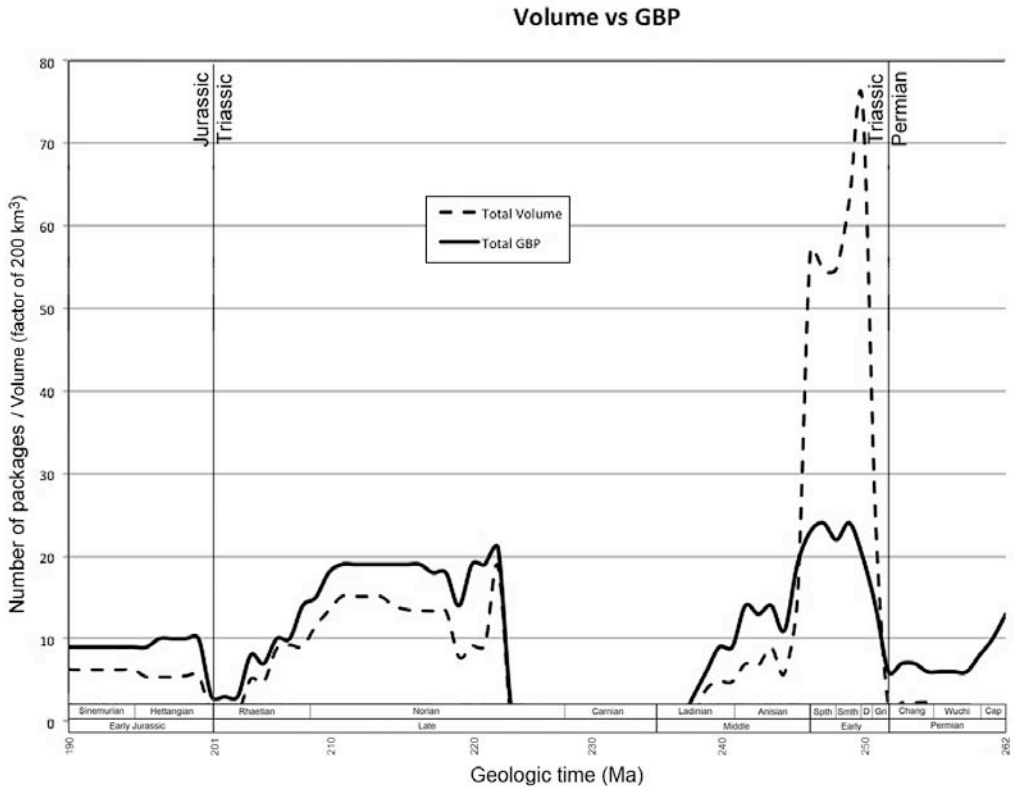

Figure 2.7—Time series showing the total volume (dashed line), and the total gap-bound packages (solid line; from Fig. 2.5) for the study interval. The gap-bound packages exhibit an Early Triassic (and early-Middle Triassic) and a mid-late Late Triassic period of sediment accumulation. Note the volume closely follows the same pattern as the number of gap-bound packages with the exception of the disproportionately high volumes in the Early Triassic. Data are plotted at age of each interval base.

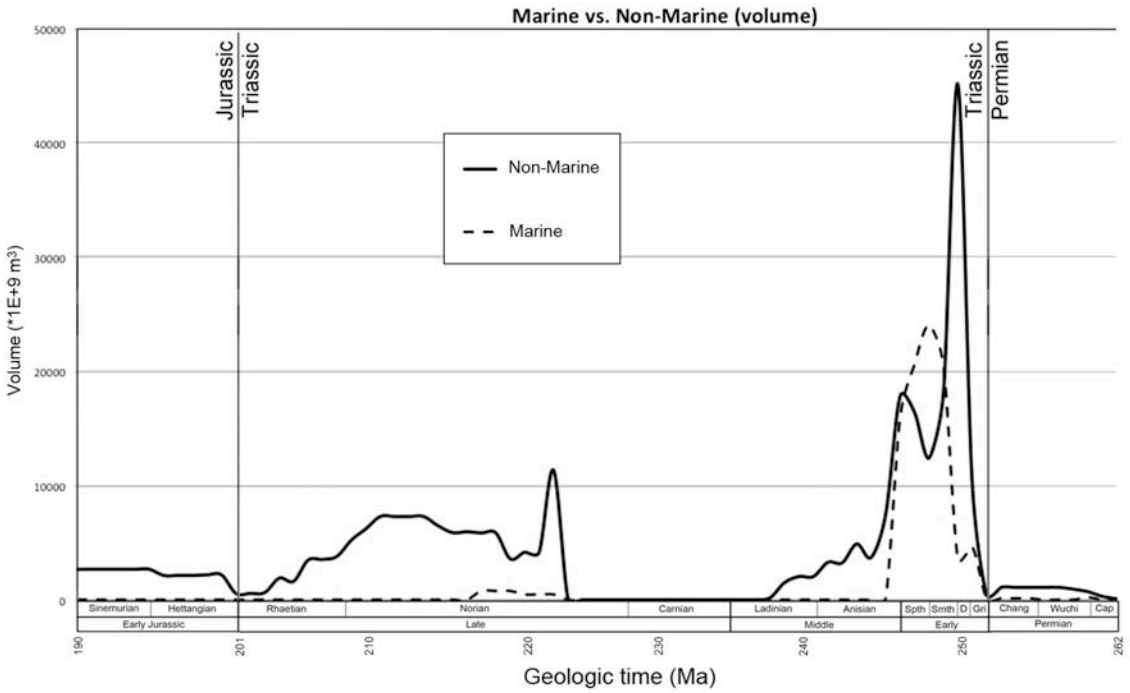

Figure 2.8—Time series displaying the differences in marine (dashed line) and non-marine rock volumes (solid line). Note the peak in the marine volume in the Early Triassic coincides with the trough of the double peak of the non-marine volume. Data are plotted at age of each interval base.

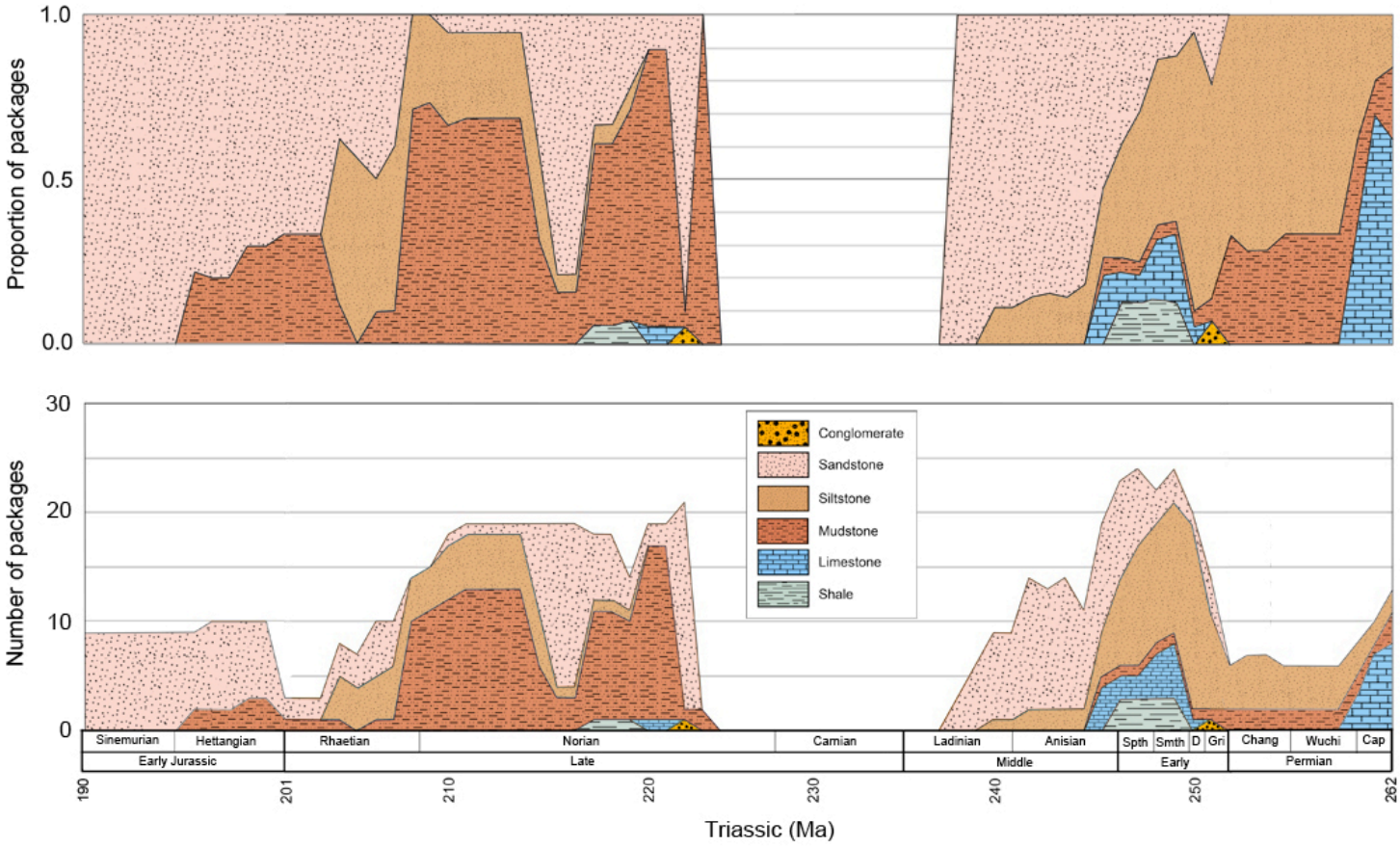

Figure 2.9—Time series of relative (top) and absolute (bottom) abundance of lithofacies measured as a total number of packages preserved in each 1 million year time bin. The most striking pattern (aside from the missing Middle/early Late Triassic packages) is the difference between a relative coarsening of sediment in the Early Triassic, and two periods (initiating at ca. 225 Ma and 218 Ma) that display a relative fining of sediment until the early Rhaetian, which displays a coarsening. Data are plotted at age of each interval base.

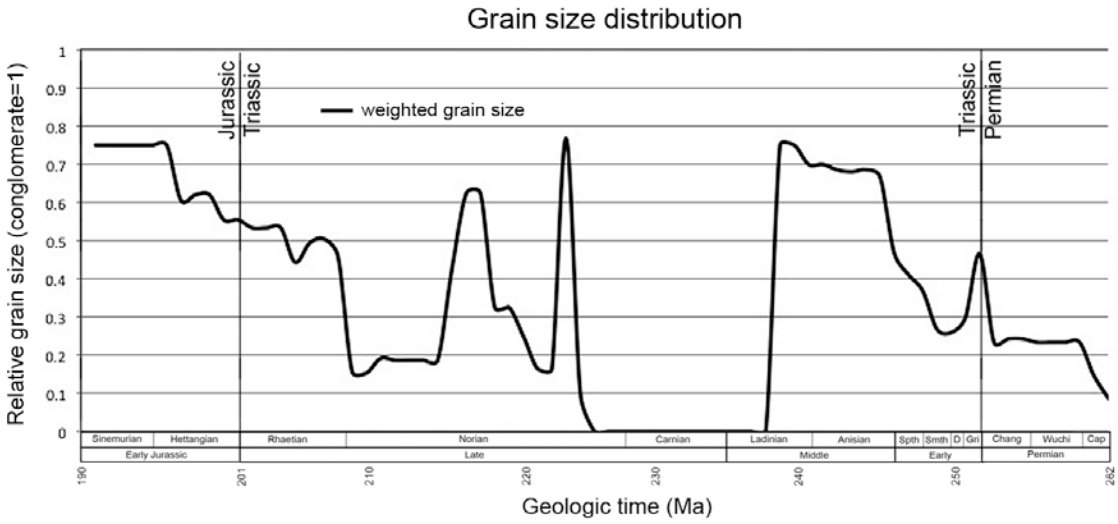

Figure 2.10—Time series of weighted grain size distribution. The overall trend shows a long-term coarsening in the Early Triassic and Late Triassic (Rhaetian)–Jurassic, two distinct short-term coarse events in the early and mid-Norian, and a pronounced coarse event at the P-T boundary is notable. Data are plotted at age of each interval base.

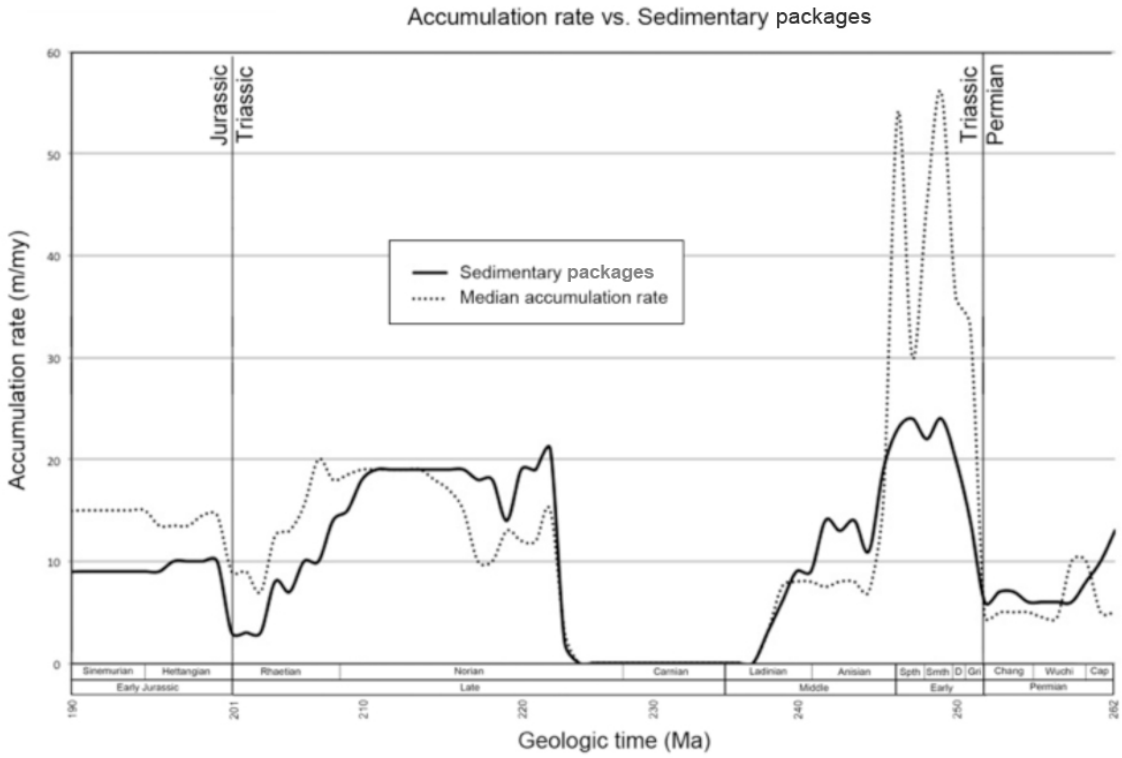

Figure 2.11—Time series showing the median accumulation rate (dotted line) compared to total sedimentary packages (solid line). Note the double pulse of increased rate of sediment accumulation in the Early Triassic. Data are plotted at age of each interval base.

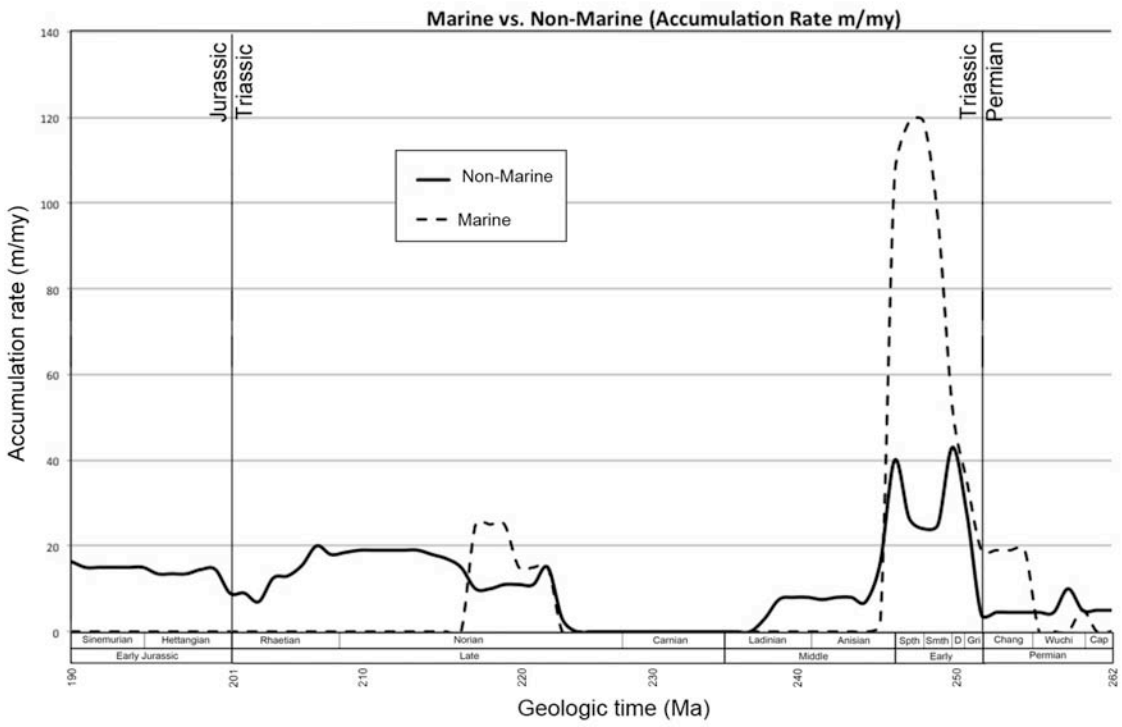

Figure 2.12—Time series comparing median marine (dotted line) and non-marine (solid line) accumulation rates. Note the double peak of increased sediment accumulation rates in the Early Triassic, and the single peak demonstrating a rapid increase in the rate of marine sediment accumulation. Data are plotted at age of each interval base.

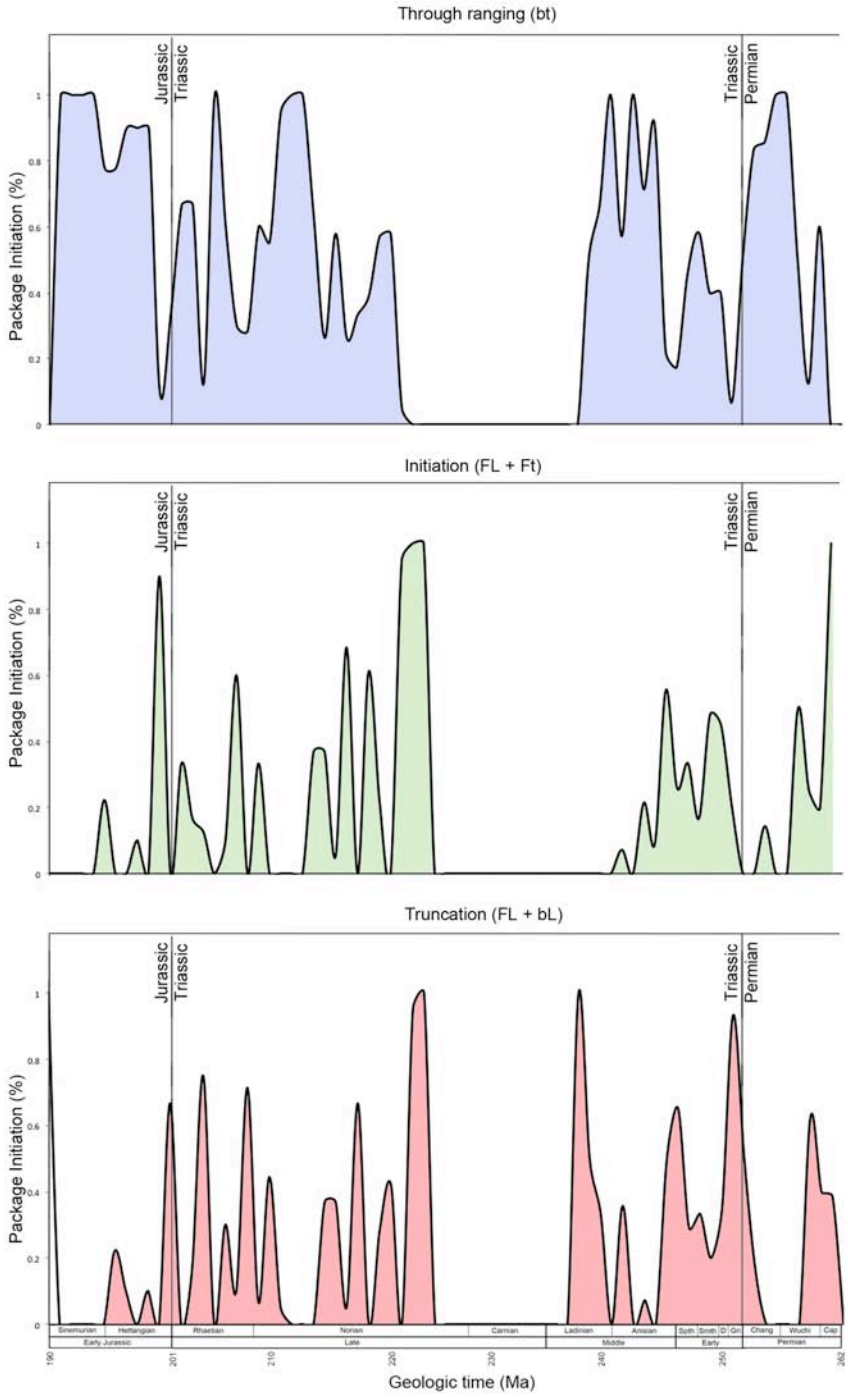

Figure 2.13—Time-series showing through ranging (bt) packages and package initiation (FL + Ft) and truncation (FL + bL). Data are plotted at age of each interval base.

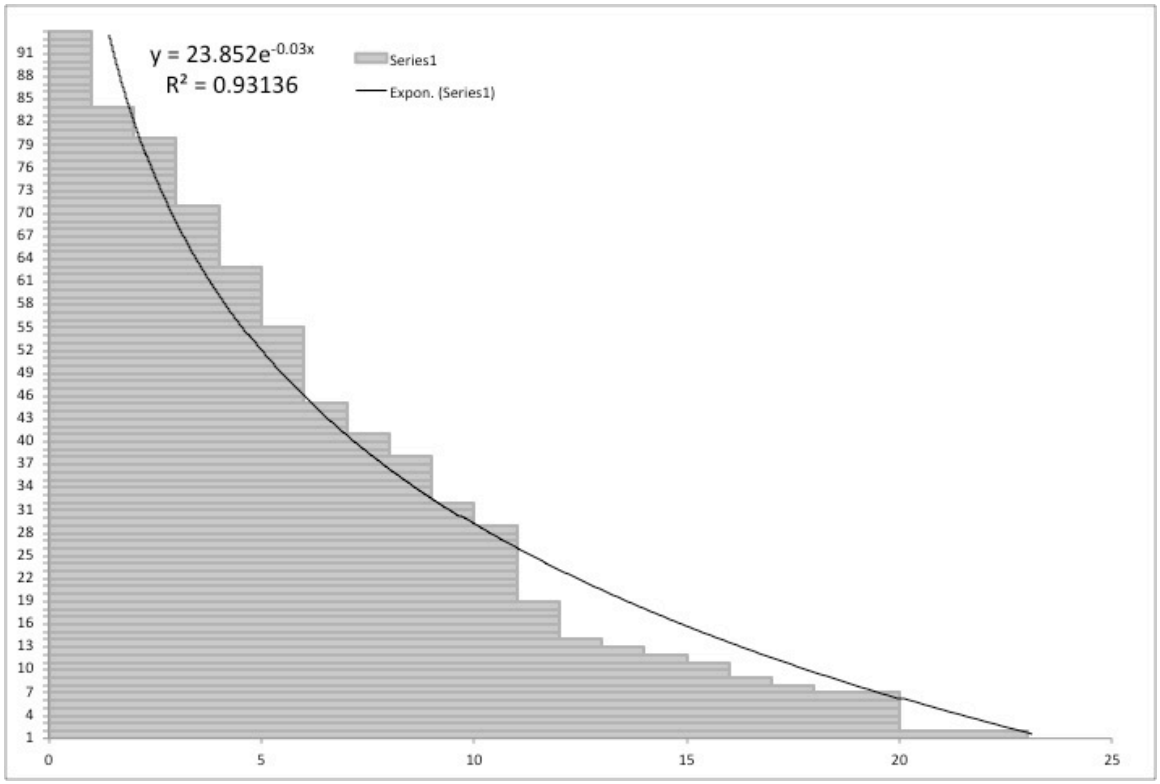

Figure 2.14—Time-series demonstrating the distribution of package duration. The decay constant -0.03t is consistent with previous calculations of package duration (at the stage level) for North America (Peters, 2006).

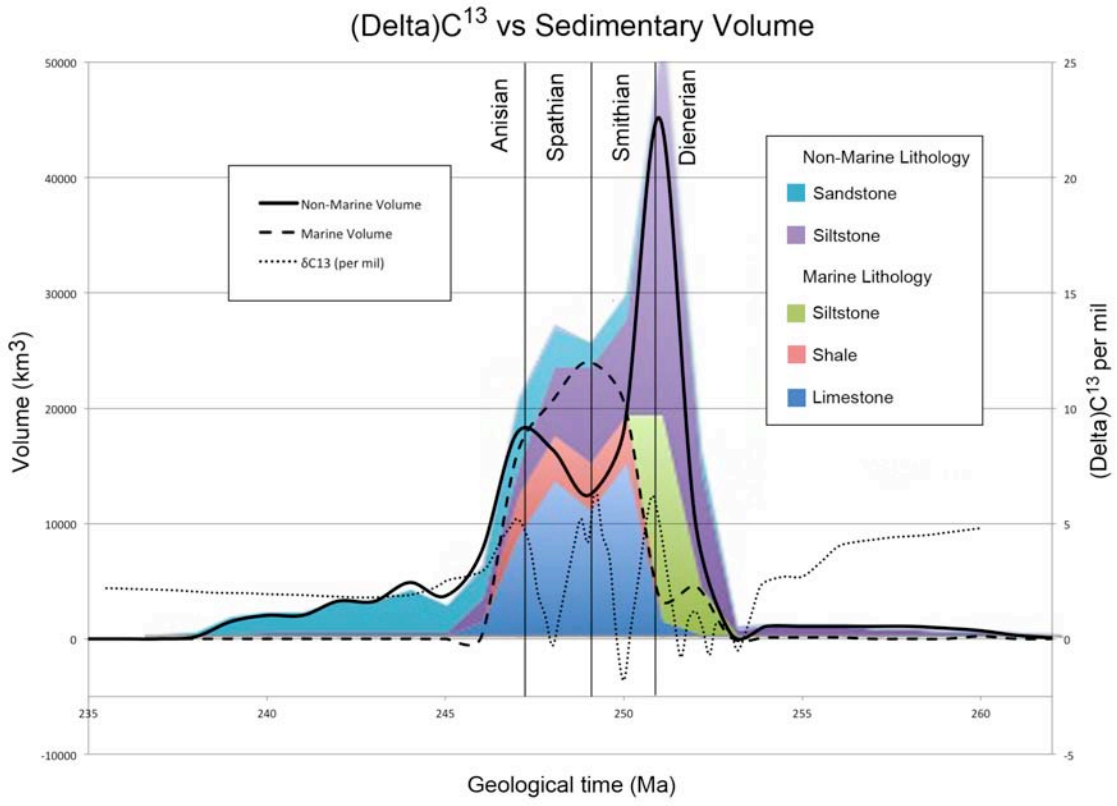

Figure 2.15—Time series showing marine (dashed line) and non-marine (solid line) volumes compared to δ^3C (dotted line). $\delta^{13}C$ data from Corsetti et al. (2005). Note the relationship between the volume excursions (up to 4.5 times greater than in the LT) and the peak carbon isotope excursions in the Early Triassic and the stabilization of $\delta^{13}C$ during the Anisian coincident with a stabilization (relative to the LT) of volume and sedimentation rate (see Fig. 2.11).

CHAPTER 3

Tracking Triassic vertebrate diversity: variability of vertebrate trace and body fossils in Triassic strata of the western USA

ABSTRACT

Recent macrostratigraphic analyses of Triassic strata from the western USA provide the first opportunity to quantify the relationships between vertebrate fossil collections and the geologic record. Vertebrate track and body fossils from the Early to early-Middle Triassic exhibit strikingly different patterns than those from the Late Triassic. Early Triassic tracks strongly correlate to the distribution of fine-grained sediments and rate of sediment accumulation, which reached a peak during the Early Triassic, although body fossils show no correlations with analyzed sedimentary properties. In contrast, Late Triassic body fossils show a strong correlation with the number of sediment packages but not with any individual lithology, while tracks exhibit poor or negative correlations. The Early Jurassic track record demonstrates a relationship between accumulation rates and track preservation similar to that seen in the Early Triassic, suggestive of a taphonomic bias in the creation of the rock and faunal record during recovery intervals. Sample space bias is accounted for, and new diversity curves suggest a rapid end-Triassic loss of diversity over 1 million years rather than a slow decline over the last 8 million years of the Triassic.

The Early to Middle Triassic biological record is better represented by track diversity (5 of 6 clades) than by body fossils (1 of 6 clades) and extends the stratigraphic

range of 4 clades into the early Spathian. This pattern of "tracks first" is consistent throughout the Triassic (6 of 8 clades), demonstrating the need to incorporate ichnologic data into analyses of diversity and molecular clock calibrations. The examination of a quantified biologic and geologic record demonstrates novel spatiotemporal relationships between track and body fossils across the Triassic of the western USA.

3.1 INTRODUCTION

The Triassic Period (252.6–201.9 Ma) records some of the most significant biological events in earth's history including the end-Permian biotic recovery, the origin of the modern fauna (lepidosaurs, crocodiles, turtles, dinosaurs [birds], and mammals); Sereno, 1997; Rieppel and Reisz, 2003; Twitchert, 2006; Muttoni et al., 2010), and the end-Triassic extinction (Raup and Sepkoski, 1982; Twitchert, 2006; Lucas and Tanner, 2007). However, our understanding of macroevolutionary trends within tetrapod lineages and their recovery in the wake of mass extinction events have traditionally been limited to the body fossil record (Tucker and Benton, 1982; Sennikov, 1996; Benton, 2010). It has more recently been argued (Brussatte et al., 2010) that the vertebrate ichnologic record can play a meaningful role not only in developing new anatomical insights within an individual taxon, but also in aiding in the recognition of larger macroevolutionary patterns not always possible with the body fossil record. Another recent study (Chapter 2) quantifies the spatial and temporal distribution of sedimentary packages and their attributes for the Triassic of the western USA, making it an ideal region to investigate the interrelationships of preserved vertebrate diversity and the sedimentary record. In this region terrestrial Triassic strata are divided by a significant hiatus that spans much of the Middle and early-Late Triassic. This effectively splits these deposits two distinct periods

of sediment accumulation. The first episode represents the Early through early-Middle Triassic where the initial end-Permian biotic recovery is recorded. The second episode represents the majority of the Late Triassic through the Early Jurassic boundary. This interval records much of early evolution of the modern fauna, the end-Triassic extinction, and the Early Jurassic recovery. Here we explore the relationship between the spatiotemporal distribution of vertebrate fossils (body and trace), sedimentary packages, and genus richness of the western USA during this important geologic interval.

3.2 DATA AND METHODS

3.2.1 Geologic Data

The sedimentary record is composed of discrete packages of sediment that represent relatively continuous periods of deposition; the packages are bound by hiatal intervals, or gaps in the rock record observable at the same temporal resolution. Properties of gap-bound packages, such as thickness, volume, accumulation rate, environment, lithology, and fossil collections, can be used to quantify the geologic record. Taken together, the data provide a means to examine the spatiotemporal relationships between the physical properties of sedimentary packages and fossil collections found within them.

Recently a macrostratigraphic analysis of Triassic sedimentary rocks was conducted for strata in the western United States (Chapter 2) where the spatiotemporal distribution of gap-bound packages and their properties were quantified. In Chapter 2, 35 area-weighted composite stratigraphic sections, composed of 233 lithostratigraphic units that represent all Triassic deposits of that region, were used to create a relational database

(Triassic Database = TDB). The data set has a temporal range of 262 Ma to 190 Ma and is composed mostly (~84%) of continental units. A minimum hiatus-recognition threshold of 1 million years was applied for macrostratigraphic analyses, yielding 93 total sedimentary packages (inclusive of all four classes of gap-bound packages; *sensu* Peters, 2006). The resultant time series demonstrate temporal variability of several major sedimentary attributes such as rock volume, accumulation rates, lithology, environment, and number of preserved sedimentary packages. These data allow the integration of biologic and geologic information to test potential interrelationships and biases.

3.2.2 Biologic Data

Genus and species data from the Paleobiology Database (PaleoDB) were compiled to quantify the stratigraphic distributions of fossil vertebrates across the Triassic and into the Early Jurassic to test hypotheses regarding the boundary extinction events on land (both end-Permian and end-Triassic boundaries), potential taphonomic variability of track and bone preservation, and paleoecological diversity (genus richness) throughout the Triassic.

A relational database similar to that created for macrostratigraphic analyses (Chapter 2) was produced from data culled from the PaleoDB that includes all recorded vertebrate taxa (genus or species level) from each lithostratigraphic unit that comprise the TDB. The database is comprised of 332 genera from both track (n = 35) and body fossils (n = 297) and includes several additional taxa not currently entered into the PaleoDB. The lithostratigraphic unit, first and last occurrence, clade, and inferred ecology (where available) are recorded for each taxon occurrence.

3.2.3 Analyses

Time-series analyses were produced from these data to quantify vertebrate diversity across the Triassic (including 10 million year tails that proceed past the Permian and Jurassic Period boundaries to account for edge effects). Taxa culled from the PaleoDB were organized into their respective clades. Because little information on stratigraphic control beyond the member level is available in the PaleoDB entries, individual genera were given a temporal range inclusive of the entire duration of the smallest assignable lithostratigraphic unit where they first and last occurred; this ensures a more conservative estimate of temporal disparity between body and trace fossil collections. The data (both geologic and biologic) were compiled using 1-my time bins (range = 262 Ma to 190 Ma), and genera (and ichnogenera) were entered into their appropriate age bins and tallied across each bin to produce time-series data, including genus richness and sediment abundance. Data are plotted at age of each interval base. Results from the study are used to interrogate the affects of geological processes on the variability of vertebrate body and trace fossil preservation and its relationship with vertebrate diversity through the Triassic.

3.3 RESULTS

Given the important biological events recorded in the Triassic, understanding the relationship between sedimentary and biological records is critical. For instance, it has not been established that the sedimentary record of the Triassic in the western USA has imparted a bias on observed biodiversity as a result of variability in sedimentary properties (e.g., volume, accumulation rate, and lithology). It has been documented that Phanerozoic marine (Raup, 1976; Peters and Foote, 2001; Peters, 2005) and non-marine (Smith, 2001) environments preserve a strong positive correlation between rock quantity

and overall genus diversity patterns, and that short-term fluctuations in diversity likely reflect changes in quantity of preserved sediments.

3.3.1 Relationships of Sediment and Fossil Diversity

Comparisons of the absolute number of packages and vertebrate body fossil and track diversity demonstrate variable relationships at different intervals in the Triassic (Fig. 3.1a). There is a high positive correlation between track diversity and the number of sedimentary packages ($r^2 = 0.748$) in the Early Triassic, as well as a very high positive correlation ($r^2 = 0.843$) with fine-grained sediments, specifically siltstone. However, there is no relationship (correlations near zero) with lithology or number of packages and number of genera represented by body fossils, nor is there a correlation between body fossil and track diversity. The lack of a relationship or correlation may be due, in part, to low sample size and limited temporal distribution of vertebrate remains, which are limited to only a few localities (Morales, 1987) prior to the Middle Triassic hiatus. The missing late-Middle to early-Late Triassic strata has been noted by others (Dubiel, 1994; Chapter 2) and succinctly divides the Early and Late Triassic strata into two distinct suites of sedimentary packages; however, little is known regarding the processes that resulted in the absence of Middle Triassic sedimentary bodies.

The Late Triassic demonstrates a different relationship between the number of sedimentary packages and vertebrate diversity. There is a weak negative correlation between absolute body and trace fossil diversity ($r^2 = -0.147$), a high negative correlation between the number of sedimentary packages and track diversity ($r^2 = -0.585$), and a very high positive correlation between sedimentary packages and body fossil diversity ($r^2 = 0.793$). Although there is a strong correlation between siltstone abundance and

tracks in the Early Triassic, there are no observed lithologies that correlate well with either body fossils or tracks in the Late Triassic.

3.3.2 Average Per-Package Diversity

The absolute diversity of body fossils observed per million year bin (Fig. 3.1a) exhibits a gradual decline in genus richness starting around 50 genera at 208 Ma and declining to near zero by the end of the Triassic 6 my later. This drop is coincident with a decline in the number of sedimentary packages that begins around 210 Ma where package quantity goes from 18 to 3 over roughly the same timeframe. To account for potential preservation bias imparted by the declining rock quantity, the number of genera were divided by the number of sedimentary packages in the same interval giving each bin an average per package diversity value (Fig. 3.1b). If genera declined at the same rate as sedimentary packages, there should be an effective flattening of the diversity curve. Instead, there is an increase in frequency of per-package diversity until around 203 Ma where the genus richness declines rapidly to near zero until it picks up again in the Early Jurassic.

A similar trend is seen in the per-package diversity of ichnogenera where ichnogenus richness increases as quantity of rock declines until rapidly dropping to near zero just before the Triassic-Jurassic boundary; for the last 2 my of the Triassic tracks are the only evidence of vertebrate presence. In the Late Triassic, genus richness positively correlates with the number of sedimentary packages, in contrast to the negative correlation between those same sedimentary packages and ichnogenus richness. However, there is a high positive correlation between the per-package body fossil and per-package track diversity in the Late Triassic ($r^2 = 0.803$). A similar correlation is not

seen in the Early Triassic or Early Jurassic, where track diversity exceeds that of body fossils by a factor of ca. 2.5 (Fig. 3.1c).

The unusual representation of Early Triassic vertebrate tracks relative to body fossils may be the result of a dramatic spike in accumulation rates across this 5 my interval. In order to test the hypothesis, accumulation rates described in Chapter 2 were plotted against the average quantity of tracks per package. There was a moderate positive correlation in the Early Triassic ($r^2 = 0.377$). Weak-moderate negative correlation exists for the Late Triassic ($r^2 = -0.267$). The Early Jurassic overrepresentation of tracks (per package) has an even stronger positive correlation with sedimentation rate ($r^2 = 0.889$) and number of packages ($r^2 = 0.811$).

Most studies of Early Triassic endemism during the initial biotic recovery, as well as the radiations that accompany the origination of the modern fauna in the western USA (Morales, 1987), have not accounted for the potential bias imparted by the number of preserved sedimentary packages. There is a significant difference in apparent diversity when potential sample space bias is considered. An exponential model was fit to a time-series of per package genus richness (Fig. 3.2) that shows a strong correlation ($r^2 = 0.833$). The model demonstrates an exponential increase in genus richness that began near the end of the Early Triassic (Spathian) and continued until immediately prior to the end of the Triassic (ca. 203 Ma), when genus richness abruptly drops to near zero at the Triassic-Jurassic boundary. Genus richness rapidly increases several fold within the first 6 my of the Jurassic.

3.3.3 Trends in the Temporal Distributions of Track and Body Fossils

Terrestrial strata of the western US that record the initial recovery interval (Griesbachian–Smithian) do not preserve vertebrate fossil material (Morales, 1987). By the Spathian, five of the six potential clades are present, although only one clade (Temnospondyli) is preserved as a body fossil (Fig. 3.3). The remaining four clades, Archosauromorpha, Crurotarsi, Dinosauromorpha, and Testudines, are represented solely by track material (Welles, 1947; Peabody, 1948; Lovelace and Lovelace, in press).

By the beginning of the Middle Triassic, two of the four clades (Crurotarsi and Archosauromorpha) are represented by body and trace fossils, as well as the addition of coeval tracks and body fossils belonging to Therapsida (Morales, 1987; Nesbitt and Angielczyk, 2002). It is not until the Late Triassic (Carnian–Norian) that another new clade emerges—Dinosauria—again first as track fossils (Lockley and Milner, 2006) and 3 my later as a body fossil (Lehman and Chaterjee, 2005). The final clade, Mammalia, appears towards the end of the Triassic (Norian–Rhaetian) represented only by ichnofossils well into the Jurassic (Lockley et al., 1992). Six of the eight tetrapod clades present during the Triassic of the western US first occur as ichnofossils. Three clades are quickly represented by bone material (within 3 my), while the other three clades range from ca. 10 to 30 Ma before body fossils appear.

3.4 DISCUSSION & IMPLICATIONS

3.4.1 Tracking the Origins of Vertebrate Clades

Vertebrate tracks have been used to extend the known range of several major clades, including: the oldest evidence for turtles in North America (Lovelace and Lovelace, in press), the oldest tetrapod (Niedzwiedzki et al., 2010), and the oldest dinosauromorphs (Brusatte et al., 2011). In addition to extending the known temporal

and paleogeographic range of clades, vertebrate trace fossils also record behavioral and anatomical evolutionary trends not preserved in the body fossil record (Wilson et al., 2005; Padian et al., 2010).

There are no known terrestrial vertebrate fossils from the first 4 my of the Triassic in the western US (Morales, 1987). It is not until the early to mid-Spathian that evidence of vertebrates begins to be represented in the fossil record (Welles, 1947; Peabody, 1948), when ichnofossils best exemplify vertebrate diversity in the Early Triassic (5 of 6 clades). The trace fossils demonstrate the existence of a diverse ichnofauna that may indicate the replacement of disaster taxa (if they were ever present) by specialists prior to the Spathian; however, the utility of track data to answer long-term diversity trends appears to be somewhat limited. Lineages and clades principally diversify exponentially (Benton, 2010), and while the pattern is well-expressed in the body fossil record of the western USA (Fig. 3.2), a similar pattern is not seen in the track record.

Track data may not be a strong indicator of biodiversity (that is, it fails to adequately reflect many aquatic vertebrates), although they provide a powerful tool for observing aspects of behavior and functional morphology (Padian, 2003; Klein et al., 2010). Furthermore, track data has recently extended the temporal range (globally) of many clades including an 18-my extension of tetrapod origins into the Middle Devonian and a 5- to 9-my extension of dinosaur stem lineages into the Early Triassic (Brusatte et al., 2010; Niedzwiedzki et al., 2010; Lovelace and Lovelace, in press). The refinement of paleontological first occurrences has a marked impact on the calibration of the fossil record and molecular clocks (Benton and Donaghue, 2007). Tracks record the first

occurrence of nearly every vertebrate clade present in the study area—in some cases, extending ranges more than 20 my deeper in time.

3.4.2 Sedimentary and Biologic Relationships

In the western USA, the Early Triassic has been demonstrated to be significantly different that the Late Triassic with respect to sedimentary package properties, even though the relative abundance of packages is roughly equivalent (Chapter 2). Differences in sediment accumulation rates, grain size distribution (which is reflective of lithology), environment, and preserved volumes are all likely to have an effect on body and trace fossil preservation (Behrensmeyer et al., 1992; Kidwell and Behrensmeyer, 1993;). Positive correlations of Early Triassic and Early Jurassic track diversity and grain size, number of packages, and sediment accumulation rates further illustrate the unusual nature of the recovery intervals. There was no similar correlation in the Late Triassic with track diversity; body fossil diversity, on the other hand, strongly and positively correlated with the number of sediment packages. Because correlations are not consistent across the interval, the positive correlation during both recovery intervals may be an effect of a common cause (Peters, 2005), such as eustatic sea level or global carbon perturbations that affected sedimentation rate, package quantity, and track preservation.

The positive correlation with sedimentary packages is consistent with previous observations of the relationship between diversity and package number (Raup, 1976; Smith, 2001, Peters and Foote, 2001; Peters, 2005). When the bias in available sample space is considered (i.e., average per-package diversity) there is a positively correlated exponential increase in biologic diversity in the Triassic. The model also predicts a continued increase in diversity throughout the missing Middle and early-Late Triassic,

which suggests that conditions that lead to the destruction or non creation of accommodation space may have been tectonically, not environmentally driven. If environmental conditions were dramatic enough to completely stop sedimentation (e.g., cessation of precipitation) the biota preserved once sediment accumulation resumed in the Late Triassic would likely display a strong faunal succession (Sahney and Benton, 2007). This hypothesis is consistent with the 'sudden' appearance of a diverse flora and fauna coincidence with the initiation of sediment accumulation in the Late Triassic.

The Late Triassic extinction event is the least studied of the five major extinction events (Twitchert, 2006). The compensation for potential sample bias due to shrinking sample space suggests a rapid loss of diversity shortly before the end of the Triassic. This shifts the initial decline of diversity during the end-Triassic extinction event roughly 5 my closer to the Triassic-Jurassic boundary suggesting a catastrophic, rather than gradual, extinction event. The loss of sedimentary packages (that is, sample space) is a result of regional erosion marked by the J0 unconformity (Pipiringos and O'Sullivan, 1978), which imparts an artificial appearance of diversity decline. Further work across the Triassic–Jurassic boundary is required to better understand the transition, and it is likely that ichnofossils will be key.

3.5 SUMMARY

The comparison of quantified biologic and geologic records suggests:

- The Early Triassic and Late Triassic demonstrate significant differences in the spatiotemporal distribution of sedimentary properties, including fossil collections.
- Track diversity correlates well with sedimentation rate, number of sediment packages, and abundance of siltstone in the Early Triassic and Early Jurassic, both

of which are post-extinction recovery intervals and may reflect a taphonomic bias in favor of track over body fossil preservation.

- The fossil record of tracks preserves a biological signal that is sometimes missing from the body fossil record. The addition of the vertebrate ichnologic data suggests an Early Triassic recovery of most major clades roughly 3 million years earlier than the body fossil record suggested (a roughly 50% error in previous recovery estimates).
- The end-Triassic extinction event may have been a much more contracted event than previously thought.

ACKNOWLEDGMENTS

I would like to thank Shanan Peters for mentoring me and patiently showing me the power of macrostratigraphy. Thanks also to the SedPaleo working group at UW–Madison for their helpful critique and conversations, and to Scott Hartman for his discussions and helpful comments.

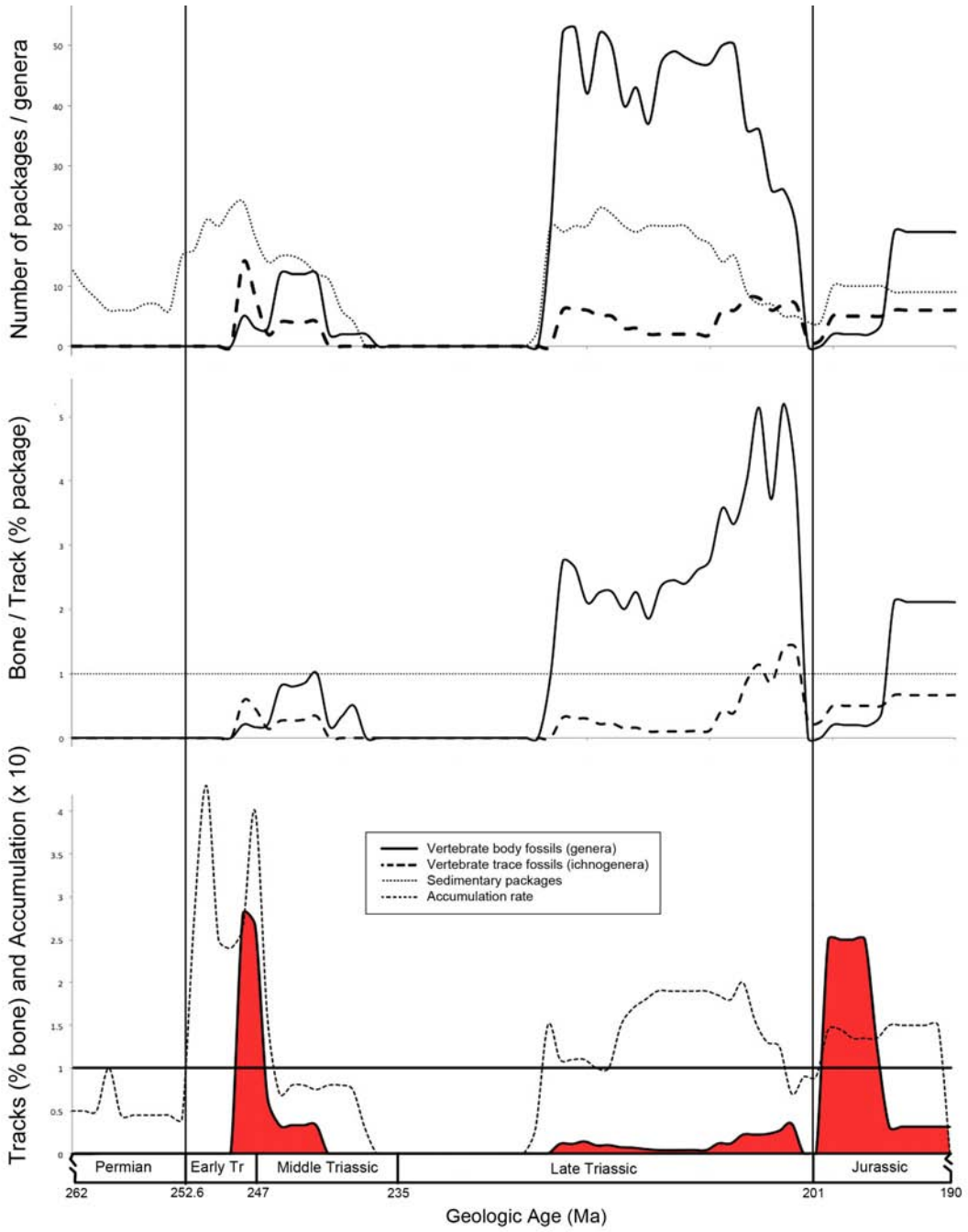

FIGURE 3.1—Upper: Time series of absolute track (dashed) and body fossil (solid) genus richness are compared to the total number of sedimentary packages (dotted). Middle: Time series of the average per-package track and body fossil genus richness. Bottom: Time series quantifying the relative proportions of tracks and body fossils compared to terrestrial accumulation rate (heavy dotted).

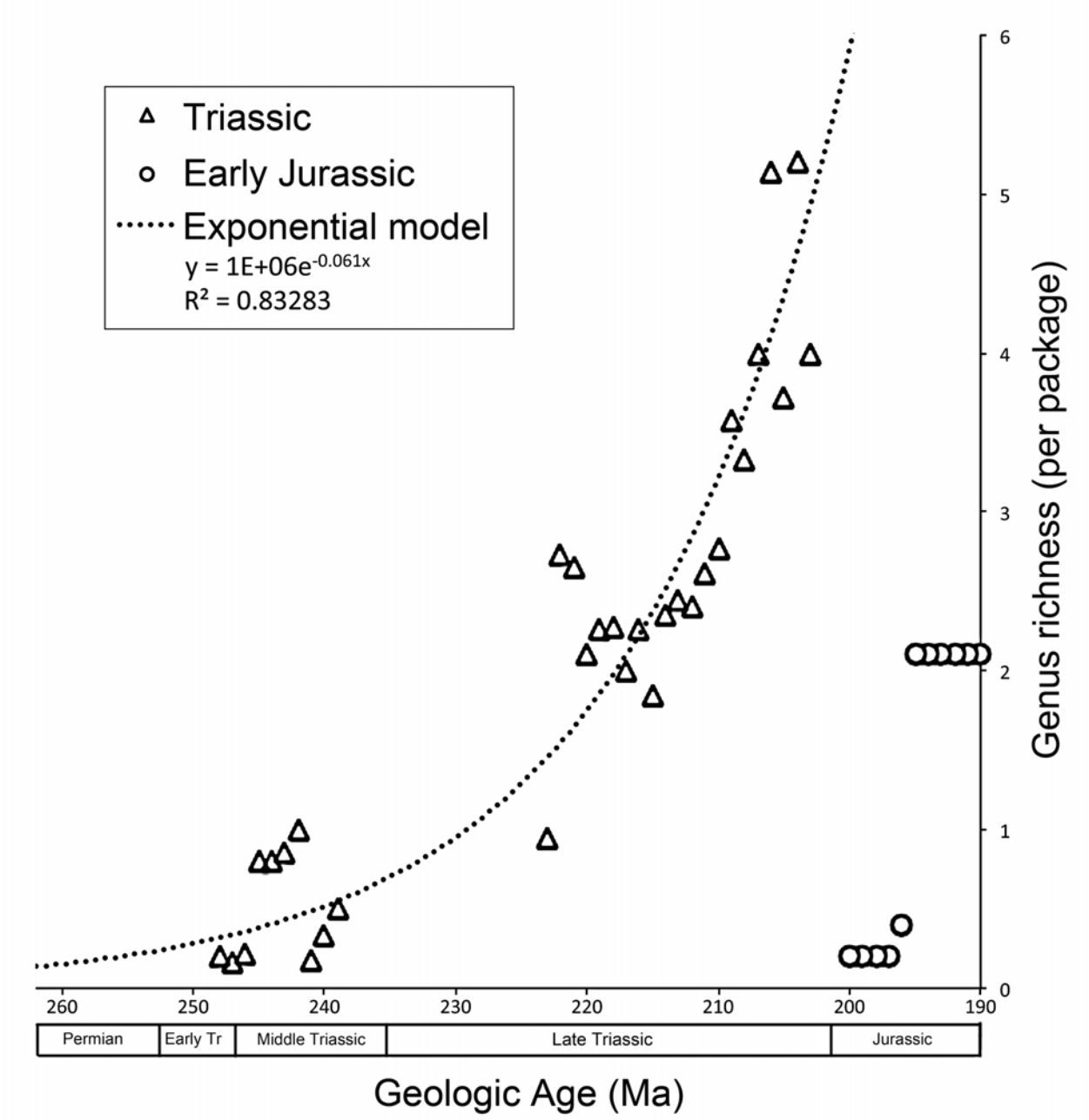

FIGURE 3.2—Exponential model of genus richness based on body fossils from the Triassic (triangles) and Early Jurassic (circles). The Early Jurassic data are not included in the model.

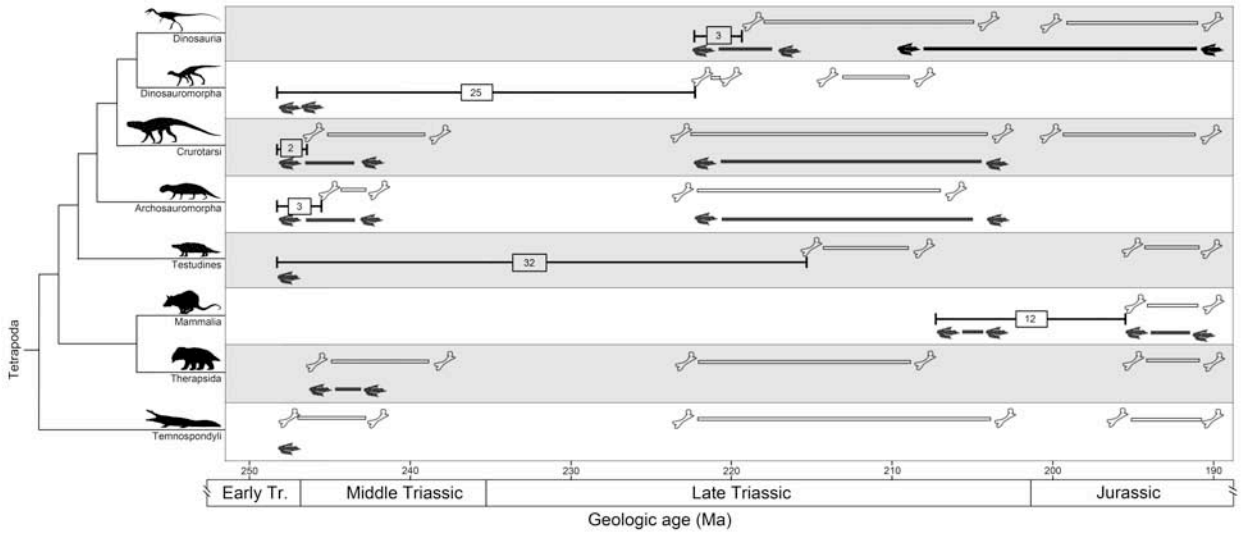

FIGURE 3.3—Phylogenetic distribution of track and body fossil ranges across the Triassic. Box plots show temporal disparities (million years) between the first track and first body fossil occurrence for each clade. Note that the majority of Early Triassic diversity is represented by ichnofossils.

CHAPTER 4

PALEOENVIRONMENTS AND PALEOECOLOGY OF AN EARLY TRIASSIC INVERTEBRATE AND VERTEBRATE ICHNOASSEMBLAGE FROM THE RED PEAK FORMATION (CHUGWATER GROUP), CENTRAL WYOMING

ABSTRACT

The Lower Triassic Red Peak Formation of the Chugwater Group has long been considered to have an extremely poor paleontological record, although the cause for the apparent dearth of fossils has yet to be been determined. During the course of fieldwork in central Wyoming numerous vertebrate and invertebrate ichnogenera ($n \geq 11$) were observed. Vertebrate tracks and trackways representative of dinosauromorph, archosaur, lepidosaur, and testudinate track makers were found (cf. *Rotodactylus*, *Chirotherium barthii*, *Rhynchosauroides*, and cf. *Chelonipus* respectively). An invertebrate ichnoassemblage composed of at least 6 ichnogenera consistent with the *Scoyenia* ichnofacies were also found (e.g., *Diplichnites*, *Lockeia*, *Fuersichnus communis*, *Palaeophycus striatus*, cf. *Scoyenia*, and cf. *Scolicia*). The majority of these tracks and traces were found in the upper platy facies (upper 10–20 m of the of the Red Peak Formation), which is thought to be no younger than late Spathian in age. Sedimentary structures, architectural elements, and lateral stratigraphic relationships support the interpretation of floodplain, fluvial, and lacustrine deposition for the upper platy facies in central Wyoming. The Red Peak Formation vertebrate and invertebrate ichnoassemblages, along with their associated depositional environments, are consistent with a fluviolacustrine (continental) setting comparable to those described from Lower to Middle Triassic strata with a Pangean distribution, including the Moenkopi Formation in the southwestern United States. This ichnoassemblage provides the first opportunity to

observe paleoecological diversity and associated paleoenvironments within the Lower Triassic of the Chugwater Group.

4.1 INTRODUCTION

Globally, rocks of Early to Middle Triassic age preserve evidence of biological recovery in the aftermath of the Permian-Triassic extinction and record the origination of many new clades of terrestrial vertebrates (e.g., the modern fauna sensu Langer et al., 2010), including stem–group turtles, lepidosaurs, archosaurs (crocodilians, dinosaurs, and birds), and stem–group mammals (Sereno, 1997; Rieppel and Reisz, 1999; Twitchert, 2006; Langer et al., 2010). Given the eventful history of this period and its paleontological significance, further studies that focus on the transition between Lower and Middle Triassic deposits are needed to better understand this important interval.

Strata that bound this time interval are often sought as a natural laboratory to test hypotheses regarding the timing of origins and evolutionary history of many clades (Demathieu, 1989; Rogers et al., 1993; Sereno, 1997; King and Benton, 1996; Langer et al., 2010; Brusatte et al., 2011). Body fossils are the principal data used to support or reject hypotheses of vertebrate evolution, but recent studies have demonstrated the utility of vertebrate tracks in addressing such issues as stance and gait evolution, dinosaur origins and diversification, and population structure where body fossils are unavailable (Avanzini and Lockley, 2002; Wilson, 2005; Marsicano et al., 2007; Kubo and Benton, 2009; Wilson et al., 2009; Brusatte et al., 2010; Padian et al., 2010). Vertebrate trace fossils are often preserved in a wide range of environments, some of which are not ideally situated for the preservation of body fossils, while others preserve both bone and tracks

together (Lockley et al., 1992, 1994; Lockley and Hunt, 1994; Lockley, 1998; Jennings and Hasiotis, 2006). Furthermore, invertebrate and vertebrate tracks and traces cannot be transported and, thus, represent evidence of direct interaction between organism and environment; these data can be used to advance paleoenvironmental reconstructions (Jennings and Hasiotis, 2006; Diedrich, 2008, 2009) and enhance our understanding of the spatiotemporal distribution of taxa (Hunt and Lucas, 2007a, 2007b; Avanzini and Mietto, 2008; Klein and Lucas, 2010).

Outcrops of the understudied Red Peak Formation (Chugwater Group) in central Wyoming were chosen to investigate the paleoecology and paleoenvironments across the Early Triassic–Middle Triassic transition along the northern mid-tropical latitudes of western Pangea. The dearth of fossils from these strata has been hypothesized to reflect harsh environmental conditions that limited habitable zones across this region (Cavaroc and Flores, 1991; Johnson, 1993a). A new invertebrate and vertebrate ichnological assemblage, however, was observed within the Lower Triassic Red Peak Formation, which demonstrates a strong paleoecological signal not captured by the body fossil record.

The new ichnological assemblage from the Early Triassic of Wyoming is herein reported. This assemblage extends the paleobiogeographic range of several vertebrate ichnogenera, including tracks interpreted as being made by dinosauromorphs, to the northern mid-tropical latitudes of western Pangea. Also reported are traces that share many affinities with known turtle trackways, thereby constituting some of the earliest evidence of this clade (e.g. Rühle von Liliestern, 1939; Haubold, 1971a).

4.2 GEOLOGICAL SETTING

4.2.1 Stratigraphy

Stratigraphy in the Rocky Mountain west (RMW) of the United States records passive margin marine-to-continental sedimentation throughout most of the Permian and Early through early-Middle Triassic along the western edge of the supercontinent Pangea (McKee et al., 1959; Blakey, 1974; Paull and Paull, 1983; Blakey et al., 1993). Even though uninterrupted intervals across the Permian-Triassic boundary are preserved in only a few areas (e.g. Goose Egg and Spearfish formations; Boyd and Maughan, 1972), Lower Triassic rocks are well represented throughout the RMW extending from the desert-southwest northward into southern Montana and western Idaho (Fig. 1).

The Chugwater Group (see Picard, 1978) in central Wyoming consists of four formations that span from Early Triassic (Deinerian) into the early-Late Triassic (Carnian; Fig. 2). The earliest Triassic rocks present in central Wyoming are Griesbachian in age and are represented by the conodont-rich Dinwoody Formation and the syndepositional continental Goose Egg Formation (Boyd and Maughan, 1972; Paull and Paull, 1983; 1994). The Red Peak Formation, the basal most formation in the Chugwater Group, conformably overlies the Dinwoody and Goose Egg formations, (High and Picard, 1967; Picard, 1967). The Red Peak Formation thickens westward from roughly 200 m in central Wyoming to 700 m in eastern Idaho (Picard, 1967; Pipiringos and O'Sullivan, 1978) and comprises the majority of rock volume in the Chugwater Group, which is thought to range in age from earliest Dienerian (Paull and Paull, 1983) to

late Spathian. The upper age limit of the Red Peak Formation is constrained by vertebrate paleontological interpretations of the Alcova Limestone (Storrs, 1991).

Though the Red Peak Formation of the Chugwater Group has been studied in some detail (High and Picard, 1967, Picard and High, 1964, 1968; Picard et al., 1969), there is little consensus regarding the nature of its depositional environments. Historically, the Red Peak Formation has been interpreted as a nearshore marine to tidal flat complex with little to no continental sedimentation (Picard, 1967; Picard et al., 1969; Johnson, 1993a). Often, laterally extensive beds have been used to support these interpretations (Picard, 1967; Picard et al., 1969; Johnson, 1993a), although there has been disagreement and such environments as sabkha and low-gradient coastal floodplains have been hypothesized for parts of the Red Peak Formation in east-central Wyoming (Cavaroc and Flores, 1991; Irmen and Vondra, 2000). Others have suggested, at least in part, that the Red Peak Formation represents coastal plain deposits that are intermixed with shallow marine and continental strata (Branson, 1947; Boyd and Loope, 1984).

Similar transitional marine-to-continental rocks of Early–Middle Triassic age are well exposed in the western United States (McKee et al., 1959). Of particular note is the Lower– to Middle Triassic Moenkopi Formation (McKee, 1954; Blakey, 1974).

4.2.2 Paleontology

The Moenkopi Formation has received much more attention than it's northern counterpart; it has a rich vertebrate body and trace fossil assemblage from Lower Triassic (Peabody, 1948; Mickelson et al., 2006a, 2006b) and Middle Triassic members (Welles, 1947; Peabody, 1948; Hunt et al., 1993; Nesbitt and Angielczyk, 2002; Lucas et al.,

2003; Heckert et al., 2005). In contrast no vertebrate body fossils have been reported from the Red Peak Formation.

In addition to a variety of environmental interpretations the Red Peak Formation is said to exhibit a perplexing dearth of fossils (Picard et al., 1969; Boyd and Loope, 1984; Johnson, 1993a; Irmen and Vondra, 2000) and is commonly thought to record little or no evidence of biological activity (Lull, 1942; Branson, 1947; Love, 1948; Picard, 1967); however, Johnson (1993a) speculated that the area should have been thriving with life but climatic and oxidizing conditions may have prevented body fossil preservation. Previous reports of fossil material consist of: one poorly preserved bivalve from the northern Wind River Basin, fish scales near Thermopolis, Wyoming, (not curated), one vertebrate track near Lysite (‘*Akropus’* = *Rhychosauroides*; site 10 of Fig. 1), two reports of tetrapod traces (site 8 of Fig. 1), and several occurrences of ‘worm burrows’ (Branson, 1947; Love, 1957; Picard, 1967; High and Picard, 1967; McLellan, 1968; Boyd and Loope, 1984; Carson, 1998).

Invertebrate trace fossils have not been formally described from the Red Peak Formation, although the presence of ‘burrows’ or ‘worm trails’ has been noted (Picard, 1967; Picard and High, 1967; Boyd and Loope, 1984; Johnson, 1993a). Lerner et al. (2007) critically evaluated the few reports of invertebrate ichnology for the Lower Triassic Moenkopi and Ankerah formations and described the occurrence of two ichnogenera new to the Moenkopi Formation ichnofauna: *Gordia* isp., and *Helminthopsis* isp. Others have described *Fuersichnus*, *Palaeophycus*, *Arenicolites*, and *Skolithos* (Mickelson et al., 2006a), as well as *Diplicnites* (Peabody, 1956), and *Kouphichnium* (Hamblin and Foster, 2000; Mickelson et al., 2006a), from the Moenkopi Formation.

Invertebrate trace fossils commonly occur with those of vertebrate tracks in the Moenkopi Formation (McKee, 1954; Peabody, 1956; Lerner et al., 2007); a similar association is seen within the Red Peak Formation ichnoassemblage as well.

R.S. Lull (1942) briefly described fossil footprints belonging to a reptile from the Red Peak Formation of central Wyoming. Soon after, Branson (1947) rediscovered the Lull's locality (not published by Lull) and figured tracks that represented Lull's ichnogenera *Eurichnus jenseni* (*nomen dubium*). Branson (1947) suggested it more closely resembled *Akropus* (Rühle von Lilienstern, 1939), which is now considered a junior synonym of *Rhynchosauroides* (Beasley in Maidwell, 1911). Unfortunately, the ichnogenus *Rhynchosauroides* is in need of taxonomic revision (Hunt and Lucas, 2007c). The only other report of vertebrate tracks from the Early-Middle Triassic of the Chugwater Group was a description of tetrapod swim traces from three localities (18, 30, and 70 m) below the Alcova Limestone (Boyd and Loope, 1984); the authors demonstrated the likely vertebrate origin of parallel 'sole marks' in several blocks. These 'sole makes' are strongly reminiscent of traces found in swim trackways near Vernal, UT (Peabody, 1956; Webb, 1980; Thomson and Lovelace, in review).

Vertebrate tracks assigned to the ichnogenera *Brachychirotherium*, *Capitosaurus*, *Chirotherium*, *Isochirotherium*, *Rhynchosauroides*, *Rotodactylus*, and *Synaptichnium*, have been reported from the Spathian aged Wupatki, Upper Red, and Torrey members of the Moenkopi Formation within Utah, Arizona and New Mexico (Peabody, 1948, 1956; McKee, 1954; Welles, 1969; Haubold, 1984; Morales, 1987; Mickelson et al., 2006a, 2006b). An additional ichnogenus, *Therapsipus*, is reported from the Holbrook Member of Anisian age (Hunt et al., 1993; Nesbitt and Angeilczyk, 2002).

4.3 METHODS

Trenched stratigraphic sections in the upper 30-40 m of Red Peak Formation were measured with a precision Jacob's staff. Colors were determined by comparisons with a Munsell soil chart (Munsell Color, 1988). Outcrops were walked out and all observed traces were photographed and catalogued with GPS coordinates captured by a Garmin eTrex device. Observed burrows were described in the field based on their architectural and surficial burrow morphology as well as burrow fill character; measurements of burrow diameter and lengths were made with a metric ruler. Where possible, invertebrate traces were collected and observed under plain light dissecting scope to better observe surficial burrow morphology and bioglyphs. Vertebrate traces and trackways were measured in the field with a standard metric ruler and photographed for further analysis in the lab. The original stratigraphic position of *ex situ* slabs was reconstructed where possible. Most specimens observed in the field were not collected. All collected vertebrate tracks were located on Bureau of Land Management lands (permit number PA09-WY-180) and are accessioned into collections at the University of Wisconsin-Madison Geology Museum (UWGM).

4.4 STRATIGRAPHY AND SEDIMENTOLOGY

The upper Red Peak Formation of the Chugwater Group is often divided into three facies (High and Picard, 1967; Picard, 1978; Johnson, 1993a): 1) alternating facies, 2) upper platy facies, and 3) sandy facies. To aid in comparison and avoid confusion with previous studies we continue to use this nomenclature, although we recognize the need for better descriptive terminology. Stratigraphic sections were measured in three

locations along Red Wall and one section at Red Hole (Fig. 3). Each measured section was initiated within the alternating facies, approximately 15 m below an apparent unconformity at the contact between the alternating facies and upper platy facies, where a change in lithologic character is clear. Measured sections were terminated at the upper contact of the Alcova Limestone and the basal sandstone of the Crow Mountain Formation.

The Alcova Limestone overlies the sandy facies and forms a prominent resistant ledge that serves as a useful datum for regional correlation. The Alcova Limestone is the only Early Triassic unit in the Chugwater Group from which vertebrate fossils have been reported; these fossils have provided the only reasonable age estimate for the underlying upper Red Peak Formation, which is likely no younger than latest Spathian (Storrs, 1991).

4.4.1 Alternating Facies of Red Peak Formation

Description.—The alternating facies is named for the repetitive muddy siltstone and silty mudstone elements typically seen in outcrop. This facies is represented by alternating units composed of 1–3-m-thick red (2.5YR4/2) calcite cemented muddy siltstone with poorly preserved bedding and sedimentary structures grading into a silty mudstone that frequently express evidence of subaerial exposure. The siltstone layers often appear massively bedded, but when sedimentary structures are present, they are expressed as faint ripple to climbing-ripple cross-laminations. The alternating siltstone-mudstone layers are laterally extensive (10^2–10^3 m) and the bases typically exhibit ghosted bedding and a heterogeneous distribution of clay, silt, and lower very fine-

grained sand grains; silt is the primary constituent (Fig 4A). The tops of most beds feature desiccation cracks, weak soil ped development, and rare rhizoliths and mangans (Figs. 4B–C).

Unidentified conchostracans (UWGM 1008) are locally present in a thin (< 5 cm) reduced, laminated mudstone interval with incipient mudcracks at the top of one alternation at Red Hole, ~15 m below the Alcova Limestone (Figs. 4D–E). The conchostracan-bearing gray mudstone is overlain by several muddy siltstone intervals containing thinly bedded gypsum layers and disturbed (brecciated) bedding prior to the last alteration, which expresses mottles, rhizoliths, and weak ped development immediately below the erosive contact with the basal sandstone of the upper platy facies.

Interpretation.—Previous interpretations suggest the alternating lithologies indicate a repetitive migration of the nearshore to tidal environment, or shallow-water accretion of reworked delta front sandstones (Picard, 1967; Caravoc and Flores, 1991). The alternating facies remains enigmatic, though we tentatively interpret this facies as distal fluvial-floodplain deposits on a low gradient coastal plain. Episodic high rates of sedimentation are indicated by the abundance of climbing-ripple cross-lamination and are thought to be the result of flood events from distant fluvial complexes; this similar to units described from the Early Permian of New Mexico (Mack et al., 2003). Deposition of each bed was followed by a period of incipient paleosol formation as evidenced by desiccation features, disturbed bedding, rare rhizoliths, and 1–2 cm blocky peds that exhibit mangans, which disrupt original bedding (Retallack, 1988; Mack et al., 2003). The discrete mudstone interval that contains the conchostracans and is overlain by several gypsum layers is thought to be from the same interval in which Picard (1967) identified

possible fish scales and likely represents a playa or local shallow lacustrine interval within this facies.

4.4.2 Upper Platy Facies of Red Peak Formation

Description.—The base of the upper platy facies consists of a laterally extensive (10^3–10^4 m) very-fine to fine grained red (2.5YR4/6) sandstone, which is incised (<2–3 m vertical relief) into an underlying muddy siltstone with medium-scale, blocky peds and mangan coatings. Gutter casts with a dominantly (present-day) east-to-west trend and abundant muddy silt rip up clasts are common along the erosive base of this sandstone (Fig. 4F). The coarsest grain sizes are upper fine, not including abundant intraformational silty mudstone rip-up clasts (0.5–3 cm).

The sandstone interval is composed of 2–5 m thick, laterally accreted barforms (Fig. 5A) with trough cross stratification at the base that transitions to upper flow regime planar cross stratification with prominent parting lineations and rare 1–2-m-long antidunes (Fig. 5B). The upper flow regime planar beds typically evolve to climbing ripples whose rates of climb decreases gradually over 50 cm and grades into multiple thinly bedded asymmetrically rippled sandstones with mud caps of variable thickness (Fig. 5B). These thinly bedded sandstones can be walked out perpendicular to the direction of flow for 10^1–10^2 m before they thin or are truncated; siltstone and mudstone content increases distally.

Multiple layers of thin (10–50 cm) very fine-grained sandstone capped by 0.5–2 m of silty mudstone to muddy siltstone comprise the majority of the upper platy facies (Fig 5C). The muddy interval typically exhibits either fine horizontal laminations and has

a platy nature, or it has disrupted bedding with blocky peds, argillan and mangan coatings, and rhizoliths (Soil Survey Staff 1999). The thin sandstones can often be traced for 10's of meters before they thin or are erosively truncated; the dominant sedimentary structures are asymmetrical rippled cross laminations, though some trough and upper flow planar cross stratification is seen in larger sandstone bodies. In addition, these thin sandstones preserve rare raindrop impressions, vertebrate and invertebrate tracks and burrows, rhizoliths, and mudcracks (Figs. 5D–E); track preservation occurs as both convex hyporelief and concave epirelief.

Interpretation.—The base of the upper platy facies is interpreted to be a fluvial complex dominated by laterally accreted barforms that transition vertically to crevasse-splay, lacustrine, and floodplain deposits. The presence of rhizoliths, evidence of clay and manganese illuviation, and faint depletion and accumulation zones suggest weak incipient pedogenic modification occurred. The scoured surface and contrasting lithology of the underlying alternating facies suggests an increase in depositional energy in the system, possibly associated with a steepening gradient from the flexure of the Moenkopi back bulge basin (Lawton, 1994) or the local Smithian–Spathian regression (Dubiel, 1994; Paull and Paull, 1994). Both hypotheses would account for decreased local stratigraphic base level and initiate incision and sediment bypass. Consequently, deposition of the upper platy and sandy facies may have initiated after relaxation of the back bulge or during late Spathian transgression (Pruss et al., 2005), either of which might have raised local stratigraphic base level.

4.4.3 Sandy Facies of Red Peak Formation

Description.—The sandy facies is characterized by 2–5 m thick fine-grained grayish orange pink (5Y 7/2) sandstone that is often massive or structureless (Picard, 1967; Johnson, 1993a; Irmen and Vondra, 2000; Fig. 5F); remnant small-scale trough cross stratification, planar-tabular cross stratification, and ripple cross-lamination are rare. The contact is conformable with the underlying upper platy facies and in the Red Wall sections the base consists of a 20–30 cm thick muddy, very fine-grained sandstone with disturbed bedding, prominent desiccation cracks, and large vertebrate tracks (Figs. 5F–I). The 20–30 cm basal sandstone is capped by a thin (5 cm) green-grey (color) silty mudstone that shows some distinct fine scale horizontal to wavy laminations (Fig. 5H). The upper few meters of the facies is more characteristic of its regional expression: disturbed very-fine grained sandstone with Liesegang banding, faint planar-tabular cross stratification, and ripple cross laminations.

The contact with the overlying Alcova Limestone is sharp, though locally a 10–20 cm fining upward alternation of mm-scale horizontally laminated silty sandstone, siltstone and silty limestone can be seen before they grade into 1–2 m of stromatolitic to laminated limestone. The base of this unit, however, more commonly exhibits an undulating surface with small-scale (1–2 m wide, 10–30 cm deep) lenticular beds that pinch or grade laterally into the overlying horizontal limestone beds (see Carini, 1964; Storrs, 1991).

Interpretation.—The sandy facies characteristically displays colorful Liesegang banding that often obscures faint original bedding surfaces. Difficulty discerning bounding surfaces and sedimentary structure makes interpretation difficult, though the presence of a conformable contact with underlying floodplain deposits, desiccation

cracks, vertebrate tracks, and sedimentary structures (where visible) are suggestive of continued low-energy fluvial or floodplain deposition. The upper portion of the facies exhibits dominantly low angle small-scale trough cross stratification and lower flow regime planar beds that may indicate marine reworking of original fluvial sediments during the late Spathian transgression; this is consistent with other regional observations (Paull and Paull, 1983, 1994; Dubiel, 1994). Caravoc and Flores (1991) discuss evidence of pedogenic processes at the top of this unit further to the east. The Liesegang banding and destruction of original bedding may be the result of fluid migration along base of the Alcova Limestone (Cavaroc and Flores, 1991; Picard, 1993; Irmen and Vondra, 2000).

4.5 ICHNOLOGY

4.5.1 Invertebrate Ichnology

Seven morphologies of invertebrate traces were observed in the Red Peak Formation. The seven morphotypes, presented below, represent the first formal description of the ichnology of Lower Triassic strata in Wyoming.

4.5.1.1 Morphotype I

Description.—The first form exhibits two parallel rows of small, linear to curved tracks, which deflect approximately 45º from the 5 mm wide trail; no medial grooves or impressions were observed. There is a single to double appearance of the parallel rows as the tracks overlap in multiple sets of 6–9 tracks per set (Fig 6A). One slab was collected (UWGM 1000) that contains at least 5 trackways that cross one another and are preserved in convex hyporelief.

Remarks.—The morphology displayed by the Red Peak Formation specimen is consistent with traces observed from the Early Triassic of the Karoo Basin and the Moenkopi Formation, which are interpreted to be arthropod trackways that belong to the ichnogenus *Diplichnites* (Peabody, 1956; Lerner et al., 2007). Others have also reported the occurrence of this ichnogenus in continental deposits of Triassic age (Bromley and Asgaard, 1979; Lucas et al., 2006; Melchor et al., 2006). Melchor et al. (2006) describe rare occurrences of *Diplichnites* from Middle Triassic floodplain deposits of Argentina; their morphology compares well with the Red Peak specimens from similar depositional settings. We refer this morphology to *Diplichnites* isp.

4.5.1.2 Morphotype II

Description.—The second form exhibits a short bilobate structure that is preserved in a very fine grained sandstone in convex hyporelief with examples ranging in size from 6–10 mm long, 4–7 mm wide, and 3–4 cm deep. The traces are bilaterally symmetrical, have gently rounded ends along the long axis, and feature a narrow median furrow; lobes express either weak or absent striae (Fig. 6B; UWGM 997). The morphology grossly resembles a small coffee bean and is found without obvious trails leading to or from the structures.

Remarks.—The bilobate morphology, median furrow, and symmetry are consistent with previous interpretations of bivalve resting traces, e.g. *Lockeia* (Lucas and Lerner, 2006). Most specimens are slightly distorted, which likely occurred during sediment compaction. The preservation of surficial morphology (Hasiotis and Mitchell, 1993) or bioglyphs (sensu Ekdale and Gilbert, 2010), such as scratch marks running

oblique to the median furrow, are rare and weakly expressed where present; this may suggest poor preservation in a soft medium incapable of capturing fine impressions (Ekdale and Gilbert, 2010).

The limited number of specimens and the quality of preservation hinders confident taxonomic identification. Traces with morphologies grossly similar to morphotype II include *Rusophycus*, *Pelecypodichnus*, *Lockeia*, and resting traces cf. *Isopodichnus* all of which have been reported from the Triassic (McKee, 1954; Bromley and Asgaard, 1979; MacNaughton and Pickerill, 1995; Buatois and Mángano, 1998; Hasiotis, 2002; Melchor et al., 2006; Lucas and Lerner, 2006). *Pelecypodichnus* and *Lockeia* are typically almond-shaped (Lucas and Lerner, 2006), and bivalves often leave an impression of their foot expressed as a midline ridge rather than furrow (e.g., Pryor, 1967), however, medium composition and competency may preclude preservation of foot expression. The presence of oblique striae, symmetry, and association with other aquatic traces lends support to the assignment of morphotype II to the ichnogenus *Lockeia*.

4.5.1.3 Morphotype III

Description.—The third morphotype is always seen in convex hyporelief on the soles of thin (2–5 cm) very-fine grained sandstone that typically overlay platy silty mudstone that preserve mudcracks and expresses a retrusive burrow complex; traces do not crosscut mudcracks. This morphotype is commonly found above the basal sand of the upper platy facies and below the sandy facies in sections ARM, BCR, and RLH (Fig. 3A). The burrow complex is composed of a multiple horizontal and subhorizontal U or J-shaped burrows 5–10 mm in diameter with associated spreite-like structures. Spreiten

never appear to be well organized (*sensu* Bromley and Asgaard, 1979) and commonly resemble stacks of conterminous, curvilinear tubes or occur as overlapping to isolated curved burrows that express weak backfilling (Fig. 6C; UWGM 999). Small lacertoid vertebrate tracks are often observed in close association, typically on the top surfaces of sandstones that preserve this morphotype.

Remarks.—Morphotype III strongly resembles the ichnospecies *Fuersichnus communis* reported from Middle Triassic lacustrine sediments of Greenland (Clemmenson, 1978; Bromely and Asgaard; 1979). Mickleson et al (2006a) reported *Fuersichnus* from the Moenkopi Formation, however Lerner et al., (2007) rejected this assignment and referred it to cf. *Lockeia* because of close resemblance to this more commonly occurring ichnogenera and similar associations with *Palaeophycus* (e.g. Lucas and Lerner, 2006). *Fuersichnus* has also been described from similar environments in the Upper Triassic Chinle and Upper Jurassic Morrison formations (Hasiotis, 2002, 2004). Although there is some disagreement regarding the assignment of the traces in question (Mickelson et al., 2006a, fig. 8), we suggest *Fuersichnus communis* occurs in the Red Peak Formation ichnoassemblage, commonly in association with vertebrate tracks. *Fuersichnus* has not been observed to co-occur with *Palaeophycus*, though both ichnogenera are well represented in slightly different depositional settings within the upper platy facies.

4.5.1.4 Morphotype IV

Description.—The fourth morphotype is always found in convex hyporelief on the soles of moderately thick (10–20 cm), very fine-grained sandstone beds with small-

scale trough cross stratification. The forms are 5–10 mm wide and show rare, weakly developed striae (intermittent where present) parallel to elongated cylindrical structures with fill material indistinguishable from the surrounding matrix that occasionally express lined burrows (Fig. 6D). The burrows are often found occurring in a roughly parallel orientation; associated traces show rounded terminations (Fig. 6D inset), interpenetration, subhorizontal forms, and most commonly contrast with surrounding sediment due to a reduced color.

Remarks.—Morphology III is characteristic of the long-ranging, facies-crossing, ichnogenera *Palaeophycus* and *Planolites* (Alpert, 1975; Pemberton and Frey, 1982; Lucas and Lerner, 2006; Mickelson et al., 2006a). McKee (1954, pl 12B) figured several "worm trails" from the Moenkopi Formation, which Lerner et al. (2007) thought might belong to *Palaeophycus*.

Based on the characteristics listed above and similarity to other reported specimens (Lucas et al., 2006, Lucas and Lerner, 2006) morphotype IV is tentatively assigned to *Palaeophycus striatus*, although the rare presence of line burrows cannot preclude a possible assignment to *Planolites striatus* (see Pemberton and Frey, 1982).

4.5.1.5 Morphotype V

Description.—The fifth morphotype is less common than the previous two morphotypes and is generally found in very fine-grained sandstone bodies, which express trough cross stratification that grades into ripple cross-laminated bedding. The burrows exhibit a 7–10 mm diameter vertical to subvertical shaft with small-scale oblique and longitudinal scratch marks adorning some wall surfaces (Fig. 6E). The burrows exhibit

differential weathering, which is dominantly expressed in cross section as concave epirelief; the burrow fill is often absent when exposed (Fig. 6E). The top of the sandstone containing this trace morphotype is truncated and the burrow entrance is not preserved.

Remarks.—The presence of such surficial morphology or bioglyphs as oblique and longitudinal scratch marks along the length of the burrow wall, size, and length are similar to those seen in *Scoyenia* and *Ancorichnus*; however, they lack any distinct meniscate structures due to poor preservation. Traces similar to this morphology have been inferred to belong to a beetle (Hasiotis, 2002). Burrows of both *Scoyenia* and *Ancorichnus* can either be actively or passively filled and may exhibit scratch marks along the burrow wall (Hasiotis, 2002). Due to poor preservation and rarity, it is difficult to confidently assign this morphotype to an ichnotaxon because of the overlap of burrow morphology with multiple ichnotaxa, however it lacks strong chevron shaped backfill suggesting a closer affinity to *Scoyenia* than *Ancorichnus*. The designation of morphotype V is tentatively assigned to the ichnogenus cf. *Scoyenia*.

4.5.1.6 Morphotype VI

Description.—The sixth morphotype consists of a horizontal trail with slightly raised lateral edges and a relatively smooth curved central canal. These are preserved in concave epirelief on the upper surfaces of planar and ripple cross-laminated, very fine-grained sandstones that sometimes feature small lacertoid vertebrate tracks (Fig. 6F). The trails vary from slightly sinusoidal to irregular, maintain a consistent width (3–5 mm), and can be up to 12 cm long.

Remarks.—This morphology is consistent with traces that been interpreted to as gastropod feeding and locomotion trails; this morphology is similar to modern gastropods observed in fluvial sediments and is assigned to the ichnogenus cf. *Scolicia* (Pryor, 1967, Turner, 1978; Hasiotis, 2002). Sediment bulldozing is inferred from the raised ridges observed on the lateral edges of trails, which is consistent with gastropod traces observed in actualistic sedimentology experiments (Baldwin, 1974). The ichnogenus *Scolicia* is typically observed in marine sediments, but its presence in fluvial, palustrine, and lacustrine settings has been noted (Turner, 1978; Hasiotis, 2002, 2004, 2008).

4.5.1.7 Morphotype VII

Description.—The seventh morphotype was only observed once in the Red Peak Formation. This morphotype consists of irregularly paired 2.5–4 mm pustules along the length of the 10 cm horizontal trace (Fig. 6G). Several isolated pustules are observed on the same slab.

Remarks.—Morphotype VII is considered *incertae sedis*, although it is reminiscent of traces reportedly associated with horizontal burrows of some spiders (Hasiotis, 2002: pg. 114), but may belong to another arthropod tracemaker (Melchor et al., 2006). Although this specimen was not found *in situ* it is constrained to an interval immediately above the basal fluvial complex in the upper platy facies and likely represents saturated floodplain deposits. This specimen is quite similar to the hypichnial bilobed ridge trace reported by Melchor et al. (2006).

4.5.2 Vertebrate Ichnology

4.5.2.1 Morphotype VIII

Description.—The most abundant tracks in the Red Peak Formation belong to morphotype VIII (Fig. 7). This morphotype is found throughout the upper platy facies (n ≥ 140 slabs with multiple tracks of morphotype VIII were observed or collected: UWGM 984, 985, 987, 988, 990, 992, 996, 998, 1001-1005, 1009, 1011, 1012). Tracks of this morphology characteristically display a pentadactyl digitigrade to semiplantigrade pes with an increasing digit length from I–IV and an interdigital divarication around 30˚ between each digit from I to IV (Fig. 7A). Digit V is much shorter than IV and exhibits a 70–90˚ interdigital divarication (Fig. 7A). Digits terminate in fine claw impressions. Some tracks, consistent with this morphology, only display the distal most portions of the digit or claw impression. This expression is often found in association with fine mm-scale desiccation cracks on thin (1–2 mm) mud laminae capping the underlying very fine-grained sandstone, which preserve the track impressions. Larger desiccation cracks are also seen to cross cut trampled surfaces (e.g. Fig. 7G)

The semiplantigrade manus is typically overstepped by the pes and possesses slightly shorter digits with a digit V perpendicular to digit IV (Figs. 7B–C, F). The pes length of greater than 75% of morphology VIII tracks are around 2.5 cm, with less than 10% in the 1.5 cm size range and only a few isolated specimens that were larger than 4 cm with a maximum size of 5.5 cm.

Remarks.—This morphology is attributable to the ichnogenus *Rhynchosauroides*. This identification is not surprising as this ichnogenus has a global distribution and is one of the more prevalent vertebrate tracks within the Lower-Middle Triassic rocks of Europe (Avanzini, 2000; Diedrich, 2002, 2008; Valdiserri and Avanzini, 2007; Avanzini and Mietto, 2008;) and North America (Peabody, 1948, 1956; Mickelson et al., 2006a, 2006b;

Hunt and Lucas, 2007). *Rhynchosauroides* tracks from the Germanic basin are dominantly found in what has been interpreted as a carbonate tidal flat where microbial mats enable the preservation of tracks through increased cohesion, early cementation, and low-energy deposition (Riding, 2000; Diedrich, 2009; Cuadrado et al., 2011). In contrast, tracks from the Red Peak vertebrate assemblages are almost exclusively found on fluvial bar-tops, the tops of crevasse splays, and as preserved casts and transmitted tracks on the undersides of very fine-grained splay sands.

In most instances, individual trackways are not present or difficult to discern due either to isolation of single manus and pes tracks in small slabs or trampled surfaces where the number of overlapping tracks increases the likelihood of misidentifying track associations (Figs. 7D–E). Individual trackways are sometimes distinct and often preserve sinusoidal tail drags along the midline of the trackway. In Figure 7F a tail drag is visible and the trackway exhibits a pace angle slightly less than 90˚, which is consistent with previous descriptions inferred to be slow walking movement within this ichnotaxon (Diedrich, 2008).

4.5.2.2 Morphotype IX

Description.—This morphology was observed at four localities within the field area. Tracks are preserved in convex hyporelief on the soles of very fine-grained sandstone that is incised into a pedogenically modified muddy siltstone. The Trampled-by-Turtle (TBT) tracksite from Red Hole (Fig. 3) preserves the best record of this morphology (Figs. 7A–E); no specimens were collected but a latex mold (UWGM 1013) was taken of the largest slab.

The footprints vary in length (1–3 cm) and width (2–5 cm), exhibit tridactyle to pentidactyle footprints whose digits face anteriorly with little interdigital divarication, and terminate in distinct triangular claw impressions of nearly equal size (Fig. 8A). The digit lengths do not vary greatly, however, digit III is the longest with slightly shorter but equal length digits II and IV; digits I and V are the shortest. All digits are connected by an arched structure that penetrated the substrate slightly less than the claw impressions (Fig. 8C). In some instances the claw impressions of digits II-IV extend into 3 parallel scratch marks that can extend anteriorly several times the footprint length (Figs. 8A, B, D).

There are few sets of successive footprints that display identifiable trackways with paired pedal and manual impressions (Fig. 8A). The manus print displays 3–4 distinct digits connected by a slightly arching structure and the digits are roughly parallel and face anteriorly; the tracks are typically digitigrade, though some semiplantigrade prints are visible (Figs. 8D, E). The pes prints are typically digitigrade with 3–4 distinct claw impressions.

Remarks.—This morphology is relatively rare in the study area, although they are well represented at the TBT tracksite. The presence of parallel digits of comparable length, low to absent interdigital divarication, digits connected by a slightly arched structure, and low pace angle all compare favorably to the ichnogenus *Chelonipus* from the Early Triassic and Late Jurassic (Rühle von Liliestern, 1939; Avanzini et al., 2005). Morphology VII is assigned to the ichnogenus cf. *Chelonipus*.

This morphology, also described from the Mesozoic of the western USA (Lockley and Foster, 2006), contrasts with the more common tracks of morphotype VIII. Morphotype VIII expresses a 30˚ interdigital divarication and an increasing digit length from I–IV, and a digit V that is shorter with a nearly 90˚ interdigital divarication between IV and V; this is markedly different than the nearly absent interdigital divarication seen in morphotype IX. The long parallel scratches are interpreted as evidence of partially to fully buoyant trackmaker that swam along the bottom of the water-filled channel (Milner et al., 2006; Michelson et al., 2006a). This interpretation is consistent with actualistic ichnologic observations of ecologically diverse extant turtle species that interacted with variable substrate and saturation conditions (Rühle von Liliestern, 1939; Foster et al., 1999; Avanzini et al., 2005). Diedrich (2005) conducted similar actualistic studies using iguanas as an analog for lacertoid trackmakers; the lacertoid tracks are notably dissimilar to morphology IX.

Some tracks display pull-up features that incorporate muddy siltstone with overlying sand deposits suggesting that trackmakers continued to inhabit the channel during deposition; at least some tracks represent transmitted undertracks. The TBT tracksite assemblage is likely time-averaged (*sensu* Falkingham et al., 2011). Lack of desiccation features and the presence of slide marks, pull-up features, and swim traces indicate that the trackmakers inhabited the waters before and after flow ebbed and as sediment was deposited, thereby preserving the muddy track-bearing surface as well as transmitted traces.

The 30 cm thick very fine-grained sandstone lens that preserves the tracks as convex hyporelief thins to 2–5 cm platy rippled sandstone interbedded with muddy

siltstone within the span of 8 m. The sandstone fills a shallow lenticular cut into underlying thinly layered muddy siltstone with mm-scale tapering rhizoliths that cap a very fine-grained sandstone with rapidly decreasing silt content. Less than 1 m north, the layer thickens and then thins northwards for several meters where it is truncated by another cut-and-fill deposit similar to that which preserves the tracksite. The original slab observed by Carson (1998) matches a section of exposed sandstone closest to the deepest part of the cut-and-fill deposit. Trackways from this slab display morphologies consistent with increased trackmaker buoyancy towards the deepest part of the channel; tracks transition from rounded traces with apparent deformation rims to long parallel scratch marks (Fig. 8B). Two meters lateral of the channel tracks made by a much larger animal exhibit characteristic swim traces such as kick off scours and z-traces (*sensu* Thomson and Lovelace, in review). These are likely chirotheroid traces, but definitive taxonomic identity is obscured by extramorphological distortion. *Chelonipus* tracks are best-expressed 3–4 meters from the thickest part of the incised channel.

4.5.2.3 Morphotype X

Description.—The second most abundant vertebrate tracks belong to morphotype X and are typically found as individual prints, paired manus-pes prints, and as partial prints or claw impressions on the soles of crevasse splays and channel barforms. This morphotype is most commonly found in the sandy facies within 1–3 m of the Alcova Limestone (Figs. 9A–C), although the best-preserved specimens are found in the underlying upper platy facies (Figs. 10–11; collected specimens include UWGM 979-982, 991, 993, 1006). The pes illustrated in Figure 10A is characterized by a print that is longer than wide with digit III being only slightly longer and more robust than digit II.

Digit I is shorter and much less robust than the more prominent digits II–IV. Interdigital divarication between digits I–III is lower (10–15º) than between digits III–IV (15-20º) or digits IV–V (25–30º). The total divarication between I and V is typically < 90º. Digit V curves outward at the distal end forming a rounded posterolateral hook and does not appear to terminate in a claw, unlike digits I–IV, each of which exhibit a wide subtriangular claw (Fig. 10B). Skin impressions are rare and have only been observed in this morphotype (Figs. 10B–C). When skin impressions are present, they are found on the phalangeal pads and display small rounded scales on the base as well as long parallel scratches on the sides of the print where scales pushed through or slid along the sediment interface (Fig. 10D).

The digitigrade manus is approximately one-third the surface area of the pes, typically exhibits the first four digits, and rarely displays digit IV (Fig. 10E). In most circumstances where paired manus-pes prints are preserved the manus is found anterior of digit III of the pes; the distance between manus and pes varies between 3 cm–10 cm. Digits II–IV are the most prominent, digit I is small, and digit V is often absent or represented by shallow impressions in the print where it appears to be similar to the length and width of digit IV. Claw impressions are prominent on digits II–IV where they are expressed as small triangular wedges at the distal end of the phalangeal pads (Fig. 10F). Skin impressions are less common in manus than in pes, but parallel scratch marks on the vertical sides of prints are present in some manus specimens.

Only one specimen was collected (UWGM 980; Fig. 11A) that displays an identifiable trackway. Most slabs observed in the field only preserve isolated prints or single manus-pes pairs. UWGM 980 exhibits one manus-pes pair and the following pes

print. An isolated manus was found in a small weathered block very nearby and is likely paired with the forward most pes. The pes is 17.2 cm long and 11.2 cm wide.

Remarks.—The trackway UWGM 980 best exemplifies this morphotype and is characteristic of the chirotheriod tracks from the Early and Middle Triassic of North America and Europe (Peabody, 1948, 1956; Avanzini and Lockley, 2002; Demathieu and Demathieu, 2004; Klein and Lucas, 2010). The glenoacetabular length is 1 m, and the stride length is 90 cm, based on the limited sample size the external trackway width is estimated to be 30 cm (Figs. 11B–C). The pedal morphology, trackway width, and stride is consistent with the ichnogenera *Chirotherium barthii* (Kaup, 1835); the pes is longer than wide, digit IV is slightly shorter than III, low angle interdigital divarication, and posterolaterally hooked distal digit V that lacks a claw impression. Fitchner and Kunz (2004) tested the stability of the many chirotheroid ichnogenera through the comparisons of reduced vs. dominant pedal digits (e.g. *Chirotherium* 3>2>1 dominant; 5>1 reduced); they suggest that the type morphology of *Chirotherium barthii* was a relatively stable ichnospecies.

The most abundant tracks in the sandy facies are referable to morphotype X, although extramorphologic features such as displacement rims obscure the true morphology and limit taxonomic assignment to *Chirotherium* isp. This assignment is largely based on the relative length of digits, size, and width to length ratio of the pes.

4.5.2.4 Morphotype XI

Description.—The eleventh morphotype was observed on three consecutive *in situ* slabs containing several pes prints (Figs. 12A–B; UWGM 1014–1015). The tracks

exhibit a long digit IV (2.5 cm) with a successively smaller III–II. Digit V is not visible on any track and digit I is poorly preserved in only a few tracks. Several tracks overlap the edges of the slab; the presence-absence of this digit cannot be confirmed. Digit I is reduced and only lightly impressed relative to II–IV. Proximally, the digits are parallel to one another and form a straight to slightly angular posterior margin. Interdigital divarication between digits I–IV is negligible and claw impressions are skewed mediolaterally.

Remarks.—This morphology is rare in the field area and consists of only six independent tracks (none appear to belong to a discrete trackway). Similar tracks have been reported from the Moenkopi Formation of the western US and from the Lower-Middle Triassic of Europe (Peabody, 1948; Demathieu and Gand, 1973; Avanzini and Mietto, 2008; Brussatte et al., 2010). The extremely low interdigital divarication between digits I-IV, absence of metatarsal impressions, and a reduction of digits V and I are consistent with a tightly bound foot; these are synapomorphic characters of dinosauromorphs. Tracks that show strong dinosauromorph affinities from the Early-Middle Triassic include *Rotodactylus* and *Protodactylus* (e.g., Brussatte et al. 2010; Fig. 12C). The small sample size and incomplete trackway make taxonomic assignment tentative. Given the similarity of the ichnoassemblages from the Red Peak and the Moenkopi and the dinosauromorph affinities, this morphotype is assigned to the ichnogenus cf. *Rotodactylus*.

4.5.3 Locality Information

Invertebrate ichnology—At a location near the ARM measured section (Fig. 3), about 10 m below the Alcova Limestone, morphotypes I–II were observed in a very fine-grained sandstone with ripple cross laminations bound above and below by 10–20 cm thick wavy bedded, muddy siltstone. This was the only observed occurrence of morphotypes I–II. Morphotypes III–IV were observed in each measured section and appear to be characteristic of the assemblage as a whole. Morphotype V was seen in all measured sections except ARM. Morphotypes III–V are commonly found on the soles of fluvial sandstones, cut and fill structures, and what are interpreted to be crevasse splays. Morphotype VI was observed at all but the RLH locality. Only one occurrence of morphotype VII was observed in an isolated slab; stratigraphic position could not be adequately determined, although the overall depositional setting is identical to that of morphotype III–V.

Vertebrate ichnology—Four vertebrate morphotypes are recognized in the Red Peak Formation of central Wyoming. Morphotypes VIII–X were found across the study area, while morphotype XI was only observed in the ARM section (Fig. 3). All morphotypes were found in the upper platy facies; only morphotype X was also observed in the overlying sandy facies.

4.6 DISCUSSION

4.6.1 Sedimentology

There are several notable differences in sedimentology between the alternating facies and the upper platy facies in central Wyoming that suggest environmental factors are responsible for the paleoecological disparity between these two facies. The alternating

facies differs in some aspects between the Red Hole locality (TBT) and those from the southern Big Horn Mountains (ARM, BCR, RLH of Fig 3). All four areas, however, contain several muddy-siltstone intervals interpreted as low-gradient floodplain deposits that received periodic influxes of fine-grained sediment during flood events from distant fluvial systems. All four also exhibit pedogenic features such as blocky peds, mangans, and rare rhizoliths; these structures along with such subaerial features as desiccation cracks often disrupt original bedding within this facies. These beds have traditionally been interpreted to be alternations of near-shore to tidal flat complexes (Picard and High, 1963; High and Picard, 1967; Picard, 1967).

In addition to the aforementioned floodplain deposits, the Red Hole locality also preserves conchostracan bearing beds that are interpreted to be playa or shallow lacustrine deposits; conchostracans (extant and fossil) are known from alkaline inland ponds, ephemeral freshwater lakes, and coastal floodplains further supporting this interpretation (Webb, 1979; Kozur and Weems, 2010). At this locality thin gypsum lenses, disturbed (brecciated) beds, and desiccation cracks are present above and below the conchostracan bearing bed are also consistent with ephemeral alkaline lake conditions (McKee, 1954; Dunagan and Driese, 1999; Mack, et al., 2003). Sedimentologic indicators of semiarid conditions (Hubert and Hyde, 1982; Mack et al., 2003) accompanied by a lack of body fossils and trace fossils limited to rare rhizoliths suggest the paleoenvironments of the alternating facies may have been unfavorable to more than a restricted flora and fauna as suggested by Johnson (1993). More likely the limited flora and fauna within this stratigraphic interval reflect the unusually high sedimentation rates

consistent with sedimentary features (abundant climbing ripples) and coincident with the maximum rate of sediment accumulation in the Triassic of the western US (Chapter 2).

In contrast, the upper platy facies erosively overlies the alternating facies across central Wyoming and displays a more diverse paleoecology. The erosional surface is most obvious at the BCR locality where there is up to 3 m of relief locally. Steiner et al. (1993) proposed the presence of an unconformity representing a period of nondeposition and erosion during the Smithian-early Spathian in the eastern portions of the Moenkopi and Chugwater depositional basins based on magnetostratigraphic reconstructions. They did not observe field evidence for the hiatus and suggested more observations were needed to test this hypothesis. The unconformable surface between the alternating facies and the upper platy facies may represent the Smithian–early Spathian hiatus (Fig. 2). Further study is needed to determine the duration of the hiatus and to locate the potential basinward correlative conformity.

Global sea level underwent an overall fall in the Early Triassic (Haq et al., 1987) and is clearly expressed regionally (McKee, 1954; Dubiel, 1994; Goodspeed and Lucas, 2007). The proposed unconformity may be related to the regressive surface associated with the termination of Sinbad Member deposition in the eastern most part of the Moenkopi basin; carbonates of the Sinbad Member are overlain by progradational delta deposits of the Torrey Member of the Moenkopi Formation (Blakey 1974; Mickelson, 2006a; Goodspeed and Lucas, 2007). Local sea-level rise is recorded during the mid-late Spathian by the onlap of the Virgin Limestone and upper Thaynes Formation across much of the western Moenkopi basin; the upper units of the Virgin Limestone and Thaynes Formation are thought to correlate with the Alcova Limestone (Reeside et al.,

1957; Picard et al., 1969; Pruss et al., 2005). This suggests the upper platy facies may be equivalent with the upper Torrey Member, whose vertebrate ichnodiversity is consistent with that reported in this study (Peabody, 1948; Mickelson, 2006a).

Within the Red Hole and Red Wall field areas the upper platy facies is interpreted to consist principally of fluvial and proximal floodplain deposits. The grain size distribution within the upper platy facies ranges from clay to upper very fine. The fine-grained nature of the fluvial deposits is suggestive of a low gradient floodplain characterized by downstream fining with little to no coarse material available for transport and may represent the distal reach of the fluvial system. The fine nature of these deposits, however, may reflect a fine-grained source material, such as the source areas for silty loessites from the Lower Permian Eagle basin of northern Colorado and the upper Permian Phosphoria Formation (Soreghan, 1992; Johnson, 1993b; Carroll et al., 1998). There were few identifiable ichnofossils observed in the dominantly fluvial component of the upper platy facies, only poorly preserved trace fossils attributed to swimming tetrapods (Thomson and Lovelace, in review). Floodplain deposits lateral to the channels, however, commonly contain both vertebrate and invertebrate trace fossils.

Upper platy facies strata above the basal sandstone are characteristic of proximal floodplain deposits (e.g., Mack et al., 2003) and consist of weakly developed paleosols, abundant crevasse splays, shallow lacustrine and small-scale fluvial deposits; all eleven ichnologic morphotypes were observed in these beds. Fine-grained, laminated mudstone and interbedded thin very-fine-grained sandstone lenses containing small laminated mudstone rip-up clasts were observed at the ARM section and are interpreted to be subaqueous deposits that received periodic courser clastic input, likely during storm or

flood events. Traces associated with this interval are characteristic of hydrophilic to shallow-water fauna (Hasiotis, 2004, 2007, 2008), although, the sample size is small (2 ichnogenera; morphotype I–II). Unlike the TBT lacustrine bed within the alternating facies, the ARM interval does not contain evaporites, brecciated sediments, or carbonates; it is thought to reflect non-alkaline freshwater shallow lacustrine environments within the floodplain.

The majority of the ichnoassemblage is associated with fluvial, crevasse-splay, and floodplain deposits. Distal floodplain sediments display evidence of pedogenic modification including small-scale rhizoliths (1–5 mm); no other discernable traces were observed. Splay deposits lateral to the fluvial complex preserve the most ichnodiversity, including all four vertebrate ichnogenera (morphotypes VIII–XI). There is an apparent paleoecological distribution of invertebrate ichnotaxa. The distal edges of crevasse splays are characterized by thin ripple marked to planar-laminated (1–10 cm) sandstone beds, which commonly preserve morphotype III (on bar soles) and morphotype VI and VII (on bar tops). Morphotypes IV–V are commonly preserved on the soles of thick trough cross-laminated sandstone bodies (10–30 cm) associated with proximal crevasse splays, small-scale fluvial, and channel bar deposits. All seven invertebrate ichnogenera are associated with hygrophilic to hydrophilic conditions suggesting they are restricted to near-channel or specific conditions where the water table is likely to remain close to, at, or briefly above the surface (Hasiotis, 2004, 2007, 2008). The abundance of desiccation features on the distal floodplain demonstrates it was not an ever-wet environment at the surface and the prevalence of red color and minor reduction mottles suggests moderate-to-well drained, or at least well-oxygenated conditions, prevailed (Retallack, 1988). No

epiterraphilic or terraphilic invertebrate traces were observed. The depositional environment for the upper platy facies was long considered to reflect a tidal flat complex (Picard, 1967, Picard, 1978; Johnson, 1993a), although Irmen and Vondra (2000) considered the upper platy facies in central Wyoming to be sabkha and sheet-flood deposits. McKee (1954) ascribed similar facies within the Moenkopi to fluvial floodplains.

Overall the upper platy facies fines upward demonstrating a relative decrease in local depositional energy, consistent with rising stratigraphic base level. The sandy facies appears to conformably overlie the upper platy facies and is distinguished by muddy fine-grained sandstone at its base that rapidly grades into clean sandstone that exhibits a high degree of disturbed to structureless bedding. The base of the sandy facies often contains a single 10-30 cm sandstone bed overlain by a thin green laminated mudstone; numerous large chirotheroid tracks and large desiccation cracks penetrate the basal sandstone. The chirotheroid tracks display collapsed sidewalls and other slump features indicating a saturated substrate (Cohen et al., 1991; Falkingham et al., 2010). The remainder of the sandy facies consists of disturbed to structureless bedding; where bedding is present it typically exhibits trough to planar-tabular cross stratification reminiscent of upper foreshore deposits. The base of the sandy facies is interpreted to represent a saturated floodplain that transitioned to marine influenced backshore to foreshore deposits of the upper sandy facies. The sandy facies appears to be conformably overlain by the marine Alcova Limestone. Picard (1967) assigned a nearshore marine environment to the sandy facies, while Irmen and Vondra (2000) interpreted the sandy facies (their facies C) to be a

siliciclastic sabkha or wet interdune setting where bioturbation was responsible for the destruction of primary structures.

4.6.2 Red Peak Formation Ichnoassemblage

The Red Peak Formation has long been considered to be nearly devoid of fossil evidence of life and representative of an Early Triassic dead zone (Picard et al., 1969; Boyde and Loope, 1984; Johnson, 1993a; Irmen and Vondra, 2000). Although the data presented here are limited to the uppermost 10–15 m of outcrops in central Wyoming, they demonstrate the presence of a moderately diverse ichnoassemblage (7 invertebrate and 4 vertebrate tracemakers; Fig. 13). The paleoecology of the invertebrate fauna is suggestive of a dominantly hygrophilic to hydrophilic community, which required high soil moisture or saturation of the sediment at the time of habitation (Hasiotis, 2004, 2007, 2008). This limited habitable zones to near channel environments or environments where the water table was near to or at the surface. The lack of ichnodiversity in the underlying alternating facies characterized by drier conditions (i.e., evaporites, alkaline lakes, desiccation features) emphasizes the local environmental control on faunal distributions within the Early Triassic of central Wyoming.

The diversity of vertebrate and invertebrate ichnogenera observed in the upper platy and sandy facies of the Red Peak Formation is similar to other Lower–Middle Triassic continental strata from around the globe. The Red Peak ichnoassemblage is comparable to fluviolacustrine strata from the Wupatki, Upper Red, and Torrey members of the Moenkopi Formation within Utah, Arizona, and New Mexico (Peabody, 1948; McKee, 1954; Hunt et al., 1993; Nesbitt and Angeilczyk, 2002; Lucas et al., 2003;

Mickelson et al., 2006a; Mickelson et al., 2006b). The Red Peak Formation vertebrate ichnoassemblage is also analogous to other fluviolacustrine strata described from Lower–Middle Triassic rocks in Germany, (Diedrich, 2008, 2009); Argentina (Melchor et al., 2006; Mariscano et al., 2010), Greenland (Bromley and Asgaard, 1979) and Italy (Sirna et al., 1994; Avanzini et al., 2001, 2008).

4.6.2.1 Invertebrate ichnology—The single location that preserved the ichnogenera *Diplichnites* and *Lockeia* is a shallow lacustrine interval (ARM locality) that exhibits laminated muds of limited extent that are weakly incised and overlain by thin very fine-grained sandstone with cm-scale mud rip-up clasts. Both of the traces are preserved in convex hyporelief on the base of the sandstone and were likely made by small arthropods resting and walking on the muddy floor and bivalves suspension feeding in a shallow subaqueous environment (Bromley and Asgaard, 1979; Machalski and Machalska, 1994; Melchor et al., 2006; Mitner et al., 2007). Similar arthropod traces have also been reported from strata in the Moenkopi Formation (McKee, 1954; Peabody, 1956).

Two of the most common invertebrate trace fossils in the Red Peak Formation ichnoassemblage are associated with saturated floodplain deposits: *Palaeophycus* and *Fuersichnus*. These two ichnogenera are often observed in convex hyporelief on the soles of crevasse-splay sands, the tops of which commonly preserve abundant *Rhynchosauroides* tracks in concave epirelief. *Palaeophycus* and *Fuersichnus* have both been reported from continental Triassic fluviolacustrine deposits (Clemmensen, 1978; Bromley and Asgaard, 1979; MacNaughton and Pickerill, 1995; Lucas and Lerner, 2006; Marsicano et al. 2010) and are thought to be the result of deposit-feeding annelids? or arthropods and mayfly larvae, respectively (Hasiotis, 2002, 2004, 2008); these trace

fossils are commonly associated with seasonal to perennial freshwater bodies (Hasiotis, 2004, 2008) and make up the bulk of the Red Peak Formation invertebrate ichnocoenoses. Also associated with *Rhynchosauroides* tracks are rare locomotion trails cf. *Scolicia* (see Fig. 4F), which are interpreted to be the result of a gastropod trace maker. *Scolicia* was commonly observed on the tops of thin asymmetric ripple cross-laminated sandstone layers overlain by muddy siltstone.

Traces tentatively assigned to cf. *Scoyenia* are relatively rare, and are typically only seen in fluvial sandstones that also contain evidence of pedogenic overprinting, although original structure can be still be seen. The cf. *Scoyenia* traces may be the result of beetle activity (Hasiotis, 2002, 2004, 2008).

The invertebrate ichnoassemblage of the Red Peak is dominated by *Fuersichnus* and *Palaeophycus* and is consistent with the *Scoyenia* ichnofacies, which is often applied to transitional shallow-subaqueous to subaerial continental sediments (Seilacher, 1967; Frey et al. 1984; Frey and Pemberton, 1987). The *Scoyenia* ichnofacies, however, is a broadly defined association, which does not adequately reflect the spatiotemporal variability seen in continental deposits (Hasiotis, 2008). This invertebrate ichnocoenoses also includes *Diplichnites*, *Lockeia*, *Scolicia,* and *Scoyenia*. The presence of *Scolicia* is not typical, but has been noted in similar fluviolacustrine settings (Hasiotis, 2004), while *Palaeophycus* is commonly found in permanently subaqueous environments (Frey and Pemberton, 1984).

4.6.2.2 Vertebrate ichnology—The vertebrate ichnogenera observed in the Red Peak Formation ichnoassemblage represent a medium-high diversity assemblage (e.g. 4–8

ichnogenera *sensu* Hunt and Lucas, 2007a) and has a similar faunal composition to the proposed *Procolophonichnium* ichnocoenoses (Hunt and Lucas, 2007a). Chirotheroid (*Chirotherium barthii*) tracks and trackways are present though they are less abundant than *Rhynchosauroides* traces, which dominate; *Rotodactylus* tracks are present but rare. Tracks that are attributed to cf. *Chelonipus* are rare, but well represented at one locality.

Confidently assigning vertebrate tracks and traces to unambiguous ichnospecies can be complicated by extramorphologic conditions (*sensu* Peabody, 1948) such as substrate composition, as well as trackmaker mass, speed (Manning, 2004; Milan and Bromley, 2006, 2008; Diaz-Martinez et al., 2009), and behavior (e.g. Fiorillo, 2005; Diedrich, 2008). This problem is further exacerbated by the number of ichnospecies associated with the ichnogenus *Rhynchosauroides* (see Hunt and Lucas, 2007c), which makes up the majority of the vertebrate component of the Red Peak Formation ichnoassemblage. The high number of *Rhynchosauroides* ichnospecies may reflect unintentional splitting based on extramorphologic variability rather than actual track maker diversity. With the above caveat in mind, the designation of the majority of observed vertebrate traces in the Red Peak Formation are assigned to *Rhynchosauroides* isp.

Rhynchosauroides is recognized globally during the Triassic and represents the primary ichnospecies observed in several megatracksites in the Middle Triassic of the Germanic Basin (Diedrich, 2002, 2008, 2009; Avanzini et al, 2008; Brusatte et al., 2010). The usefulness of *Rhynchosauroides* as biostratigraphic ichnotaxon has been demonstrated in the Southern Italian Alps, but its utility globally remains to be determined (Avanzini et al., 2001; Avanzini et al., 2008). Klein and Lucas (2010)

compared the known stratigraphic range of the majority of Triassic vertebrate ichnogenera and suggest their utility in biostratigraphy and biochronology, at least at a course scale; they further suggest *Rhynchosauroides* may be less useful due to is presence across the entire Triassic.

Of the four vertebrate ichnogenera in the Red Peak Formation ichnoassemblage, *C. barthii* appears to be the most temporally constrained ichnospecies and is limited to the Spathian through Anisian (i.e., *Chirotherium barthii* biochron of Klein and Lucas, 2010). The presence of *C. barthii* in the Red Peak Formation ichnoassemblage is consistent with a Spathian age as suggested by others (Storrs, 1991; Steiner et al., 1993) but does not fully exclude a possible early Anisian age. *Chelonipus* is known from the Early and Late Triassic, but due to limited occurrences it may not make a reliable taxon for biostratigraphic comparisons (Rühle von Liliestern, 1939; Haubold 1971a, 1971b; Avanzini et al., 2005; Lockley and Foster, 2006).

Although the presence of cf. *Chelonipus* in the Red Peak Formation ichnoassemblage may not be useful for biostratigraphy, it does help highlight the richness of the Early Triassic turtle track record. The debate over turtle origins (aquatic vs. terrestrial) has been reinvigorated with the discovery of toothed marine turtles from the Late Triassic of China (Li et al., 2008). Joyce and Gauthier (2004) suggest that stem turtles were terrestrial and not aquatic. Their interpretation is based in part on morphological differences in the manus of aquatic vs. terrestrial turtles and association of terrestrial vertebrates with the majority of turtle remains (see Lucas et al., 2000). The *Chelonipus* tracks from the Red Peak Formation, however, are found in fluvial deposits and demonstrate variable impressions consistent with changing buoyancy suggesting an

aquatic bottom walking behavior (Avanzin et al., 2005). *Chelonipus* tracks are not seen in conjunction with terrestrial *Rhynchosauroides* tracks, but they are found with associated chirotheroid swim traces. The observed *Chelonipus* tracks support an aquatic habit for some stem turtles as early as the late Early Triassic, however, this is far from conclusive as to the nature of turtle origins as a whole. No body fossils of turtles have been reported from any earlier than the Late Triassic (Lucas et al., 2000; Joyce et al., 2009).

Swim tracks attributable to chirotheroid and turtlelike trackmakers are associated with fluvial channel deposits. No swim traces consistent with *Rotodactylus* or *Rhynchosauroides* tracemakers were observed suggesting these ichnogenera principally occupied nonaquatic proximal floodplain environments; although, the rarity of *Rotodactylus* tracks does not preclude the possibility of aquatic behavior, or occupancy of distal floodplain environments as well. While traces of swimming chirotheroids are present, only terrestrial trackways were found to preserve adequate morphological detail to assign the specific designation of *Chirotherium barthii*.

Both *Rhynchosauroides* and *Chelonipus* are found with associations of tracks of different size co-occurring together indicating these ichnogenera may have been semigregarious (e.g. Demathieu, 1985), whereas, close associations of different sized individuals was not observed in the chirotheroid or *Rotodactylus* track bearing surfaces. The gregarious behavior of *Rhynchosauroides* and *Chelonipus* trackmakers, and the relative abundance of *Rhynchosauroides* suggest they may represent lower trophic level clades (herbivorous or insectivorous diets; Demathieu, 1985; Nesbitt and Angielczyk, 2002; Diedrich, 2008). The isolated tracks and trackways of *Chirotherium* are characteristic of large (3-5 m) carnivorous archosaurs and represent the dominant form at

the peak trophic level in the Red Peak Formation ichnoassemblage (Diedrich, 2009). Lacking in this ichnoassemblage are tracks of large herbivores such as dicynodonts, which are known from the Moenkopi Formation. (Nesbitt and Angielczyk, 2002).

The few pes prints attributed to cf. *Rotodactylus* suggests the presence of dinosauromorphs in the Red Peak Formation fauna. This is not unexpected given the similarities to the fauna and proximity of the Moenkopi Formation of the southern Rocky Mountain west. Unfortunately, given the limited sample size and absence of trackways it is difficult to make further comparisons with other early dinosauromorph track sites (e.g. Brusatte et al., 2010).

4.7 CONCLUSIONS

Lower Triassic rocks of central Wyoming, classically considered to be nearly devoid of fossils or evidence of life, preserve a previously undescribed ichnoassemblage that demonstrates a diverse paleoecology comparable to that observed in the better-studied equivalent strata of the southwestern United States. The upper Red Peak Formation was traditionally thought to be composed of tidal to nearshore marine deposits; the lack of fossils confounded matters and made environmental interpretation difficult. The ichnoassemblage from the mid-late Spathian upper platy and sandy facies of the Red Peak Formation, Chugwater Group, provides a new means to test previous paleoenvironmental hypotheses and lends new insights into paleoecological diversity.

The sediments of the upper platy facies are well exposed in central Wyoming and exhibit a 3-5 m basal sandstone that preserve abundant channel barforms and reactivation surfaces consistent with an amalgamated channel complex. The channel complex grades

into thinly bedded sandstones, floodplain paleosols, abundant desiccation features, and laminated silty-mudstone to muddy-siltstone intervals. The sedimentology of the upper platy facies is consistent with a semi-arid fluviolacustrine depositional environment. The general upward fining of the upper platy facies and the conformable contacts of the sandy facies and overlying Alcova Limestone record the transition from continental to marine deposition at the end of the Spathian or earliest Anisian; this event likely records the easternmost extent of the Thaynes-Virgin Formation transgression. Future work focusing on this transitional zone may help place the Red Peak Formation of central Wyoming in a sequence stratigraphic framework more conducive to broader scale correlations with better-studied units to the south and west facilitating further comparisons of paleoenvironments and paleoecology within the Moenkopi and Red Peak formations.

The Lower Triassic Red Peak Formation ichnoassemblage demonstrates a rich vertebrate and invertebrate ichnofauna. The dominance of the invertebrate ichnogenera *Palaeophycus* and *Fuersichnus*, and the presence of *Diplicnites*, *Lockeia*, and *Scoyenia*, is consistent with a shallow–ephemeral freshwater ichnocoenoses. All of the observed invertebrate trace fossils are representative of hygrophilic to hydrophilic tracemakers and are restricted to near-channel and floodplain environments where the water table is near, at, or above the surface. No epiterraphilic or terraphilic invertebrate traces were found.

The presence of the vertebrate ichnogenera *Rhynchosauroides*, *Chirotherium barthii*, and *Rotodactylus* extend the paleobiogeographic range of these ichnogenera into the northern Rocky Mountain west, and the presence of *Chelonipus* marks the first Triassic occurrence of the ichnogenus in North America. Vertebrate tracks and traces

record trackmaker behaviors associated with distinct paleoenvironments, which range from aquatic (*Chelonipus*), semi-aquatic (chirotheroid), to terrestrial (*Rhynchosauroides* and *Rotodactylus*) habitats. In the absence of body fossils, the ichnologic record of the Red Peak Formation provides the first evidence of the hidden biodiversity preserved during the Early Triassic of central Wyoming.

The Early-Middle Triassic transition is a crucial time in the evolution of the modern continental fauna, many members of which are represented in the Red Peak Formation vertebrate ichnofauna (e.g. lepidosaur, crocodilian, chelonian, and avian lineages). The *Rotodactlyus* specimens are amongst the oldest dinosaurmorph tracks in North America, but not as old as the Smithian dinosauromorphs from Poland. The tracks referred to cf. *Chelonipus* suggest an aquatic habitat for some Early Triassic chelonians. Notably, tracks attributable to amphibian and synapsid trackmakers are unknown from the Red Peak Formation ichnofauna, although they are both represented in the Moenkopi Formation by trace and body fossils. The absence of body fossils in the Red Peak Formation remains unexplained.

The Lower Triassic Red Peak, Alcova Limestone, and the Middle Triassic Jelm and Crow Mountian formations of the Chugwater Group preserve a nearly continuous record of deposition from Early Triassic through at least early Middle Triassic. This striking stratigraphic unit is greatly understudied considering the nature of the geologic interval it preserves; a great deal remains to be done to better understand the paleoclimate, paleoecology, and paleoenvironments of these units and their relation to equivalent units in the desert southwest.

ACKNOWLEDGEMENTS

We thank Jenn Drake, Mary Lovelace, Rich Slaughter, Shanan Peters, Angeline Catena, Amalia Doebbert, Eric Williams, Debra Jennings, Laura Vietti, and the UWGM 2010 field crew for their invaluable discussions and assistance in the field. Special thanks go to the Geological Society of America, American Association of Petroleum Geologists, the University of Wisconsin-Madison Geology Museum, and the University of Wisconsin-Madison Department of Geoscience for financial support. Our sincere thanks go to the Red Canyon Ranch (The Nature Conservancy), Wyoming Dinosaur Center, and Bureau of Reclamation and the Bureau of Land Management for access. We are grateful for the critical and editorial comments of three anonymous reviewers, Martin Lockley, and Stephen Hasiotis, their insight was extraordinarily helpful. Finally, we extend our sincere appreciation for all workers who have spent many a frustrated hour trying to puzzle out the character and history of the Chugwater Group. Any and all errors are ours and ours alone.

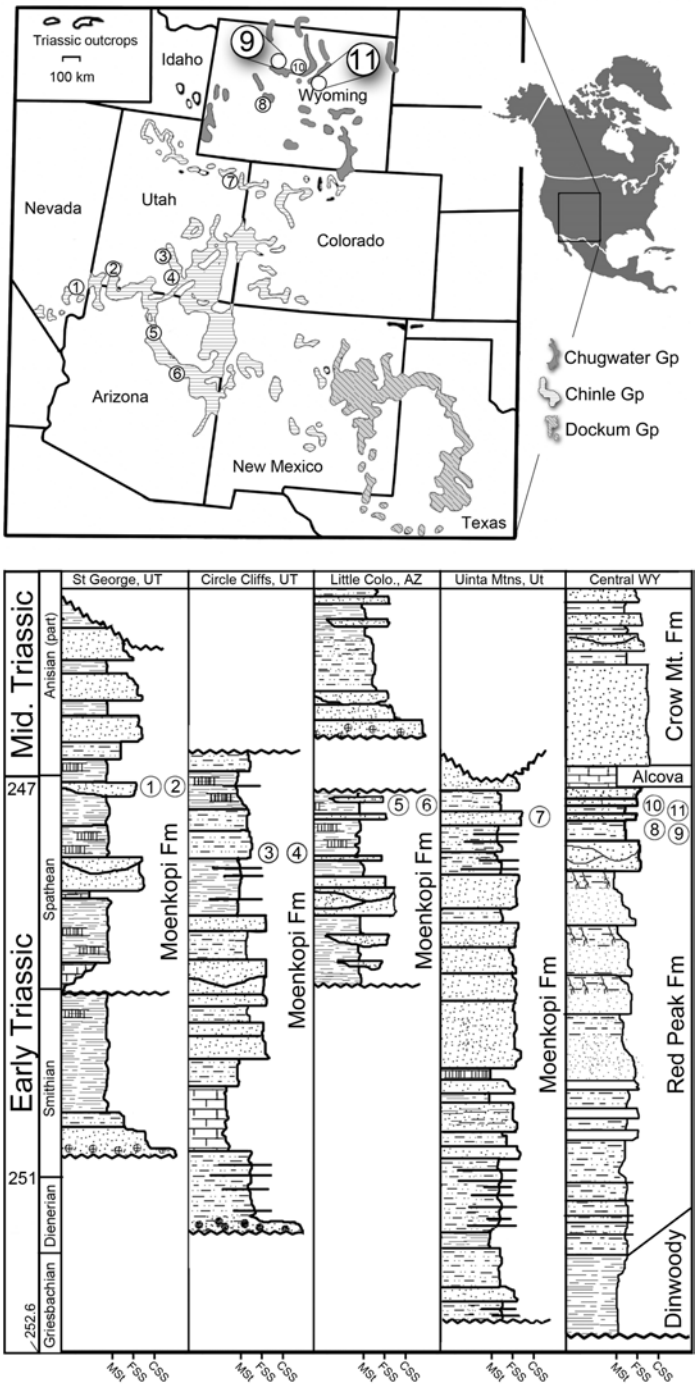

FIGURE 4.1—Outcrops of Triassic age rocks where vertebrate tracks have been observed. Circled numbers represent field locations of Lower-Middle Triassic track sites. The Moenkopi Formation (within horizontal hatching) has numerous reports of vertebrate tracks (sites 1-7; Welles, 1947; Peabody, 1948; McKee, 1954; Peabody, 1956). Lower Triassic vertebrate tracks or traces from the Chugwater Group (solid gray) of Wyoming are poorly understood (sites 8 and 10; Boyde and Loope, 1984; and Branson, 1946; respectively). Sites 9 and 11 are the new track localities described in this paper. Outcrop map modified after Hunt and Lucas (2007b).

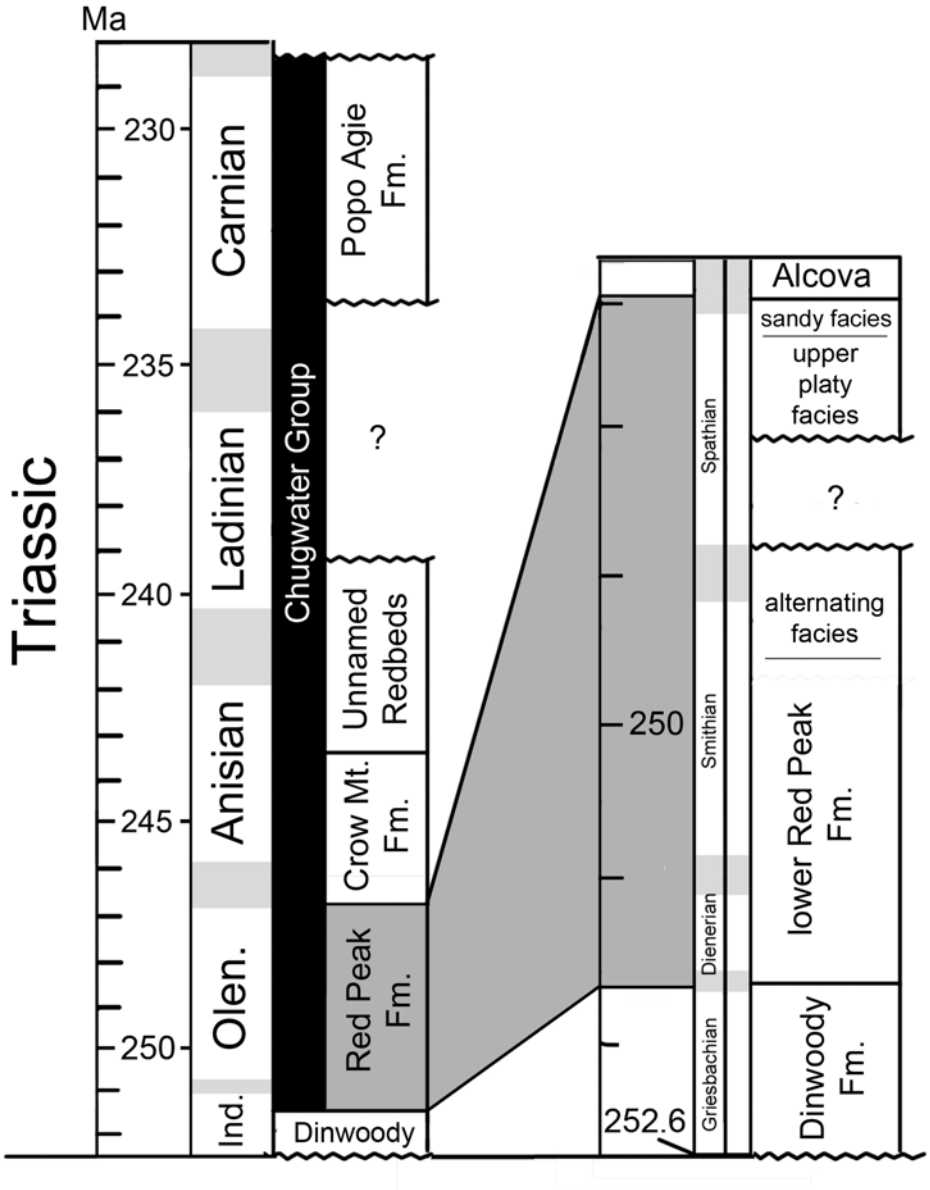

FIGURE 4.2—Chronostratigraphic position of the four formations within the Chugwater Group; The Red Peak Formation is extended to the right demonstrating the position of the sandy, upper platy, and alternating facies. The duration and boundaries of interpreted hiatuses in the Early and Late Triassic are poorly constrained.

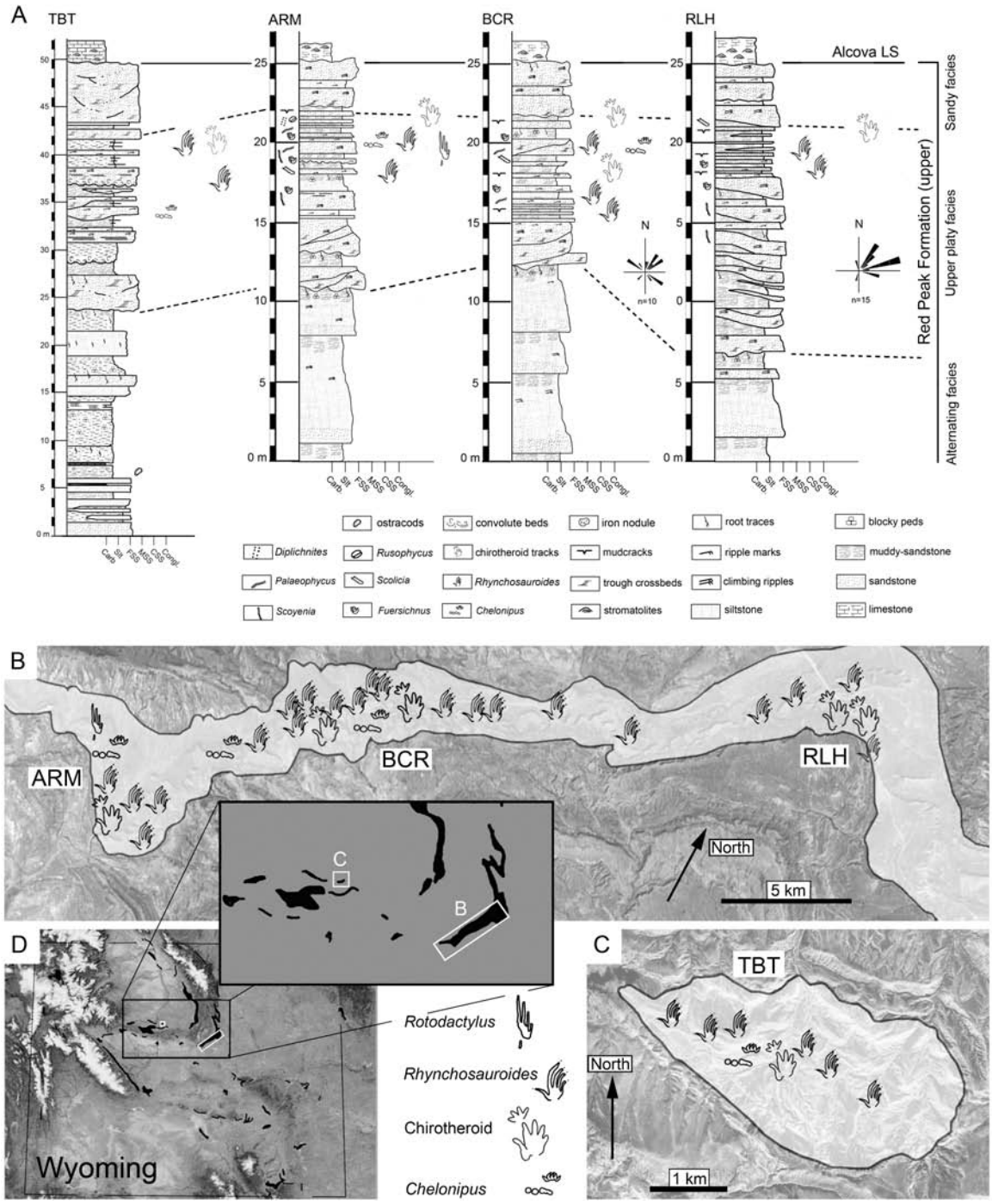

FIGURE 4.3—Representative measured sections, outcrop, and vertebrate track locations in central Wyoming. A) Four measured stratigraphic sections from Red Wall and Red Hole. B) Track locations along the Red Wall on the south slope of the Bighorn Mountains, Natrona County; ARM = Arminto, BCR = Baker Cabin Road, RLH = Roughlock Hill. C) Track locations along Red Hole, Hot Springs County; TBT = Trampled-by-Turtles tracksite. D) Study area in central Wyoming; inset displays locations of Red Wall (B) and Red Hole (C)

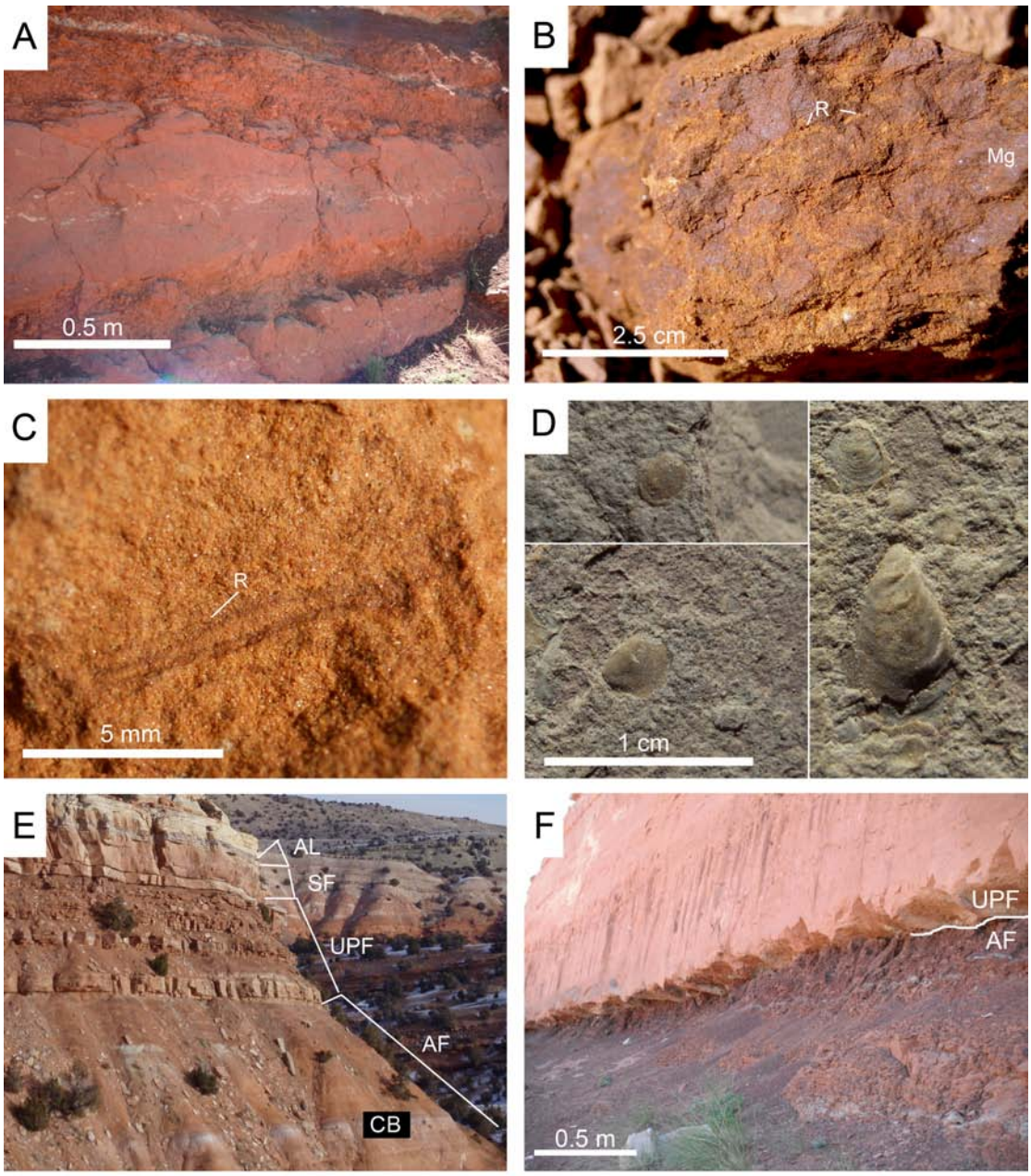

FIGURE 4.4—Outcrop, sedimentary features, and trace and body fossils of the alternating facies. A) Alternating beds typical within the alternating facies. B) Blocky peds that exhibit rhizoliths and mangans. R = rizolith; Mg = mangan. C) Rhizoliths are rare but present on the tops of several alternations, usually associated with other pedogenic features. D) Unidentified conchostracans from the TBT locality. E) Outcrop near the TBT locality. AL = Alcova Limestone; SF = sandy facies; UPF = upper platy facies; AF = alternating facies; CB = conchostracan bed. F) Erosional base of the fluvial complex at the base of the upper platy facies with scour surface incised into the alternating facies.

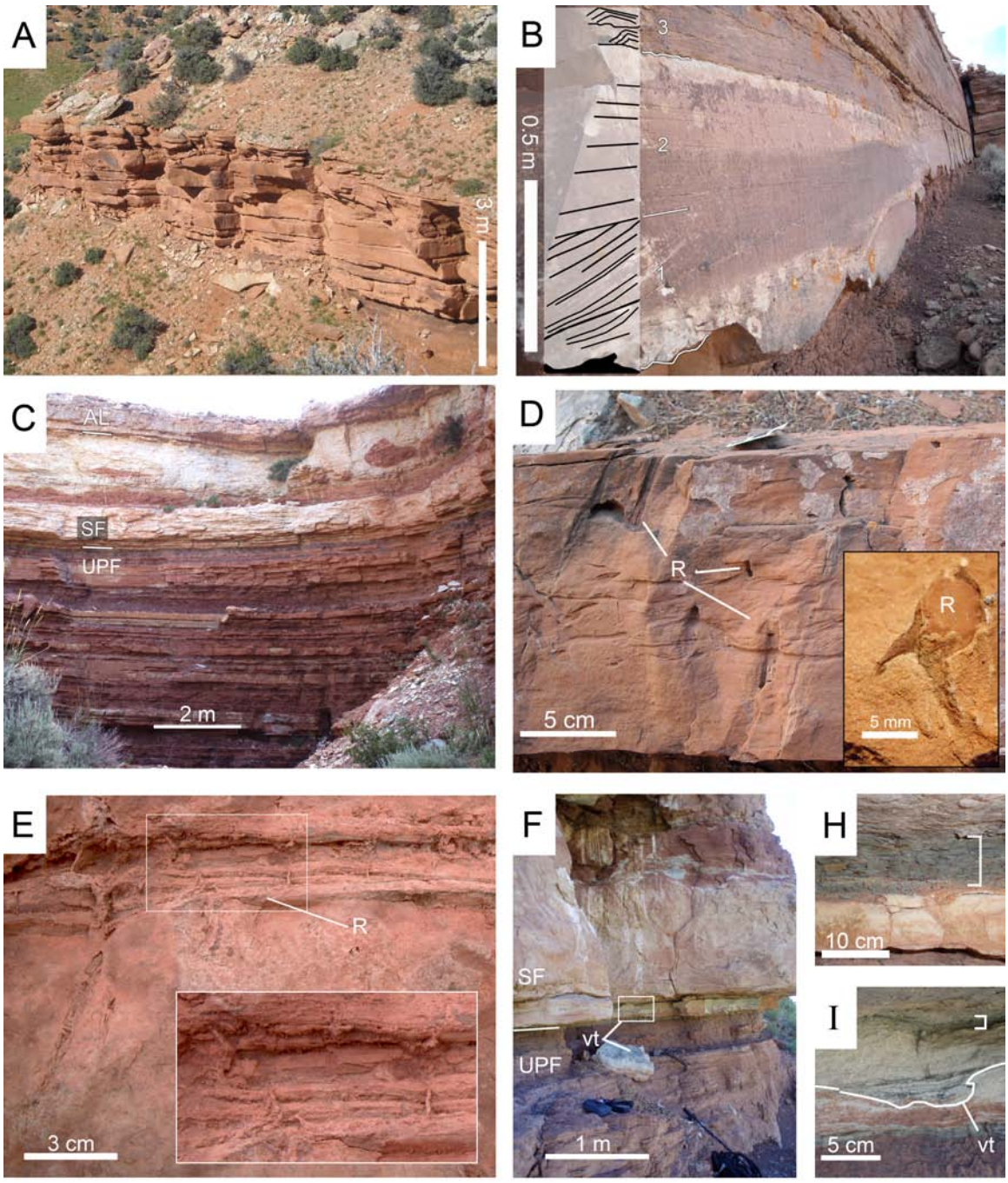

FIGURE 4.5 (see caption next page)

FIGURE 4.5—Outcrop, sedimentary structures, and trace fossils of the upper platy facies. A) Lateral accretion beds in the basal sandstone. B) Typical elements observed in fluvial barforms. 1 = trough cross stratification; 2 = upper flow regime planar and antidunes beds; 3 = asymmetrical ripples with vertically decreasing angle of climb. C) Erosional cut demonstrating the contact between the track bearing surfaces of the upper platy facies, the sandy facies, and the Alcova Limestone. AL = Alcova Limestone; SF = sandy facies; UPF = upper platy facies. D) Rhizoliths in a crevasse splay, upper platy facies; inset is a mud infilled rhizolith with bifurcating segment to the left (from unweathered section of D). R = rhizolith. E) Rhizolith along base of crevasse splay sand; inset showing larger view of bifurcating structures. F) Contact of sandy facies and upper platy facies. The base of the sandy facies preserves numerous chirotheroid tracks suggestive of a saturated base, which is commonly overlain by laminated mudstone of variable thickness (see Fig. 9). vt = vertebrate track. H) Laminated mudstone (bracket) overlying basal sand of the sandy facies. I) Laminated mudstone (bracket) overlying cross section of track (close up view of box in F), note the mixed muddy infill of the track.

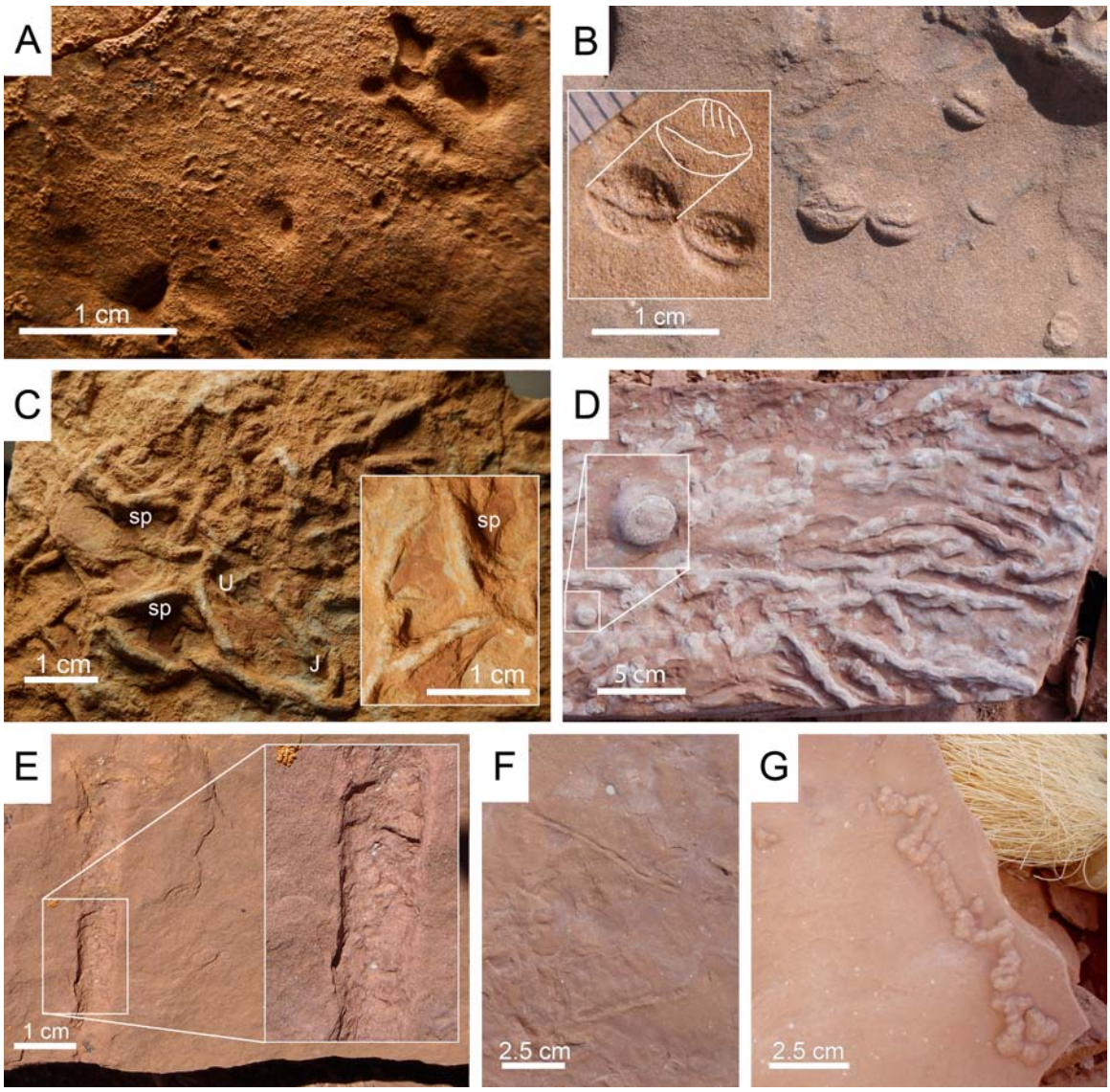

FIGURE 4.6—Invertebrate trace fossils from the upper Red Peak Formation. A) Morphotype I: *Diplicnites* isp. B) Morphotype II: *Lockeia* isp; inset demonstrates the weakly preserved striations (inset scale in mm divisions). C) Morphotype III: *Fuersichnus communis*; inset showing spreiten. Sp = spreiten; U = u-shaped burrow; J = j-shaped burrow. D) Morphotype IV: *Palaeophycus striatus*; inset displays enlarged view of a vertical termination with distinct lining. E) Morphotype V: cf. *Scoyenia*; inset demonstrates longitudinal and oblique bioglyphs. F) Morphotype VI: *Scolicia*. G) Morphotype VII: *incertae sedis*.

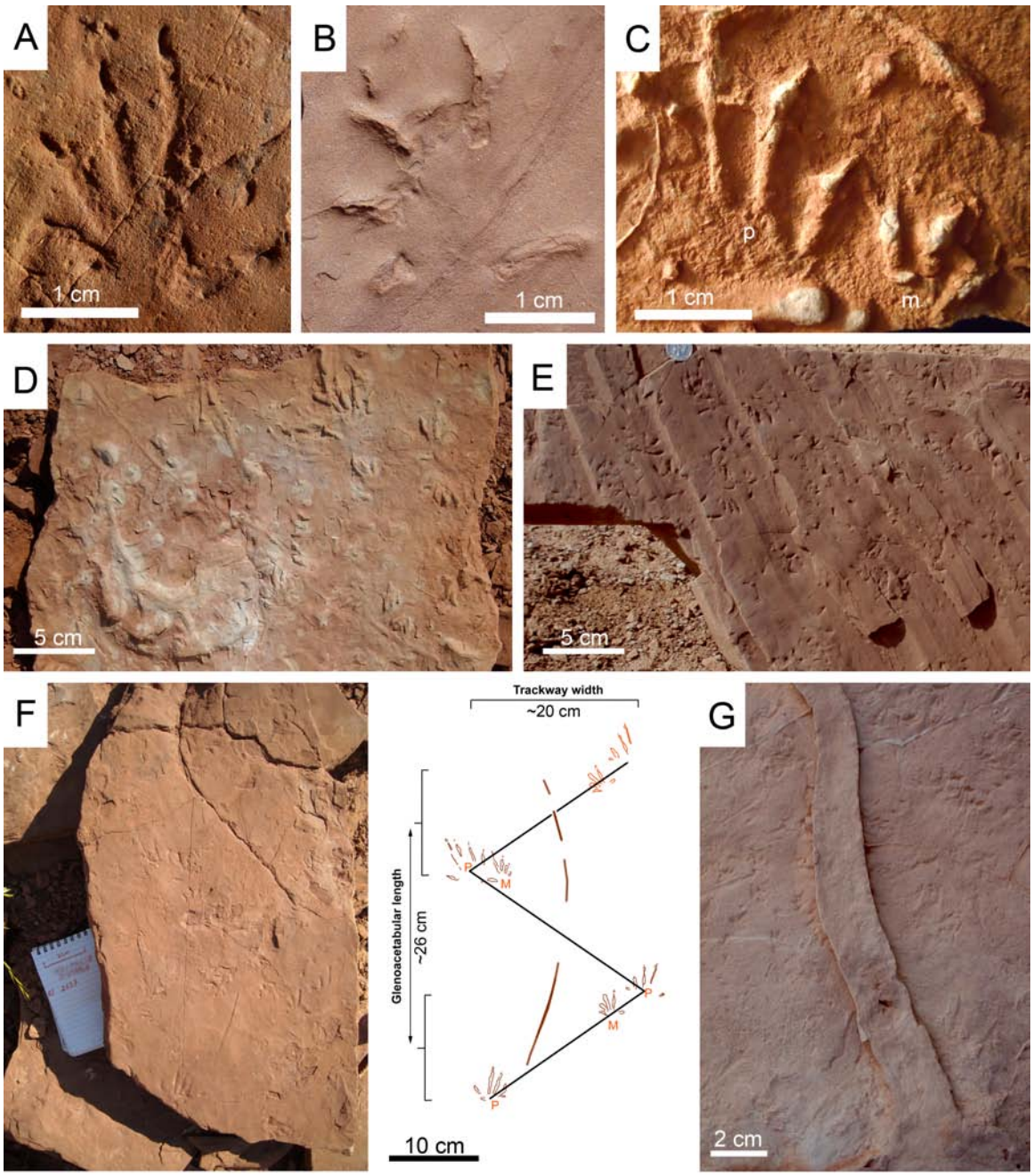

FIGURE 4.7 —Tracks and traces of *Rhynchosauroides* (morphotype VIII). A) Pes exhibiting deep impressions of claws; IV = digit IV B) Manus print. C) Pes and manus pair in convex hyporelief (partial); note pes oversteps manus. m = manus; p = pes. D) Trampled surface in convex hyporelief with tail drag from bottom right to top left. E) Trampled surface in concave epirelief on a low-angle asymetrically rippled surface. F) Trackway with three consecutive manus-pes pairs and tail drag; schematic drawing to the right. F) Desiccation crack crosscutting trampled surface (dominantly transmitted tracks and claw impressions).

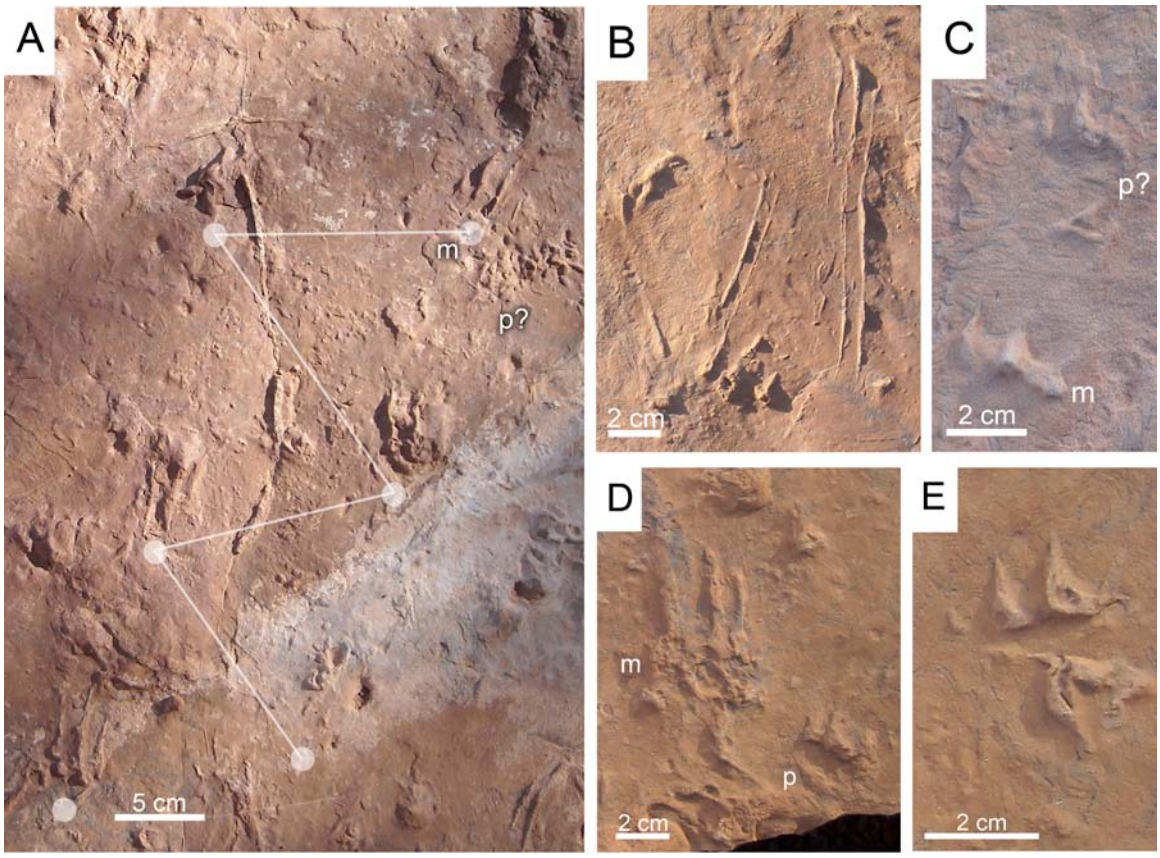

FIGURE 4.8—Tracks and traces of *Chelonipus* (morphotype IX). A) *Chelonipus* trackway exhibiting dominantly manual impressions. Solid gray circles = manus print; m = manus; p = pes. B) Scratch marks made by a partially bouyant trackmaker. C-D) Manus and pes tracks. E) Manus track.

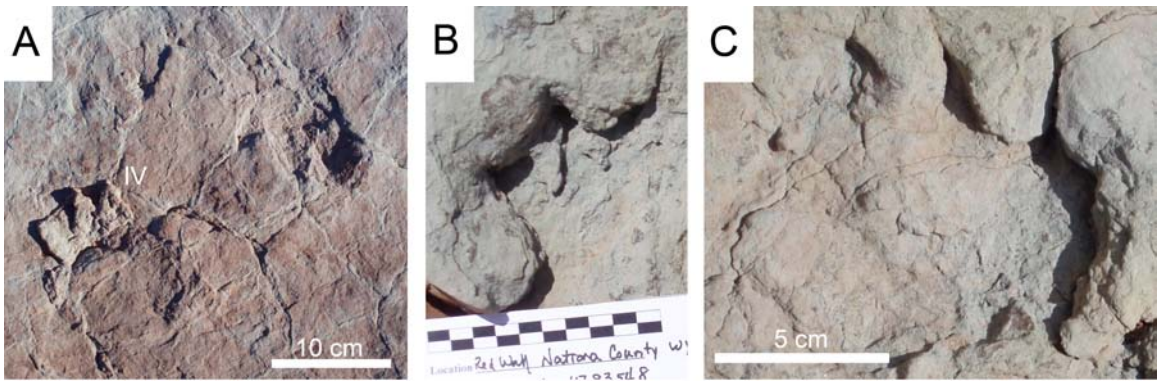

FIGURE 4.9—Chirotheriod tracks from the basal sand of the sandy facies. A) Mudcracked surfaces demonstrating shallow (transmitted?) impressions in concave epirelief (top of image), and a pes (lower left) exhibiting pull-up features associated with adhesion of the substrate. IV = digit IV. B) Manus impression demonstrating sidewall collapse due to saturated substrate. Scale in cm. C) Pes impression also demonstrating a saturated substrate that partially deformed as foot was withdrawn.

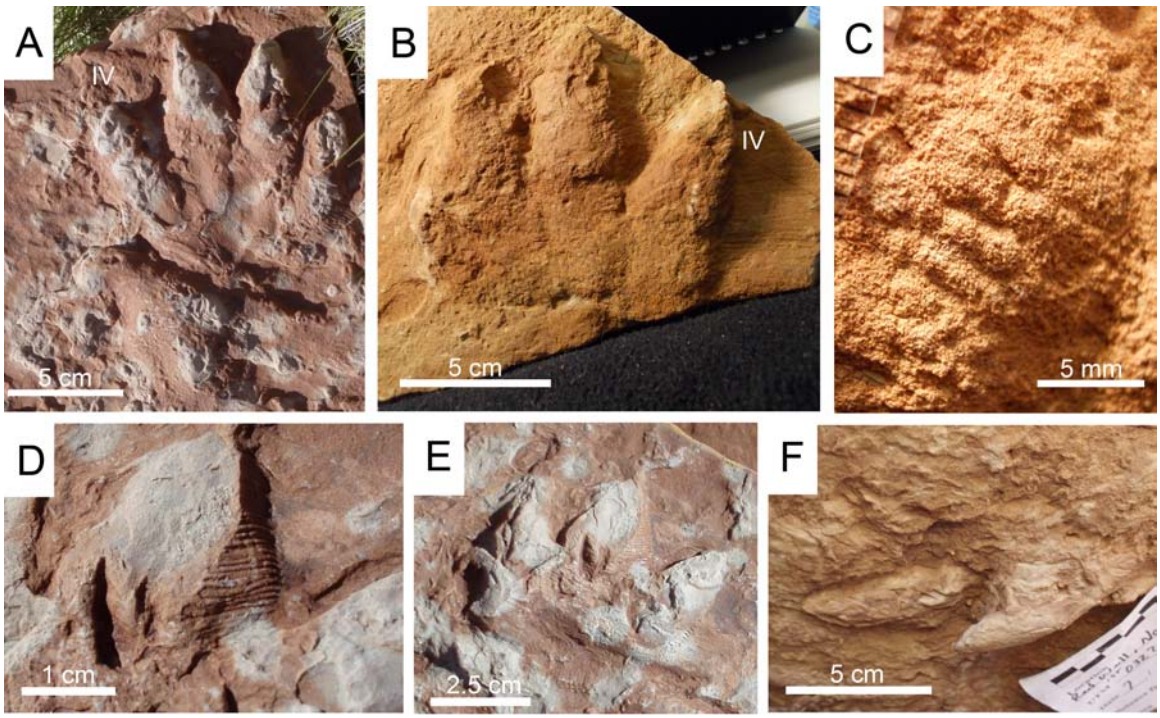

FIGURE 4.10—Tracks and traces of chirotheroids and *Chirotherium barthii (*morphotype X). A-B) Pes tracks in convex hyporelief demonstrating skin impressions. IV = digit IV. C) Skin imprints exhibiting small rounded scale impressions. D) Scale drag marks on manus (digit III; 10F). E) Claw impressions on the base of a fluvial barform, attributed to a swimming chirotheroid. F) Manus in convex hyporelief, digit I is not evident.

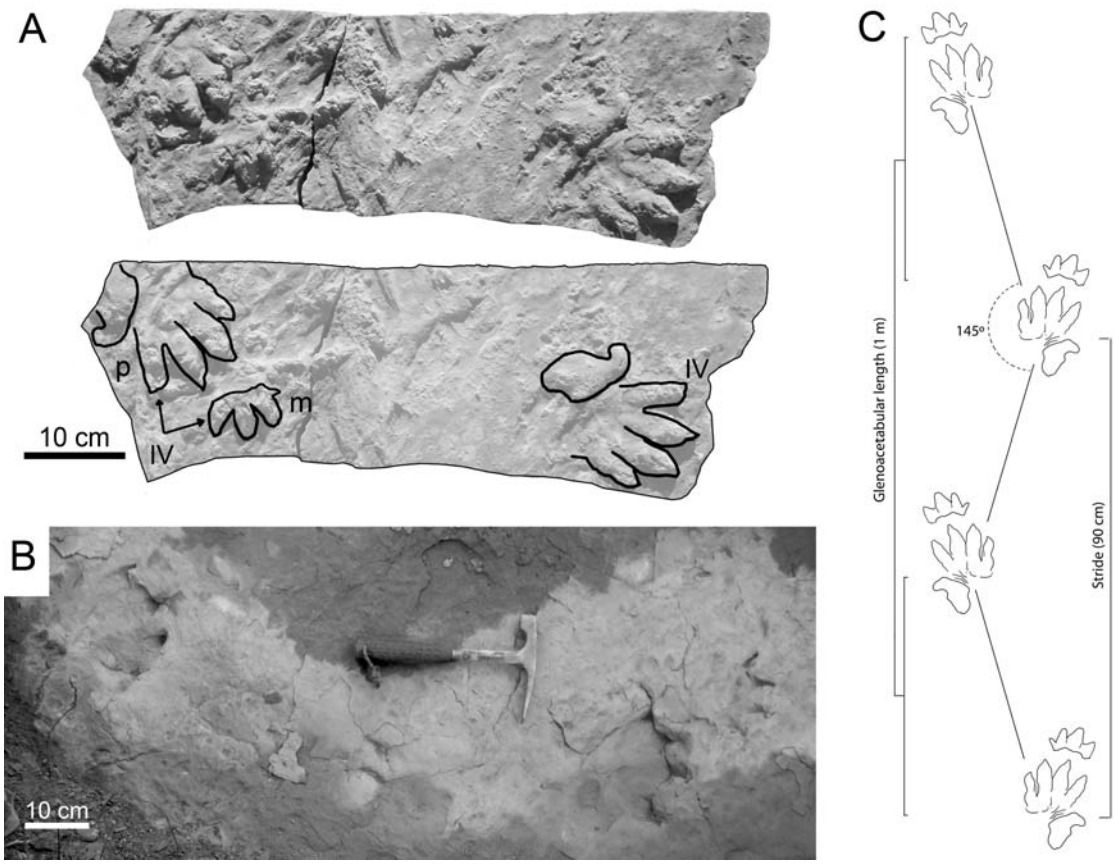

FIGURE 4.11—Trackways of chirotheroids and *Chirotherium barthii* (morphotype x). A) Trackway (UWGM 980) in convex hyporelief preserved on the sole of a crevasse splay sandstone, lower image outlines the individual tracks. p = pes; m = manus. B) Trackway preserved in concave epirelief near the Red Hole locality. C) Trackway pattern with stride and glenoacetabular length inferred from UWGM 980.

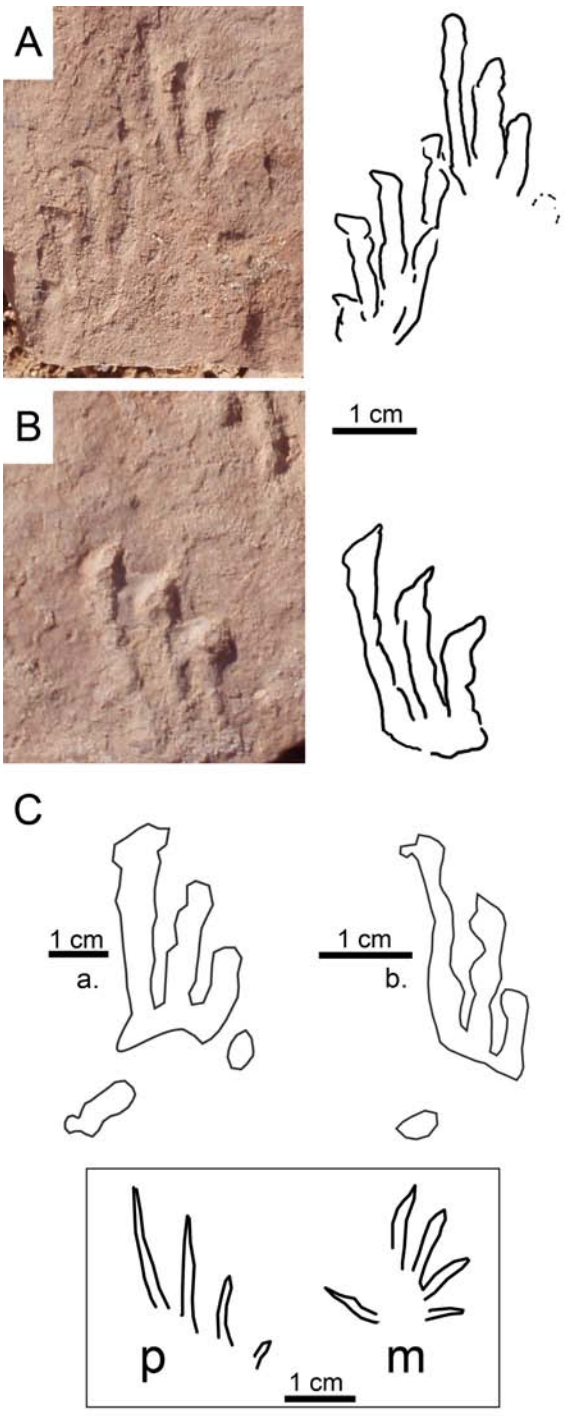

FIGURE 4.12—Tracks of cf. *Rotodactylus* (morphotype XI). A-B) Pes impressions on a single slab expressed in convex hyporelief; schematic drawing to the right of each image. C) Schematic drawings of *Rotodactylus* (modified after Brusatte et al., 2011, supplemental figure S7). Inset, schematic drawing of *Rhynchosauroides* manus-pes pair for comparison (see also Fig. 7).

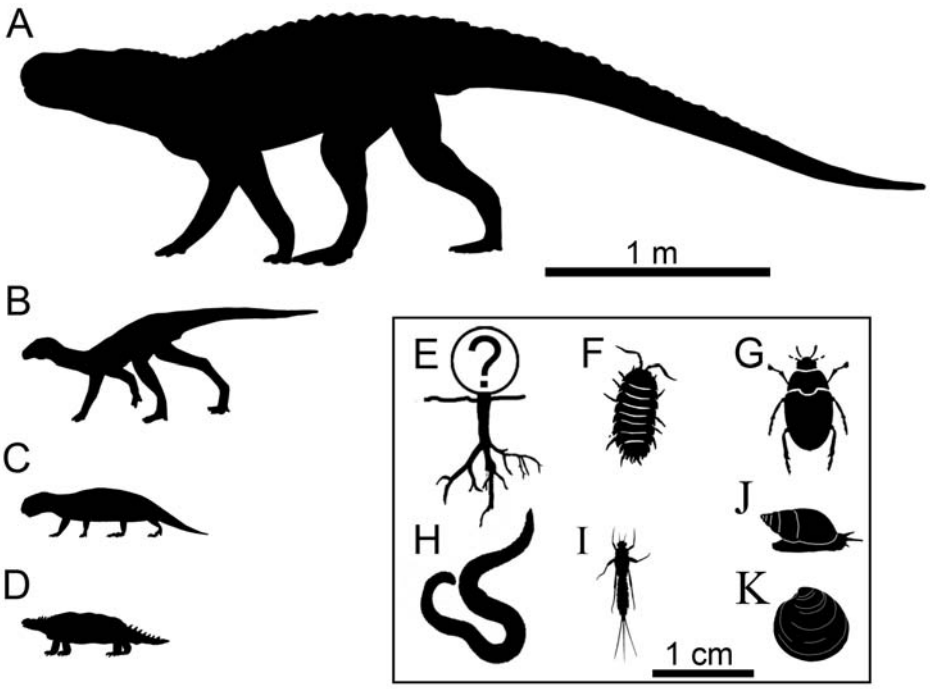

FIGURE 4.13—Representative body forms of the hidden biodiversity (*sensu* Hasiotis 2004, 2008) not recorded in the body fossil record of the Red Peak Formation. A) Chirotheroids (*Chirotherium barthii*). B) Dinosauromorphs (*Rotodactylus* isp.). C) Lepidosaur trackmaker (*Rhynchosauroides* isp.). D) Turtle-like trackmaker (*Chelonipus*). E) Rhizoliths of unidentified plants. F) Unidentified arthropod track and tracemaker (*Diplichnites* isp.). G) Unidentified beetle tracemaker (cf. *Scoyenia*). H) Unidentified annelid? (possibly arthropod) tracemaker (*Palaeophycus stiatus*). I) Unidentified larval mayfly tracemaker (*Fuersichnus communis*). J) Unidentified gastropod tracemaker (cf. *Scolicia*). K) Unidentified bivalve tracemaker (*Lockeia*).

CHAPTER 5

A new age constraint for the Early Triassic (Spathian) marine Alcova Limestone (Chugwater Group), Wyoming

ABSTRACT

The Alcova Limestone is a widely exposed but poorly studied Triassic unit found throughout Wyoming. While it is used as a regional lithostratigraphic marker bed, the age of the limestone is not well constrained and contention regarding the depositional nature (marine vs. non-marine saline lake) has not been adequately resolved, although the marine hypothesis is more widely accepted. Currently, its age is based on the occurrence of a single phylogenetically primitive vertebrate taxon whose estimated geologic age has ranged from Early Triassic to late Middle Triassic.

Marine sediments record the $^{87}Sr/^{86}Sr$ ratios that reflect the composition of seawater at the time of formation, providing a global strontium curve across the Phanerozoic; the curve demonstrates a significant monotonic increase in global seawater $^{87}Sr/^{86}Sr$ starting in the Early Triassic that quickly drops in the Middle Triassic. We provide the first $^{87}Sr/^{86}Sr$ analysis of the Alcova Limestone, which corresponds with the apex of the Early Triassic strontium curve. The data strongly support a marine origin for this unit. Furthermore, the data provide an age range, based on their placement on the strontium curve, that limits the deposition of the Alcova Limestone to the latest Spathian to earliest Anisian (Early Triassic–Middle Triassic boundary). This placement is consistent with the timing of the Spathian regression recorded in other transitional marine to non-marine strata of the western USA.

5.1 INTRODUCTION

The Alcova Limestone (Alcova) is a thin (1–4 m) carbonate unit that marks a pronounced break from clastic deposition of the underlying Red Peak Formation and overlying Crow Mountain and Jelm formations. The Alcova Limestone has long been used as a regional stratigraphic marker bed because of its restricted stratigraphic thickness, distinct lithology, and regional continuity. The Alcova has had an unstable nomenclatural history (for review, see High and Picard, 1969). Storrs (1991) suggested the unit was unmappable at the 1:24000 and should remain as a member of the Crow Mountain Formation. Correlation of Alcova Limestone with the upper Thaynes Formation was proposed by Love (1957) and further supported by Picard et al. (1969), although direct correlation is made difficult by Laramide structures that disrupt an otherwise relatively continuous series of outcrops in central Wyoming. The depositional environment of the Alcova Limestone has been hypothesized to be an isolated nonmarine limestone (Carini, 1964) or, according to the more widely accepted hypothesis, a marine limestone deposited on the broad and shallow Wyoming shelf (Picard, 1967; Picard et al., 1969; Storrs, 1991). While a marine environment of deposition is more often proposed, little evidence exists that strongly favors either hypothesis.

Storrs (1991) argued that the predominantly micritic limestone preserves a faithful isotopic signal, although Storrs (1991) and Carini (1964) both demonstrated early diagenetic recrystallization of calcite. Cavaroc and Flores (1991) reported $\delta^{13}C$ and $\delta^{18}O$ for three samples from stromatolitic horizons of the Alcova along the western flanks of the Big Horn Mountains (about 20 km from the Baker Cabin Road locality) and also suggest minimal diagenetic dissolution and cementation for the unit.

The $\delta^{13}C$ (1.0-3.4‰ PDB; avg. 1.8‰) and heavy $\delta^{18}O$ (2.8-3.2‰ PDB; avg. 3.0‰) demonstrated by Storrs (1991) were interpreted as a lagoonal or restricted marine environment with a high rate of evaporation. In further support of a marine origin, Storrs suggests anatomical features (maxillary pits) on the skull of the primitive nothosaur *Corosaurus alovensis* may represent receptacles for subcutaneous salt glands suggestive of a marine lifestyle. Carini (1964) suggested the prevalence of sedimentary features, such as ripple marks, desiccation cracks, and minor micro-karsting, coupled with thinning in all directions from a maximum thickness (4 m) near the town of Alcova, WY supported a lacustrine or "lake-sea" origin of the Alcova Limestone. He further suggested that fossil evidence, including poorly preserved gastropods and ostracods (each of which are ambiguous to origin as both morphologies are commonly found in marine and non-marine environments), and more specifically a lack of halobiotic fauna, supported fresh to brackish water conditions rather than open marine.

Although the value of the Alcova Limestone as a lithostratigraphic marker within Wyoming has long been acknowledged (Picard, 1967; Picard et al., 1969; Cavaroc and Flores, 1991; Johnson, 1993), the ability to confidently correlate this unit with rocks outside of the state is not well established. The age attributed to the Alcova Limestone has ranged from Early to Late Triassic (Colbert, 1957; Zangerl, 1963; Picard et al., 1969), but its age has more recently been estimated to be late Spathian to early Anisian (Storrs, 1991; Rieppel, 1998; Lovelace and Lovelace, in press). The estimates are weakly supported claims based largely on vertebrate traces and a single species (*Corosaurus alcovensis*; Storrs, 1991) represented by a body fossil.

The $^{87}Sr/^{86}Sr$ record is a well-established tool that has been used to correlate and date marine sediments and differentiate marine and non-marine depositional environments (DePaolo and Ingram, 1985; McArthur et al., 2001; for review see McArthur, 2007). The $^{87}Sr/^{86}Sr$ of seawater has a long residence time ($2–5 \times 10^6$ yr) relative to oceanic mixing times (10^3 yr) such that it takes timescales greater than 10^4 years to affect ocean $^{87}Sr/^{86}Sr$ (Elderfield, 1986; Veizer, 1989; McArthur, 2007). Burke et al. (1982) demonstrated the utility of this system for stratigraphic purposes when they determined that isotopic composition of $^{87}Sr/^{86}Sr$ in seawater fluctuated, at times dramatically, across the Phanerozoic.

There have been several revisions of the marine $^{87}Sr/^{86}Sr$ curve of Burke et al. (1982) that focus on Mesozoic intervals (e.g., Koepnick et al., 1990; Korte et al., 2003), which show an abrupt rise in $^{87}Sr/^{86}Sr$ from the latest Permian to the Early–-Middle Triassic boundary followed by a similarly rapid decline through the Middle Triassic. Given the inconsistency of reported values of carbon and oxygen stable isotopes (Storrs, 1991; Cavaroc and Flores, 1991) and the extreme Early Triassic global $\delta^{13}C$ isotopic excursions (Payne et al., 2004), another isotopic system was chosen. Seven samples were collected to measure the $^{87}Sr/^{86}Sr$ (Appendix 5.1) in order to further test hypotheses of a marine or inland lake-sea origin of the Alcova Limestone, and provide a dataset for chemostratigraphic correlation with regional strata of similar age.

5.2 METHODS

5.2.1 Sampling

Hand samples (AS-1-7, 10) were collected between the base of the micritic limestone (10 cm above the contact with the sandy facies of the Red Peak Formation) and the first 20 cm of the overlying sandstone of the Crow Mountain Formation. Carbonate samples were micro-drilled from layers that did not exhibit stylolitic, spar-rich, or fractured surfaces.

5.2.2 $^{87}Sr/^{86}Sr$ Analysis

Carbonate was extracted from 5 to 6 milligrams of powdered bulk sample in 1M Acetic Acid. Between 74% and 97% of sample mass was carbonate in these samples, based on dry sample mass difference pre- and post-carbonate extraction. Extracted carbonate was spiked with a mixed ^{87}Rb-^{84}Sr tracer, dried down, and redissolved in HNO_3 for Sr separation using Sr spec resin (Sr Resin SPS, 50-100mm, manufactured by EIChrom Industries, Inc., Lot # SRS07101). Rb was further purified using cation exchange resin (AG MP-50) and 2.2M HCl. A total procedural blank processed with the samples included 77 pg of Sr and 7 pg Rb.

Mass analysis of Sr was conducted using a three-jump multi-collector analysis routine using a Micromass Sector 54 thermal ionization mass spectrometer. Samples were loaded on tantalum filaments for analysis. Reported $^{87}Sr/^{86}Sr$ ratios are the average of 120 ratios (outliers excluded) run at an ^{88}Sr ion intensity of 3×10^{-11} A. The error reported for the $^{87}Sr/^{86}Sr$ ratios is 2 standard errors of the mean from the internal statistics of an individual analysis. Analysis of the NIST SRM 987 Sr standard run under the same conditions yielded an $^{87}Sr/^{86}Sr$ ratio of 0.71027 ± 0.00001 (2-SD; n=6). Rubidium was analyzed using a multi-collector static analysis. $^{87}Rb/^{85}Rb$ ratios are the average of 50

ratios (outliers excluded). Mass fractionation corrections of the $^{87}Rb/^{85}Rb$ ratio (fractionation factor = 1.00857) were applied based on the average ratio of the NIST SRM 984 standard $^{87}Rb/^{85}Rb$ ratio of 0.382 ± 0.003 (2-SD; n=7).

All $^{87}Rb/^{86}Sr$ ratios for these data are less than 0.01. However, an observed correlation between $^{87}Rb/^{86}Sr$ and $^{87}Sr/^{86}Sr$ suggests that variable contribution of silicate-derived high-$^{87}Sr/^{86}Sr$ may account for variability of as much as 0.0002 in the $^{87}Sr/^{86}Sr$ ratio.

5.3 RESULTS

Six of seven hand samples were taken from a well-exposed section of the Alcova Limestone near Grey Reef, southern Natrona County, Wyoming. AS-7 is the stratigraphically lowest sample from the Grey Reef locality and sequentially decrease up-section, culminating with sample AS-1 from the gradational contact with the Crow Mountain Formation. The $^{87}Sr/^{86}Sr$ ratio increases from AS-7 to AS-6, and then decreases through AS-3 (Appendix 5.1). An isolated sample, AS-10 (0.708187±1.0E-5), was collected at the Baker Cabin Road locality in northern Natrona County, Wyoming, approximately 50 cm below the Alcova–Crow Mountain contact. AS-10 is lithologically similar to the Alcova sample AS-3 (0.708217±1.0E-5) and from an equivalent stratigraphic position, which provides a preliminary test for potential regional $^{87}Sr/^{86}Sr$ differences. Both of the sample localities are near the two localities from which samples for previous stable isotope measurements were collected (Storrs, 1991; Cavaroc and Flores, 1991).

The stratigraphically highest sample (AS-2), a silty-micritic limestone, produced a higher $^{87}Sr/^{86}Sr$ ratio (0.708428±1.0E-5) than the 5 lower samples (Figure 1). Sample

AS-1 did not yield enough carbonate to analyze. These two samples (AS-1–2) were chosen to represent transitional mixed clastic-carbonate sediments above the micritic limestone that characterizes the Alcova Limestone.

5.4 DISCUSSION

5.4.1 Depositional setting

The $^{87}Sr/^{86}Sr$ ratios of the seven Alcova samples and single Baker Cabin Road sample are consistent with a marine origin for the Alcova Limestone. The carbonate-cemented thinly interbedded (less than 1 cm laminae) siltstone-sandstone interval at the base of the unit are thought to represent shoreline sediments composed of reworked coastal plain deposits of the upper Red Peak Formation (Lovelace and Lovelace, in press). The two highest samples are from an interval of thinly bedded silty carbonate that rapidly coarsen upward into the carbonate-cemented basal silty-sand of the overlying Crow Mountain Formation. The basal deposit is thought to represent deposition from a progradational shoreline, which was subsequently reworked by eolian processes (Cavarac and Flores, 1991; Jonson, 1993; Irmen and Vondra, 2000). This analysis is consistent with a regional regression observed in related strata of the western USA (Paull and Paull, 1994; Chapter 2).

The elevated $^{87}Sr/^{86}Sr$ of sample AS-2 may be the result of an increased silicate contribution from the silt component of the upper mixed carbonate-siliciclastic interval. It is in this interval that the Alcova Limestone rapidly (but gradationally) transitions into the basal sandstone of the overlying Crow Mountain Formation. Samples AS-3–7 are

composed of relatively pure limestone and more likely reflect ocean $^{87}Sr/^{86}Sr$ at the time of deposition.

5.4.2 $^{87}Sr/^{86}Sr$ Age estimates

The analytical precision of the data are high, although the possibility of addition of radiogenic Sr through diagenesis or the contribution from silicates (as suggested for sample AS-2) must be considered. Veizer and Compston (1976) suggested that detrital grains would have radiogenic Sr which, would elevate $^{87}Sr/^{86}Sr$ ratios (of sedimentary carbonate) and that minimum values at any given time would likely be the most reliable indicator of seawater composition. It is suggested that the diagenetic alteration of original marine $^{87}Sr/^{86}Sr$ is likely limited considering the regional consistency (for instance, sample AS-10 vs AS-3-7) with no covariance with oxygen and carbon stable isotopes (Storrs, 1991; Cavaroc and Flores, 1991).

A Spathian to earliest Anisian age is supported by $^{87}Sr/^{86}Sr$ ratios (Figure 1). This interpretation confirms the inferred age based on the vertebrate ichnofauna of the underlying Red Peak (Lovelace and Lovelace, in press) and hypothesized regional correlations with strata that have associated age control such as conodonts, vertebrates, and ammonites (Picard et al., 1969). $^{87}Sr/^{86}Sr$ results from the study are consistent with regional $^{87}Sr/^{86}Sr$ ratios (Appendix B) from those same correlated rocks (Kummel, 1954; Solien, 1979; Burke et al., 1982; Koepnick et al., 1990; Storrs, 1991; Marenco et al., 2008). Furthermore, the age range allows workers to make more accurately calibrate molecular phylogenies of clades such as Lepidosauromorpha (e.g., the proposed oldest

sauropterygian *Corosaurus*, which is thought to be the oldest lepidosauropmorph). Previously, specimens of *Corosaurus alcovensis* from the Alcova Limestone lacked convincing ages, making the timing of lepidosaur origins difficult to ascertain (Storrs, 1991; Rieppel, 1998; Benton and Donoghue, 2006).

5.5 CONCLUSIONS

The $^{87}Sr/^{86}Sr$ ratios reported herein from seven samples of the Alcova Limestone are indicative of a marine origin for this unit and may facilitate correlation with other regional strata. This marine interpretation based on new geochemical data is consistent with the sedimentological data. The Alcova Limestone conformably overlies the coastal plain to near-shore deposits of the underlying upper Red Peak Formation the upper Red Peak. The Alcova, in turn, is overlain by shoreface to foreshore and backshore eolian deposits of the Crow Mountain Formation. This is consistent with a short lived but extensive marine flooding of the former Wyoming platform followed by a progradational shoreline during the late Spathain regression.

The $^{87}Sr/^{86}Sr$ results also permit estimation of the age of the Alcova Limestone. A Spathian age is suggested by the position of the $^{87}Sr/^{86}Sr$ data on the global marine $^{87}Sr/^{86}Sr$ curve. The assignment of an age range for the Alcova Limestone confirms previously hypothesized timing of the origins of lepidosaurs, and provides a temporal minimum for the underlying upper Red Peak vertebrate ichnocoenoses. Further studies exploiting this isotopic system are suggested for more accurate regional correlation with specific beds of the Thaynes and Virgin formations, and to test hypotheses regarding the time-transgressive nature of the Alcova Limestone.

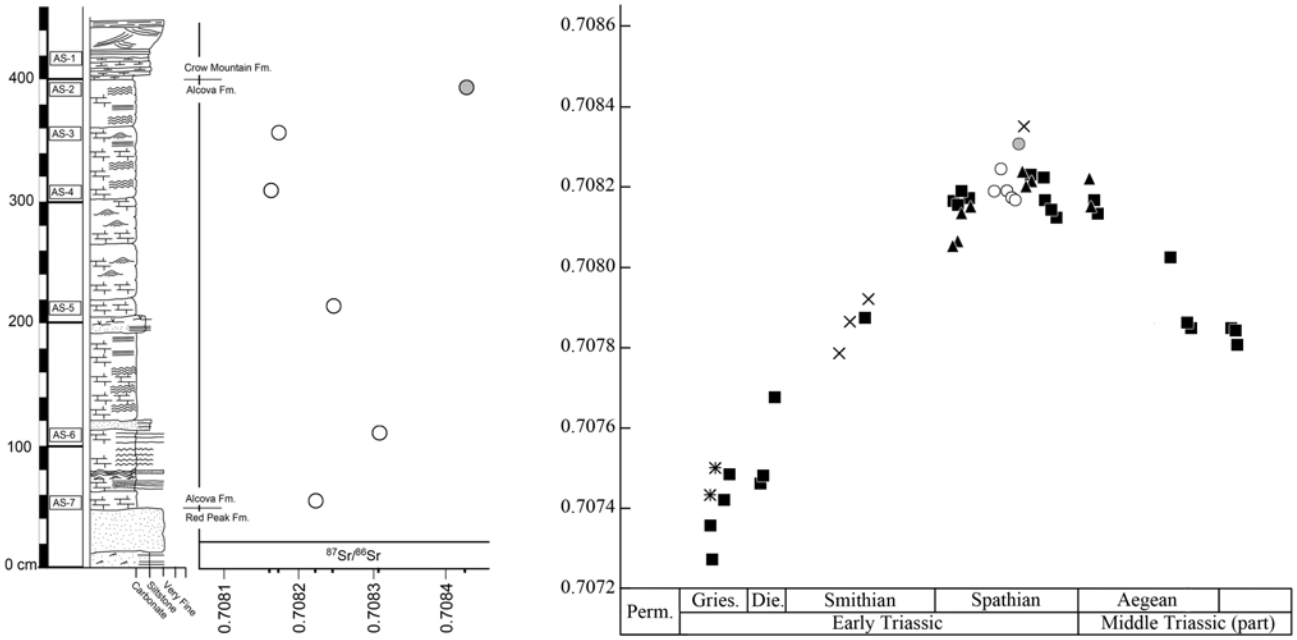

Figure 1—The figure above is a representative plot of regional and global $^{87}Sr/^{86}Sr$ values reported from Early–Middle Triassic strata. The stratigraphic column and associated $^{87}Sr/^{86}Sr$ values are shown on the left; the data are plotted (circles) in the inset box showing sample distribution with respect to stratigraphic position (*x*-axis). The data are arbitrarily placed on the *x*-axis along with the normally plotted data within the rectangle to demonstrate consistency with an Spathian–earliest Anisian age. Squares = Europe (Korte et al., 2003). Exes = Thaynes Formation (Burke et al., 1982). Asterix = Dinwoody Formation (Koepnick et al., 1990). Triangle = Virgin Limestone (Marenco et al., 2008). The X and shaded circle that lie above the rectangular box are both thought to represent data with slightly elevated radiogenic strontium (Koepnick et al., 1990).

CHAPTER 6

CONCLUSIONS

6.1 Summary of Conclusions

6.1.1 Chapter 2

The quantification of the sedimentary record provides a way to measure and compare changes in a dynamic systemdavid . This chapter is the first effort to quantify the sedimentary record of the Triassic of the western USA, which provides a means to test multiple hypotheses of local and regional significance.

The higher rates of sediment accumulation result in the obvious difference in sedimentary rock volume between the ET and LT suites. This quantitative result suggests that tectonic and climate-linked sedimentary supply (for instance, increase in sediment supply due to drying of the continental interior during the accretion of Pangea) played a strong role in the Early Triassic deposition. Late Triassic sedimentation, most notably the two widespread coarse-grained and conglomerate rich sandstone pulses, may represent the far-field effect of continental margin tectonics associated with arc terrane accretion events. Comparisons of the distribution of package duration is nearly identical to that calculated for the Phanerozoic of North America, which suggests that there are similar underlying tectonic controls, even at the continental, regional, and basin scales, that affect sediment accumulation and truncation.

6.1.2 Chapter 3

The Early Triassic and Late Triassic strata demonstrate significant differences in the spatiotemporal distribution of sedimentary properties, including fossil collections. The spatiotemporal distribution of track and body fossil diversity was quantified using data culled from the PaleoDB. Track diversity correlates well with sedimentation rate, number of sediment packages, and abundance of siltstone in the Early Triassic and Early Jurassic; both are post-extinction recovery intervals and may reflect a taphonomic bias in favor of track over body fossil preservation. The fossil record of tracks preserves a biological signal that is sometimes missing from the body fossil record such as: evolutionary transitions (e.g., Late Triassic sauropodomorph transition from facultative bipeds to columnar quadrupedality), expansion of temporal ranges, paleoecologic, and ethology. For instance the addition of vertebrate ichnologic data culled from the PaleoDB suggests an Early Triassic recovery of most major clades roughly 3 my earlier than the body fossil record suggested (a roughly 50% error in previous recovery estimates); and extends the stratigraphic range (and origins) of several clades, some more than 30 my (for instance, turtles). When the number of sedimentary packages (sample space) are considered, the end-Triassic extinction event appears to have been a much more contracted event than previously thought. The combination of biologic and geologic data sets allow for more rigorous testing of hypotheses and a broader understanding of the interdependent histories of these two systems.

6.1.3 Chapter 4

Lower Triassic rocks of central Wyoming, classically considered to be nearly devoid of fossils or evidence of life, preserve a previously undescribed ichnoassemblage that demonstrates a diverse paleoecology comparable to that observed in the better-

studied equivalent strata of the southwestern USA. The sedimentology of the upper platy facies is consistent with a semi-arid fluviolacustrine depositional environment. The general upward fining of the upper platy facies and the conformable contacts of the sandy facies and overlying Alcova Limestone record the transition from continental to marine deposition at the end of the Spathian; the event likely records the easternmost extent of the Thaynes-Virgin Formation transgression.

The Lower Triassic Red Peak Formation ichnoassemblage demonstrates a rich vertebrate and invertebrate ichnofauna. The dominance of the invertebrate ichnogenera *Palaeophycus* and *Fuersichnus*, and the presence of *Diplicnites*, *Lockeia*, and *Scoyenia*, is consistent with a shallow to ephemeral freshwater ichnocoenoses.

The presence of the vertebrate ichnogenera *Rhynchosauroides*, *Chirotherium barthii*, and *Rotodactylus* extend the paleobiogeographic range of these ichnogenera into the northern Rocky Mountain west, and the presence of *Chelonipus* marks the first Triassic occurrence of the ichnogenus in North America extending the known stratigraphic range by more than 30 my.

6.1.4 Chapter 5

The Alcova Limestone has long been used as a regional marker bed, but its utility effectively ended at its depositional edge. The $^{87}Sr/^{86}Sr$ ratios of the seven samples analyzed from this unit are indicative of a marine origin and may facilitate correlation with other strata in the region, and globally. The $^{87}Sr/^{86}Sr$ results support a conservative estimate of a late Spathian age for the Alcova Limestone. The assignment of an age for the Alcova Limestone confirms previously hypothesized timing of the origins of

lepidosaurs, and provides a temporal minimum for the underlying upper Red Peak vertebrate ichnocoenoses, making global comparisons possible.

6.2 Implications

The macrostratigraphic analysis of Triassic biologic and geologic records preserved in the well-exposed outcrops of the western USA provides a powerful tool to further interrogate these deposits. The studies in this dissertation make testable predictions regarding issues, such as the problem of the missing Middle Triassic sediments, the relationship between CIE's and Early Triassic sedimentation, and taphonomic biases that favor the preservation of tracks over body fossils, making tracks a highly useful proxy to temporally constrain the evolutionary origins of many major clades.

The prediction that tracks precede bone in the Early Triassic was supported during the investigation of the upper Red Peak Formation, a unit of rock previously thought to be nearly devoid of life; body fossils have yet to be observed. New occurrences of *Chelonipus*, the oldest occurrence in North America, push the presence of turtles on the continent back more than 30 million years. The remaining vertebrate ichnofuana is consistent with late Early Triassic assemblages around the globe, demonstrating a cosmopolitan distribution of most major clades by the end of the Early Triassic.

The $^{87}Sr/^{86}Sr$ ratios measured from the Alcova Limestone not only indicate a marine origin for this unit, but also provide a means to reasonably constrain the timing of deposition. An age range of mid-late Spathian supports the hypothesis that *Corosaurus* is the oldest sauropterygian and offers a minimum constraint for the origin of

Lepidosauromorpha confirming the proposed minimum range for molecular phylogenic calibrations of this clade. Refinement of dates, ages, or age ranges, such as this study of the Alcova Limestone, provide constraints required to increase the temporal resolution of future macrostratigraphic analyses. Combined quantitative and descriptive sedimentology and paleontology enable a more robust understanding of macroevolutionary patterns, the geological context in which they take place, and their relationships to each other.

BIBLIOGRAPHY

Armstrong, R.L., and Ward, P.L., 1993, Late Triassic to earliest Eocene magmatism in the North American Cordillera: implications for the Western Interior Basin: in Caldwell, W.G.E. and Kauffman, E.G., Eds., Evolution of the western interior basin: Geological Association of Canada, Special Paper 39, p. 472.

Aswasereelert, W., Meyer, S., Carroll, A.R., Peters, S.E., Smith, M.E., and Fiegl, K.L., in press, Basin-scale Cyclostratigraphy of the Green River Formation, Wyoming. Geology.

Avanzini, M., 2000, *Synaptichnium* tracks with skin impressions from the Anisian (Middle Triassic) of the Southern Alps (Val di Non – Italy): Ichnos, v. 7, p. 243–251.

Avanzini, M., Ceoloni, P., Conti, M.A., Leonardi, G., Manni, R., Mariotti, N., Mietto, P., Muraro, C., Nicosia, E., Sacchi, E., Santi, G., and Spezzamonte, M., 2001, Permian and Triassic tetrapod ichnofaunal units of Northern Italy: their potential contribution to continental biochronology: Natura Brescianna, Monografie 25, p. 89–107.

Avanzini, M. and Lockley, M., 2002, Middle Triasic archosaur population structure: interpretation based on *Isochirotherium delicatum* fossil footprints (Southern Alps, Italy): Palaeogeography, Palaeoclimatology, Palaeoecology, v. 185, p. 392–402.

Avanzini, M., GARCIA-RAMOS, J.C., LIRES, J., MENEGON, M., PIÑUELA L., and FERNANDEZ, L.A., 2005, Turtle tracks from the Late Jurassic of Asturias, Spain: Acta Palaeontologica Polonica, v. 50, n. 4, p. 743–755.

Avanzini, M., and Mietto, P., 2008, Lower and Middle Triassic footprint-based biochronology in the Italian Southern Alps: Oryctos, v. 8, p. 3–13.

Baldwin, C.T., 1974, The control of mud crack patterns by small gastropod trails: Journal of Sedimentary Petrology, v. 44, p. 695–697.

Beer, J., 2005, Sequence stratigraphy of fluvial and lacustrine deposits in the lower part of the Chinle Formation, south central Utah, United States: paleoclimatic and tectonic implications: Dissertation: University of Minnesota, 2005, 180 p.

Behrensmeyer, A.K., Damuth, J.D., DiMichele, W.A., Potts, R., Sues, H.-D., Wing, S.L. (Eds.), 1992. Terrestrial Ecosystems through Time—Evolutionary Paleoecology of Terres- trial Plants and Animals. University of Chicago Press, Chicago. 568 pp.

Benton, M., 1983, Dinosaur success in the Triassic: a noncompetitive ecological model: Quarterly Review of Biology, v. 58, no. 1, p. 29–55.

Benton, M. J., 2003, *When life nearly died: the greatest mass extinction of all time. London*, UK: Thames & Hudson.

Benton, M.J., 2010, The origins of modern biodiversity on land: Philosophical Transactions of the Royal Society B: Biological Sciences, v. 365, no. 1558, p. 3667–3679.

Benton, M., and Donoghue, P., 2007, Paleontological evidence to date the tree of life: Molecular biology and evolution, v. 24, no. 1, p. 26.

Berner, R., 2005, The carbon and sulfur cycles and atmospheric oxygen from middle Permian to middle Triassic: Geochimica et Cosmochimica Acta, v. 69, no. 13, p. 3211–3217.

Bestougeff, M.A., 1980, Bestougeff: Summary of world coal resources and reserves: 26th Int. Geol. Cong. Paris Colloq C-2, v. 35, p. 353–366.

Blakey, R., 1973, Stratigraphy and origin of the Moenkopi Formation (Triassic) of southeastern Utah: The Mountain Geologist, v. 10, no. 1, p. 1–17.

Blakey, R.C., 1974, Stratigraphic and depositional analysis of the Moenkopi Formation, Southeastern Utah: Utah Geological and Mineral Survey Bulletin 104, 81 p.

Blakey, R., 1977, Petroliferous lithosomes in the Moenkopi Formation, southern Utah: ds.heavyoil.utah.edu.

Blakey, R., and Gubitosa, R., 1984, Controls of sandstone body geometry and architecture in the Chinle Formation (Upper Triassic), Colorado Plateau: Sedimentary Geology, v. 38, no. 1-4, p. 51–86.

Blakey, R.C., Basham, E.L., and Cook, M.J., 1993, Early and Middle Triassic Pale~geography of the Colorado Plateau and Vicinity: Museum of Northern Arizona Bulletin, v. 59, p. 13–26.

Boyd, D.W., and Maughan, E.K., 1972, Permian-Triassic boundary in the middle Rocky Mountains: Bulletin of Canadian Petroleum Geology, v. 20, p 676.

Boyd, D.W., and Loope, D.B., 1984, Probable vertebrate origin for certain sole marks in Triassic Red Beds of Wyoming: Journal of Paleontology, v. 5, p. 467–476.

Branson, E.B., 1947, Triassic (Chugwater) footprints from Wyoming: Journal of Paleontology, v. 21, p. 588–590.

Bromley, R., and Asgaard, U., 1979, Triassic freshwater ichnocoenoses from Carlsberg Fjord, east Greenland: Palaeogeography, Palaeoclimatology, Palaeoecology, v. 28, p. 39–80.

Brusatte, S.L., Niedzwiedzki, G., and Butler, R.J., 2011, Footprints pull origin of diversification of dinosaur stem lineage deep into Early Triassic: Proceedings of the Royal Society B: Biological Sciences, v. 278, p. 1107–1113, doi: 10.1098/rspb.2010.1746.

Buatois, L.A., and Mángano, M.G., 1998, Trace fossil analysis of lacustrine facies and basins: Palaeogeography, Palaeoclimatology, Palaeoecology, v. 140, p. 367–382.

Burke, D.B., and Silberling, N.J., 1973, The Auld Lang Syne Group, of Late Triassic and Jurassic (?) age, north-central Nevada: Contributions to Stratigraphy: USGS Bulletin 1394-E, p. E1–E14.

Carson, C.J., 1998, The structural and stratigraphic framework of the Warm Springs Ranch area, Hot Springs County, Wyoming: Unpublished M.S. thesis: Oklahoma State University, 90 p.

Cavaroc, V.V., and Flores, R.M., 1991, Red beds of the Triassic Chugwater Group, Southwestern Powder River Basin, Wyoming: U.S. Geological Survey Bulletin 1917-E, 17 p.

Carini, G.F., 1964, Regional petrographic and paleontologic analysis of the Triassic Alcova Limestone Member in central Wyoming: Unpublished Ph.D. dissertation, University of Missouri, Columbia, 165 p.

Carroll, A.R., Stephens, N.P., Hendrix, M.S., and Glenn, C.R., 1998, Eolian-derived siltsone in the Upper Permian Phosphoria Formation: Implications for marine upwelling, Geology, v. 26, p. 1023– 1026, doi: 10.1130/0091-7613(1998)026<1023:EDSITU>2.3.CO;2.

Chan, M., 1999, Triassic loessite of north-central Utah; stratigraphy, petrophysical character, and paleoclimate implications: Journal of Sedimentary Research, v. 69, no. 2, p. 477–485.

Childs, O.E., 1985, Correlation of Stratigraphic Units of North America, COSUNA: American Association of Petroleum Geologists Bulletin, v. 69, no. 2, p. 173–180.

Clark, D.L., 1957, Marine triassic stratigraphy in the eastern Great Basin: American Association of Petroleum Geologists Bulletin, v. 41, no. 10, p. 2192–2222.

Clemmensen, L.B., 1978, Lacustrine facies and stromatolites from the Middle Triassic of East Greenland: Journal of Sedimentary Research, v. 48, p. 1111– 1127.

Cleveland, D., and Atchley, S., 2007, Continental Sequence Stratigraphy of the Upper Triassic (Norian Rhaetian) Chinle Strata, Northern New Mexico, USA: Allocyclic and Autocyclic Origins of Paleosols: Journal of Sedimentary Research.

Cohen, A., Lockley, M., Halfpenny, J., and Michel, A.E., 1991, Modern vertebrate track taphonomy at Lake Manyara, Tanzania: PALAIOS, v. 6, p. 371–389.

Colbert, E.H., 1957, Triassic Vertebrates of the Wind River Basin: Wyoming Geological Association Guidebook, v. 12, p. 89–93.

Colombi, C.E., and Parrish, J.T., 2008, Late Triassic environmental evolution in southwestern Pangea: PLANT taphonomy of the Ischigualasto Formation: PALAIOS, v. 23, no. 12, p. 778–795, doi: 10.2110/palo.2007.p07–101r.

Corsetti, F., Baud, A., Marenco, P., and Richoz, S., 2005, Summary of Early Triassic carbon isotope records: Comptes Rendus Palevol, v. 4, no. 6-7, p. 473–486.

Cuadrado, D.G., Carmona, N.B., and Bournod, C., 2011, Biostabilization of sediments by microbial mats in a temperate siliciclastic tidal flat, Bahia Blanca estuary (Argintina): Sedimentary Geology, v. 237, p. 95–101, doi: 10.1016/j.sedgeo.2011.02.008.

Demathieu, G.R., 1989, Appearance of the first dinosaur tracks in the French Middle Triassic and their probable significance, in Gillette, D.D., and Lockley, M.G., eds, Dinosaur Tracks and Traces: Cambridge University Press, New York, p. 201– 207.

Demathieu, G., and Gand, G., 1992, La palichnofaune des bassins permiens provençaux: Geobios, v. 25, p. 19– 54.

Demathieu, G., and Demathieu, D., 2004, Chirotheria and other ichnotaxa of the European Triassic: Ichnos, v. 11, p 79–88.

Depaolo, D.J., and Ingram, B.L., 1985, High-resolution stratigraphy with strontium isotopes: Science, v. 227, no. 4689, p. 938.

Dickinson, W.R., and Gehrels, G., 2000, Sandstone petrofacies of detrital zircon samples from Paleozoic and Triassic strata in suspect terranes of northern California: in Soreghan, M.J., and Gehrels., G.E., eds., Paleozoic and Triassic Paleogeography and Tectonics of Western Nevada and California: Boulder, CO, Geological Society of America Special Paper 347, p. 151–171.

Dickinson, W.R., and Gehrels, G.E., 2008, U-Pb Ages of Detrital Zircons in Relation to Paleogeography: Triassic Paleodrainage Networks and Sediment Dispersal Across Southwest Laurentia: Journal of Sedimentary Research, v. 78, no. 12, p. 745–764, doi: 10.2110/jsr.2008.088.

Dickinson, W.R., Gehrels, G.E., and Stern, R.J., 2010, Late Triassic Texas uplift preceding Jurassic opening of the Gulf of Mexico: Evidence from U-Pb ages of detrital zircons: Geosphere, v. 6, no. 5, p. 641–662.

Díaz-Martínez, Pérez-Lorente, F., Canudo, J.I., and Pereda-Suberbiola, X., 2009, Causas de la variabilidad en icnitas de dinosaurios y su aplicación en icnotaxonomía: Actas de las IV Jornadas Internacionales sobre Paleontología de Dinosaurios y su Entorno, p. 207–220.

Diedrich, C., 2002, Vertebrate track bed stratigraphy at new megatrack sites in the Upper Wellenkalk Member and *orbicularis* Member (Muschelkalk, Middle Triassic) in carbonate tidal flat environments of the western Germanic Basin: Palaeogeography, Palaeoclimatology, Palaeoecology, v. 183, p. 185–208.

Diedrich, C., 2005, Actuopalaeontological track experiments with *Iguana* on intertidal flat carbonates of the Arabian Gulf—a comparison to fossil *Rhynchosauroides* tracks of Triassic carbonate tidal flat megatrack sites in the European Germanic Basin: Senckenbergiana maritima, v. 35, p. 203–220.

Diedrich, C., 2008, Millions of reptile tracks–Early to Middle Triassic carbonate tidal flat migration bridges of Central Europe–Reptile immigration into the Germanic Basin: Palaeogeography, Palaeoclimatology, Palaeoecology, v. 259, p. 410–423, doi: 10.1016/j.palaeo.2007.09.019.

Diedrich, C., 2009, Palaeogeographic evolution of the Middle Triassic marine Germanic Basin changements – With emphasis on the carbonate tidal flat and shallow marine habitats of reptiles in Central Pangea: Global and Planetary Change, v. 65, p. 27–55, doi: 10.1016/j.gloplacha.2008.11.002.

Dubiel, R.F., 1994, Triassic deposystems, paleogeography, and paleoclimate of the western interior: in Mesozoic Systems of the Rocky Mountain Region, USA, Caputo, Mario V., Peterson, James A., and Franczyk, Karen J., (eds.),, p. 133–168.

Dunagan, S.P., and Driese, S.G., 1999, Control of terrestrial stabilization of late Devonian palustrine carbonate deposition: catskill magnafacies New York, USA: Journal of Sedimentary Research, v. 69, p. 772–783.

Ekdale, A.A., and De Gilbert, J.M., 2010, Paleoetholigic significance of bioglyphs: fingerprints of the subterraneans: PALAIOS, v. 8, p. 540–545, doi: 10.2110/palo.2009.p09–066r.

Elderfield, H., 1986, Strontium isotope stratigraphy: Palaeogeography Palaeoclimatology Palaeoecology, v. 57, no. 1, p. 71–90.

Embry, A.F., 1988, Otapirian Stage: Its fauna and microflora: International Association of Sedimentologists Special Publication 42, p. 249–260.

Erwin, D., 1990, The end-Permian mass extinction: Annual Review of Ecology and Systematics, v. 21, no. 1, p. 69–91.

Falkingham, P.L., Margetts, L., and Manning, P.L., 2010, Fossil vertebrate tracks as paleopenetrometers: confounding effects of foot morphology: PALAIOS, v. 25, p.356.360, doi: 10.2110/palo.2009.p09–164r.

Fagerstrom, J.A., 1987, The Evolution of Reef Communities. John Wiley & Sons, New York, NY. 600 pp.

Fielding, C.R., 2011, Foreland basin structural growth recorded in the Turonian Ferron Sandstone of the Western Interior Seaway Basin, USA: Geology, v. 39, no. 12, p. 1107–1110, doi: 10.1130/G32411.1.

Fitcher, J., and Kunz, R., 2004, New genus and species of chirotheroid tracks in the Detfurth-Formation (Middle Triassic) of central Germany: Ichnos, v. 11, p. 183–193, doi: 10.1080/10420940490444997.

Fiorillo, A.R., Turtle tracks in the Judith River Formation (Upper Creataceous) of south-central Montana: Paleontologica Electronica, v. 8, 11 p.

Foster, J., Lockley, M.G., and Brockett, J. 1999, Possible turtle tracks from the Morrison Formation of southern Utah: Utah Geological Survey Miscellaneous Publication 99, p. 185–191.

Foote, M., 2000, Origination and extinction components of taxonomic diversity: Paleozoic and post-Paleozoic dynamics: Paleobiology, v. 26, no. 4, p. 578–605.

Galfetti, T., Bucher, H., Brayard, A., Hochuli, P., Weissert, H., Guodun, K., Atudorei, V., and Guex, J., 2007, Late Early Triassic climate change: Insights from carbonate carbon isotopes, sedimentary evolution and ammonoid paleobiogeography: Palaeogeography Palaeoclimatology Palaeoecology, v. 243, no. 3-4, p. 394–411.

Gregor, C. B., 1985, The mass-age distribution of Phanerozoic sediments, in Snelling, N. J., ed., The chronology of the geologic record: Geol. Soc. America Mem. 10, p. 284– 289.

Goodspeed, T., and Lucas, S.G., 2007, Stratigraphy, sedimentology, and sequence stratigraphy of the Lower Triassic Sinbad Formation, San Rafael Swell, Utah: in Lucas S.G. and Spielmann J.A., eds., Triassic of the American West: New Mexico Museum of Natural History and Science Bulletin, v. 40, p. 91–102.

Hallam, A., 1992, Phanerozoic Sea-Level Changes. Columbia University Press, New York, NY. 277 pp.

Hallam, A., and Wignall, P.B., 1999, Mass extinctions and sea-level changes: Earth-Science Reviews, v. 48, no. 4, p. 217–250.

Hamblin, A.H. and Foster, J.R., 2000, Ancient animal footprints and traces in the Grand Staircase-Escalante National Monument, South-Central Utah: Utah Geological Association, Publication 28, p. 557– 568.

Hannisdal, B., and Peters, S.E., 2010, On the Relationship between Macrostratigraphy and Geological Processes: Quantitative Information Capture and Sampling Robustness: The Journal of Geology, v. 118, no. 2, p. 111–130, doi: 10.1086/650180.

Haq, B., Hardenbol, J., and Vail, P., 1987, Chronology of fluctuating sea levels since the Triassic: Science, v. 235, no. 4793, p. 1156.

Hasiotis, S.T., 2002, Continental Trace Fossils: Society of Sedimentary Geology Short Course Notes 51, 132 p.

Hasiotis, S.T., 2004, Reconnaissance of Upper Jurassic Morrison Formation ichnofossils, Rocky Mountain Region, USA: Paleoenvironmental, stratigraphic, and paleoclimatic significance: Sedimentary Geology, v. 167, p. 177–268, doi: 10.1016/j.sedgeo.2004.01.006.

Hasiotis, S.T., 2007, Continental ichnology: Fundamental processes and controls on trace fossil distribution, *in* Miller, W., III, ed., Trace Fossils: Concepts, Problems, Prospects: Elsevier, Amsterdam, p. 262–278.

Hasiotis, S.T., 2008, Reply to the Comments by Bromley et al. of the paper "Reconnaissance of the Upper Jurassic Morrison Formation ichnofossils, Rocky Mountain Region, USA: Paleoenvironmental, stratigraphic, and paleoclimatic significance of terrestrial and freshwater ichnocoenoses" by Stephen T. Hasiotis: Sedimentary Geology, v. 208, no. 1-2, p. 61–68, doi: 10.1016/j.sedgeo.2008.04.004.

Haubold, H., 1971a, Ichnia Amphibiorum et Reptiliorum fossilium, *in* Kuhn, O., ed., Handbuch der Palaeoherpetologie: Fischer, Stuttgart, v. 18, p.1–24.

Haubold, H. 1971b, Die Tetrapodenfährten des Buntsandsteins in der DDR und WD und ihre Äquivalente in der gesamten Trias: Paläontologische Abhandlungen A Paläozoologie, v. 4, p 395–548.

Haubold, H., 1984, Saurierfährten: DieNeueBrehm−Bücherei, A. Ziemsen, Wittenberg−Lutherstadt. 231 p.

Hay, W., and Wold, C., 1998, The role of mountains and plateaus in a Triassic climate model: Tectonic Boundary Conditions for Climate Reconstructions.

Heckert, A.B., Lucas, S.G., and Hunt, A.P., 2005, Triassic vertebrate fossils in Arizona, *in* Heckert, A.B., and Lucas, S.G., eds., Vertebrate Paleontology in Arizona: New Mexico Museum of Natural History and Science Bulletin 29, p. 16–44.

Heckert, A. B., Lucas, S. G., Dickinson, W. B., Mortensen, J. K., 2009. New ID-TIMS U-Pb ages for Chinle Group strata (Upper Triassic) in New Mexico and Arizona, correlation to the Newark Supergroup, and implications for the "long Norian." Geological Society of America, Abstracts with Programs 41 (7), 123.

Heim, N.A., Peters, S.E., 2011, Covariation in macrostratigraphic and macroevolutionary patterns in the marine record of North America. Geol Soc Am Bull 123:620–630

Heller, P.L., Dueker, K., and Mcmillan, M.E., 2003, Post-Paleozoic alluvial gravel transport as evidence of continental tilting in the U.S. Cordillera: Geological Society of America Bulletin, v. 115, no. 9, p. 1122, doi: 10.1130/B25219.1.

High JR., L.R., and Picard, D.M., 1967, Rock units and revised nomenclature, Chugwater Group (Triassic), western Wyoming: Mountain Geology, v. 4, p.73–81.

High, L.R., and Picard, M.D., 1969, Stratigraphic Relations Within Upper Chugwater Group (Triassic), Wyoming: American Association of Petroleum Geology Bulletin, v. 53, no. 5, p. 1093–1104.

Horacek, M., Brandner, R., and Abart, R., 2007, Carbon isotope record of the P/T boundary and the Lower Triassic in the Southern Alps: evidence for rapid changes in storage of organic carbon: Palaeogeography Palaeoclimatology Palaeoecology, v. 252, no. 1-2, p. 347–354.

Hubert, J.F., and Hyde, M.G., 1982, Sheet-flow deposits of graded beds and mudstones on an alluvial sandflat-playa system: upper Triassic Blomidon redbeds, St Mary's Bay, Nova Scotia: Sedimentology, v. 29, p. 457-474.

Hunt, A.P., Santucci, V., Lockley, M., and Olson, T., 1993, Dicynodont trackways from the Holbrook Member of the Moenkopi Formation (Middle Triassic: Anisian), Arizona, USA: The Nonmarine Triassic. New Mexico Museum of Natural History & Science Bulletin, v. 3, p. 213–218.

Hunt, A.P., and Lucas, S.G., 2007a, The Triassic tetrapod track record: Ichnofaunas, ichnofacies and biochronology, *in* Lucas S.G. and Spielmann, J.A., eds., The Global Triassic: New Mexico Museum of Natural History and Science Bulletin 41, pg. 78–87.

Hunt, A.P., and Lucas, S.G., 2007b, Late Triassic tetrapod tracks of western North America, *in* Lucas S.G. and Spielmann J.A., eds., Triassic of the American West: New Mexico Museum of Natural History and Science Bulletin 40. p. 215–230.

Hunt, A.P., and Lucas, S.G., 2007c, A new tetrapod ichnogenus from the Upper Triassic of New Mexico, with notes on the ichnotaxonomy of *Rhynchosauroides*, *in* Lucas, S.G. and Spielmann, J.A., eds., The Global Triassic: New Mexico Museum of Natural History and Science Bulletin 41, p 71–77.

Irmen, A., and Vondra, C., 2000, Aeolian sediments in lower to middle (?) Triassic rocks of central Wyoming: Sedimentary Geology, v. 132, no. 1-2, p. 69–88.

Irmis, R., Nesbitt, S., Padian, K., and Smith, N., 2007, A Late Triassic Dinosauromorph Assemblage from New Mexico and the Rise of Dinosaurs: Science.

Irmis, R.B., Mundil, R., Martz, J.W., and Parker, W.G., 2011, High-resolution U–Pb ages from the Upper Triassic Chinle Formation (New Mexico, USA) support a diachronous rise of dinosaurs: Earth and Planetary Science Letters, v. 309, no. 3-4, p. 258–267, doi: 10.1016/j.epsl.2011.07.015.

Jennings, D.S., and Hasiotis, S.T., 2006, Taphonomic analysis of a dinosaur feeding site using geographic information systems (GIS), Morrison Formation, southern Bighorn Basin, Wyoming, USA: PALAIOS, v. 21, p. 480–492, doi: 10.2110/palo.2005.P05-062R.

Jenny, H., 1941, Factors of soil formation: a system of pedology, p. 281.

Johnson, E.A., 1993a, Depositional history of Triassic rocks in the area of the Powder River Basin, northeastern Wyoming and southeastern Montana: U.S. Geological Survey Bulletin 1917-P, 30 p.

Johnson, S.Y, 1993b, Significance of loessite in the Maroon Formation (middle Pennsylvanian to lower Permain), Eagle Basin, Northwest Colorado: Journal of Sedimentary Research, v. 59, p. 782–791.

Joyce, W.G., and Gauthier, J.A., 2004, Palaeoecology of Triassic stem turtles sheds new light on turtle origins: Proceedings of the Royal Society B: Biological Sciences, v. 271, p. 1–5, doi: 10.1098/rspb.2003.2523.

Joyce, W.G., Lucas, S.G., Scheyer, T.M., Heckert, A.B., and HUNT, A.P., 2009, A thin-shelled reptile from the Late Triassic of North America and the origin of the turtle shell: Proceedings of the Royal Society B: Biological Sciences, v. 276, p. 507–513, doi: 10.1098/rspb.2008.1196.

Kanhalangsy, K., 1997, Petrography, geochemistry, and clay mineralogy of a paleosol in the Dockum Group (Triassic), Texas Panhandle: dspace.lib.ttu.edu.

Kaup, J.J., 1835, Mitteilung über Tierfärhten bei Hildburghausen: Neues Jahrbuch für Mineralogie Geologie und Paläontologie, 1835, p. 327–328.

Kidwell, S.M., Behrensmeyer, A.K. (Eds.), 1993. Taphonomic Approaches to Time Resolution in Fossil Assemblages. Paleontological Short Course, vol. 6. 302 pp.

Klein, H., and Lucas, S., 2010, Tetrapod footprints-their use in biostratigraphy and biochronology of the Triassic: Geological Society London Special Publications, v. 334, no. 1, p. 419–436, doi: 10.1144/SP334.14.

Klein, H., Voigt, S., Hminna, A., Saber, H., Schneider, J., and Hmich, D., 2010, Early Triassic Archosaur-Dominated Footprint Assemblage from the Argana Basin (Western High Atlas, Morocco): Ichnos, v. 17, no. 3, p. 215–227, doi: 10.1080/10420940.2010.510030.

Knoll, A.H., Bambach, R.K., Canfield, D.E., and Grotzinger, J.P., 1996, Comparative Earth History and Late Permian Mass Extinction: Science, v. 273, no. 5274, p. 452–457, doi: 10.1126/science.273.5274.452.

Knoll, A.H., 2003, The geological consequences of evolution: Geobiology, v. 1, no. 1, p. 3–14.

Koepnick, R., Denison, R., and Burke, W., 1990, Construction of the Triassic and Jurassic portion of the Phanerozoic curve of seawater $^{87}Sr/^{86}Sr$: Chemical Geology, no. 80, p. 327–349.

Korte, C., Kozur, H., Bruckschen, P., and Veizer, J., 2003, Strontium isotope evolution of Late Permian and Triassic seawater: Geochimica et Cosmochimica Acta.

Korte, C., Kozur, H., and Veizer, J., 2005, [delta] 13C and [delta] 18O values of Triassic brachiopods and carbonate rocks as proxies for coeval seawater and palaeotemperature: Palaeogeography Palaeoclimatology Palaeoecology, v. 226, no. 3-4, p. 287–306.

Kozur, H.W., and Weems, R.E., 2010, The biostratigraphic importance of conchostracans in the continental Triassic of the northern hemisphere: Geological Society, London, Special Publications v. 334, p. 315–417, doi: 10.1144/SP334.13.

Kubo, T., and Benton, M.J., 2009, Tetrapod postural shift estimated from Permian and Triassic trackways: Palaeontology, v. 52, p. 1029-1037, doi: 10.1111/j.1475-4983.2009.00987.x.

Kummel, B., 1954, Triassic Stratigraphy of Southeastern Idaho and adjacent areas: Geological Survey Professional Paper 254-H, p. 1–28.

Langer, M.C., Ezcurra, M.D., Bittencourt, J.S., and Novas, F.E., 2010, The origin and early evolution of dinosaurs: Biological Reviews, v. 85, p. 55–110.

Lawton, T.F., 1994, Tectonic setting of Mesozoic sedimentary basins, Rocky Mountain Region, USA: in Mesozoic Systems of the Rocky Mountain Region, USA, Caputo, Mario V., Peterson, James A., and Franczyk, Karen J., (eds.), p. 1–25.

Lehman, T., and Chatterjee, S., 2005, Depositional setting and vertebrate biostratigraphy of the Triassic Dockum Group of Texas: Journal of Earth System Science, v. 114, no. 3, p. 325–351.

Lerner, A.J, Lucas, S.G., and Spielmann, J.A., 2007, Invertebrate ichnoassemblage from the Triassic Moenkopi Group in North-Central Utah, *in* Lucas S.G., and Spielmann, J.A., eds., Triassic of the American West: New Mexico Museum of Natural History and Science Bulletin 40, p. 203–207.

Li, C., Xiao-Chun, W., Rieppel, O., Li-Ting, W., and Li-Jun, Z., 2008, An ancestral turtle from the Late Triassic of southwestern China: Nature, v. 456, p. 497-501.

Lockley, M.G., 1998, The Vertebrate Track Record: Nature, v. 396, p. 429–432.

Lockley, M.G., and Hunt, A.P., 1994, A review of vertebrate ichnofaunas of the western interior United States: evidence and implications, *in* Caputo, M.V., Peterson, J.A., and Franczyk, K.J., eds., Mesozoic Systems of the Rocky Mountain Region, United States, p. 95–108.

Lockley, M.G. AND Foster, J., 2006, Dinosaur and turtle tracks from the Morrison Formation (Upper Jurassic) of Colorado National Monument, with observations on the taxonomy of vertebrate swim tracks. *in* Foster, J.R. and Lucas, S.G., eds., Paleontology and Geology of the Upper Jurassic Morrison Formation, New Mexico Museum of Natural History and Science Bulletin 36, p. 193–198.

Lockley, M.G., and Milner, A.C., 2006, Tetrapod tracksites from the Shinarump Formation (Chinle Group, Upper Triassic) of Southwestern Utah: In: Harris et al., eds., 2006, The Triassic-Jurassic Terrestrial Transition. New Mexico Museum of Natural History and Science Bulletin, v. 37, p. 257–262.

Lockley, M.G., Conrad, K., Paquette, M., and Hamblin, A., 1992, Late Triassic vertebrate tracks in the Dinosaur National Monument area: Geological Society of America Miscellaneous Publication 92-3, p. 383–392.

Lockley, M.G., Hunt, A.P., and Meyer, C.A., 1994, Vertebrate tracks and the ichnofacies concept: implications for palaeoecology and palichnostratigraphy, *in* Donovan, S.K., ed., The Palaeobiology of Trace Fossils: Wiley, Chinchester, p. 241–268.

Love, J.D., 1948, Mesozoic stratigraphy of the Wind River Basin, central Wyoming: Wyoming Geological Association 3rd Annual Guidebook, p. 96–111.

Love, J.D., 1957, Stratigraphy and correlation of Triassic rocks in central Wyoming: Wyoming Geological Association 12th Annual Guidebook, p. 39–45.

Lovelace, D.M., and Lovelace, S.D., In Press, Paleoenvironments and paleoecology of an Early Triassic invertebrate and vertebrate ichnoassemblage from the Red Peak Formation (Chugwater Group), central Wyoming: PALAIOS.

Lucas, S., 1991, Sequence stratigraphic correlation of nonmarine and marine Late Triassic biochronologies, western United States: Albertiana.

Lucas, S. G., 1998, Global Triassic tetrapod biostratigraphy and biochronology: Palaeogeography, Palaeoclimatology, Palaeoecology, v. 143, p. 347–384.

Lucas, S.G., 1999. Tetrapod-based correlation of the nonmarine Triassic. Zentralblatt für Geologie und Paläontologie Teil I 7–8, 497–521.

Lucas, S.G., 2010, The Triassic timescale based on nonmarine tetrapod biostratigraphy and biochronology: Geological Society London Special Publications, v. 334, no. 1, p. 447–500.

Lucas, S.G., Heckert, A.B., and Hunt, A.P., 2000, Probable turtle from the Upper Triassic of east-central New Mexico: Neues Jahrbuch für Geologie und Paläontologie, Monatshefte, v. 5, p. 287–300.

Lucas, S.G., Heckert, A.B., and Hunt, A.P., 2001, Triassic stratigraphy, biostratigraphy and correlation in east-central New Mexico: Geology of the Llano Estacado: New Mexico Geological Society 52nd Annual Field Conference, p. 85–102.

Lucas, S.G., Heckert, A.B., and Hotton-III, N., 2002, The ryhnchosaur Hyperodapedon from the Upper Triassic of Wyoming and its global biochronological significance: in Heckert, A.B., and Lucas, S.G., (eds) Upper Triassic Stratigraphy and Paleontology, New Mexico Museum of Natural History and Science Bulletin, v. 21, p. 149–156.

Lucas, S.G, Lerner, A., Spielmann, J.A., and Hunt, A.P., 2006, Invertebrate ichnofossils from the Upper Triassic Bull Canyon Formation, east-central New Mexico, *in* Harris et al., eds., The Triassic-Jurassic Terrestrial Transition: New Mexico Museum of Natural History and Science Bulletin 37, p. 118–121.

Lucas, S.G., Heckert, A.B., and Hunt, A.P., 2003, Tetrapod footprints from the Middle Triassic (Perovkan-early Anisian) Moenkopi Formation, west-central New Mexico: New Mexico Geological Society Guidebook, v. 52, p. 177–180

Lucas, S.G., and Lerner, A.J., 2006, Invertebrate ichnofossil assemblages of the Upper Triassic Redonda Formation at Mesa Redonda, east-central New Mexico, *in* Harris et al., eds., The Triassic-Jurassic Terrestrial Transition: New Mexico Museum of Natural History and Science Bulletin 37, p. 122–127.

Lucas, S., and Tanner, L., 2007, Tetrapod biostratigraphy and biochronology of the Triassic-Jurassic transition on the southern Colorado Plateau, USA: Palaeogeography Palaeoclimatology Palaeoecology, v. 244, no. 1-4, p. 242–256.

Lucas, S.G., Krainer, K., and Milner, A.R.C., 2007, The type section and age of the Timpoweap Member and stratigraphic nomenclature of the Triassic Moenkopi Group in southwestern Utah: Triassic of the American West: New Mexico Museum of Natural History and Science, Bulletin, v. 40, p. 109–117.

Lucas, S.G., Tanner, L.H., Kozur, H.W., Weems, R.E., and Heckert, A.B., 2012, The Late Triassic timescale: Age and correlation of the Carnian-Norian boundary: Earth-Science Reviews,, p. 1–89, doi: 10.1016/j.earscirev.2012.04.002.

Lull, R.S., 1942, Chugwater footprints from Wyoming: American Journal of Science, v. 240, p. 500–504.

Machalski, M., and Machalska, K., 1994, Arthropod trackways, "*Diplichnites*" *triassicus* (Link, 1943), from the Lower Triassic (Buntsandstein) fluvial deposits of the Holy Cross Mts, Central Poland: Acta Geologica Polonica, v. 44, p. 267–275.

Mack, G.A., Leeder, M., Perez-Arlucea, M., and Bailey, B.D.J., 2003, Early Permain silt-bed fluvial sedimentation in the Orogrande basin of the Ancestral Rocky Mountains, New Mexico, USA: Sedimentary Geology, v. 160, p. 159–178, doi: 10.1016/S0037-0738(02)00375-5.

Maidwell, F.T., 1911, Notes on footprints from the Keuper of Runcorn Hill, Proceedings of the Liverpool Geological Society, v. 11, p. 140–152.

Manning, P.L., 2004, A new approach to the analysis and interpretation of tracks: Examples from the dinosauria, *in* McIlroy, D., ed., The Application of Ichnology to Palaeoenvironmental and Stratigraphic Analysis: Geological Society, London, p. 93–123.

Marenco, P., Corsetti, F., and Kaufman, A., 2008, Environmental and diagenetic variations in carbonate associated sulfate: An investigation of CAS in the Lower Triassic of the western USA: Geochimica et Cosmochimica Acta.

Mariscano, C.A., Domnanovich, N.S., and Mancuso, A.C., 2007, Dinosaur origins: evidence from the footprint record: Historical Biology, v. 19, p. 83–91, doi: 10.1080/08912960600866920.

Mariscano, C.A., Mancuso, A.C., Palma, R.M., and Krapovickas, V., 2010, Tetrapod tracks in a marginal lacustrine setting (Middle Triassic, Argentina): Taphonomy and significance: Palaeogeography, Palaeoclimatology, Palaeoecology, v. 291, p. 388-399, doi: 10.1016/j.palaeo.2010.03.009.

Martz, J.W., and Parker, W.G., 2010, Revised Lithostratigraphy of the Sonsela Member (Chinle Formation, Upper Triassic) in the Southern Part of Petrified Forest National Park, Arizona: PloS one, v. 5, no. 2, p. e9329, doi: 10.1371/journal.pone.0009329.g014.

Marzolf, J.E., 1994, Reconstruction of the Early Mesozoic cordilleran cratonal margin adjacent to the Colorado plateau : in: Mesozoic Systems of the Rocky Mountain Region, USA, Mario V. Caputo, James A. Peterson and Karen J. Franczyk, eds., p. 181–216.

McArthur, J., 2007, Recent trends in strontium isotope stratigraphy: Terra Nova, v. 6, no. 4, p. 331–358.

Mccormick, C., and Picard, M., 1969, Petrology of gartra formation (triassic), uinta mountain area, utah and colorado: Journal of Sedimentary Research, v. 39, no. 4, p. 1484.

McKee, E.D., 1954, Stratigraphy and History of the Moenkopi Formation of Triassic Aga: The Geological Society of America Memoir, v. 61, p. 1–123.

Mckee, E.D., Oriel, S.S., Ketner, K.B., Maclachlan, M.E., Goldsmith, J.W., Maclachlan, J.C., and Mudge, M.R., 1959, Paleotectonic maps of the Triassic System: U.S. Geological Survey Miscellaneous Geological Investigations Map I-300, 33 p.

Mclellan, R.C., 1968, Stratigraphy of Chugwater Group (Triassic), east side of Bighorn Mountains, Wyoming and Montana: Unpublished M.S. thesis, University of Nebraska, Lincoln, 212 p.

Mcnaughton, R.B., and Pickerill, R.K., 1995, Invertebrate ichnology of the nonmarine LePreau Formation (Triassic), southern New Brunswick, eastern Canada: Journal of Paleontology, v. 69, p. 160–171.

Melchor, R.N, Bedatou, E., De Balais, S., and Genise, J.F., 2006, Lithofacies of invertebrate and vertebrate trace-fossil assemblages in an Early Mesozoic ephemeral fluvio-lacustrine system from Argentina: implications for the *Scoyenia* ichnofacies: Palaeogeography, Palaeoclimatology, Palaeoecology, v. 239, p. 253–285, doi:10.1016/j.palaeo.2006.01.011.

Michaelsen, P., 2002, Mass extinction of peat-forming plants and the effect on fluvial styles across the Permian–Triassic boundary, northern Bowen Basin, Australia: Palaeogeography Palaeoclimatology Palaeoecology, v. 179, no. 3, p. 173–188.

Mickleson, D.L., Huntoon, J. and Kvale, E.P., 2006a, The diversity and stratigraphic distribution of pre-dinosaurian communities from the Triassic Moenkopi Formation: New Mexico Museum of Natural History and Science Bulletin 34, p. 132–137.

Mickleson, D.L., Milner, A.R.C., Deblieux, D.D. and Mcguire, J.L., 2006b, The oldest Early Triassic fossil vertebrate footprints in North America, from Zion National Park, Utah: New Mexico Museum of Natural History and Science Bulletin 34, p. 141–144.

Milán, J., and BROMLEY, R.G., 2006, True tracks, undertracks and eroded tracks, experimental work with tetrapod tracks in laboratory and field: Palaeogeography, Palaeoclimatology, Palaeoecology, v. 231, p. 253–264.

Milán, J., and BROMLEY, R.G., 2008, The impact of sediment consistence on track and undertrack morphology: Experiments with emu tracks in layered cement: Ichnos, v. 15, p. 19–27.

Milner A.R.C., Lockley M.G., and Kirkland J.I., 2006, A large collection of well preserved theropod dinosaur swim tracks from the Lower Jurassic Moenave Formation, St. George, Utah, *in* Harris J.D., Lucas S.G., Spielmann J.A., Lockley M.G., Milner A.R.C., et al., eds., The Triassic-Jurassic Terrestrial Transition: New Mexico Museum of Natural History and Science Bulletin, v. 37, p. 315–328.

Minter, N.J., Krainer, K., Lucas, S.G., Braddy, S.J., and Hunt, A.P., 2007, Palaeoecology of an Early Permian playa lake trace fossil assemblage from Castle Peak, Texas, USA: Palaeogeography, Palaeoclimatology, Palaeoecology, v. 246, p. 390–423, doi: 10.1016/j.palaeo.2006.10.009.

Morales, M., 1987, Terrestrial fauna and flora from the Triassic Moenkopi Formation of the southwestern United States: Journal of the Arizona-Nevada Academy of Science, v. 22, p. 1–19.

Mundil, R., Palfy, J., Renne, P. R., and Brack, P. 2010, The Triassic timescale: new constraints and a review of geochronological data. In: LUCAS, S. G. (ed.) The Triassic Timescale. Geological Society, London, Special Publications, 334, p. 41–59.

Muttoni, G., Kent, D., Jadoul, F., Olsen, P., and Rigo, M., 2010, Rhaetian magneto-biostratigraphy from the Southern Alps (Italy), Palaeogeography Palaeoclimatology Palaeoecology, v. 285, p. 1–16.

Nesbitt, S.J., 2011, The Early Evolution of Archosaurs: Relationships and the Origin of Major Clades: http://dx.doi.org/10.1206/352.1.

Nesbitt, S., and Angielczyk, K., 2002, New evidence of large dicynodonts in the upper Moenkopi Formation (Middle Triassic) of northern Arizona: PaleoBios, v. 22, p. 10–17.

Nesbitt, S.J., and Whatley, R.L., 2004, The first discovery of a rhynchosaur from the upper Moenkopi Formation (Middle Triassic) of northern Arizona: PaleoBios, v. 24, no. 3, p. 1–10.

Nichols, K.M., and Silberling, N.J., 1977, Stratigraphy and depositional history of the Star Peak Group (Triassic), northwestern Nevada: Geological Society of America. p. 1–73.

Niedzwiedzki, G., Szrek, P., Narkiewicz, K., Narkiewicz, M., and Ahlberg, P.E., 2010, Tetrapod trackways from the early Middle Devonian period of Poland: Nature, v. 463, no. 7277, p. 43–48, doi: 10.1038/nature08623.

Olsen, P.E., Kent, D.V., Cornet, B., Witte, W.K., and Schlische, R.W., 1995, High-resolution stratigraphy of the Newark rift basin (early Mesozoic, eastern North America): Geological Society of America Bulletin, v. 108, no. 1, p. 40–77, doi: 10.1130/0016-7606(1996)108<0040:HRSOTN>2.3.CO;2.

Padian, K., 2003, 2003. Pterosaur stance and gait, and the interpretation of trackways. Ichnos, v. 10, p. 115–126.

Padian, K., Li, C., and Pchelnikova, J., 2010, The trackmaker of *Apatopus* (Late Triassic, North America): implications for the evolution of archosaur stance and gait: Palaeontology, v. 53, p. 175–189, doi: 10.1111/j.1475-4983.2009.00924.x.

Parrish, J., 1993, Climate of the supercontinent Pangea: The Journal of Geology, v. 101, no. 2, p. 215–233.

Paull, R.K., and Paull, R.A., 1983, Revision of type Lower Triassic Dinwoody Formation, Wyoming, and designation of principal reference section: University of Wyoming Contributions to Geology, v. 56, p. 261–282.

Paull, R.A., and Paull, R.K., 1990, Persistant myths about the Lower Triassic Little Medicine Member of the Goose Egg Formation and the Lower Triassic Dinwoody Formation, central Wyoming: Wyoming Geological Association Guidebook 41, p. 57–68.

Paull, R.A., and Paull, R.K., 1993, Interpretation of Early Triassic nonmarine–marine relations, Utah, USA: The Nonmarine Triassic. New Mexico Museum of Natural History & Science Bulletin.

Paull, R.K., and Paull, R.A., 1994, Lower Triassic Transgressive-regressive sequences in the Rocky Mountains, Eastern Great Basin, and Colorado Plateau, USA: in Mesozoic Systems of the Rocky Mountain Region, USA, Caputo, Mario V., Peterson, James A., and Franczyk, Karen J., (eds.), p. 169–180.

Payne, J.L., Lehrmann, D.J., Wei, J., Orchard, M.J., Schrag, D.P., and Knoll, A.H., 2004, Large perturbations of the carbon cycle during recovery from the end-Permian extinction: Science, v. 305, no. 5683, p. 506–509, doi: 10.1126/science.1097023.

Payne, J.L., Lehrmann, D.J., Follett, D., Seibel, M., Kump, L.R., Riccardi, A., Altiner, D., Sano, H., and Wei, J., 2007, Erosional truncation of uppermost Permian shallow-marine carbonates and implications for Permian-Triassic boundary events: Geological Society of America Bulletin, v. 119, no. 7-8, p. 771–784.

Payne, J., and Kump, L., 2007, Evidence for recurrent Early Triassic massive volcanism from quantitative interpretation of carbon isotope fluctuations: Earth and Planetary Science Letters, v. 256, no. 1-2, p. 264–277.

Peabody, F.E., 1948, Reptile and amphibian trackways form the Lower Triassic Moenkopi Formation of Arizona and Utah: University of California Bulletin of the Department of Geological Sciences, v. 27, no. 8, p. 295–468.

Peabody, F.E., 1956, Ichnites from the Triassic Moenkopi Formation of Arizona and Utah: Journal of Paleontology, v. 30, p. 731–740.

Pemberton, S.G., and Frey, R.W., 1982, Trace fossil nomenclature and the *Palolites*-*Palaeophycus* dilemma: Journal of Paleontology, v. 56, p. 843–881.

Peters, S., 2005, Geologic constraints on the macroevolutionary history of marine animals: Proceedings of the National Academy of Sciences of the United States of America, v. 102, no. 35, p. 12326–12331

Peters, S.E., 2006a, Macrostratigraphy of North America: The Journal of Geology, v. 114, p. 391–412.

Peters, S.E., 2006b, Genus extinction, origination, and the durations of sedimentary hiatuses: Paleobiology, v. 32, no. 3, p. 387–407.

Peters, S.E., 2008, Macrostratigraphy and its promise for paleobiology: In From Evolution to Geobiology: Research Questions Driving Paleontology at the Start of a New Century, Paleontological Society Short Course, Paleontological Society Papers, Volume 14, Patricia H. Kelley and Richard K. Bambach. (Eds.), v. 14, p. 205–231.

Peters, S.E., and Foote, M., 2001, Biodiversity in the Phanerozoic: a reinterpretation: Paleobiology, v. 27, no. 4, p. 583–601.

Peters, S.E., and Gaines, R.R., 2012, Formation of the "Great Unconformity" as a trigger for the Cambrian explosion: Nature, v. 484, no. 7394, p. 363–366, doi:10.1038/nature10969.

Peters, S., and Heim, N., 2010, The geological completeness of paleontological sampling in North America: Paleobiology, v. 36, no. 1, p. 61.

Picard, M., 1967, Stratigraphy and depositional environments of the Red Peak Member of the Chugwater Formation (Triassic), west-central Wyoming: Rocky Mountain Geology, v. 6, no. 1, p. 39–67.

Picard, M.D., 1978, Stratigraphy of Triassic Rocks in west-central Wyoming: Wyoming Geological Association 30th Annual Field Conference Guidebook, p. 101–130.

Picard, M.D., 1993, The early Mesozoic history of Wyoming, *in* Snoke, A.W., Steidtmann, J.R., and Roberts, S.M., eds., Geology of Wyoming: Geological Survey of Wyoming Memoir 5, p. 210–248.

Picard, M.D, and High JR., L.R., 1964, Pseudo rib-and-furrow marks in the Chugwater (Triassic) Formation of west-central Wyoming: Rocky Mountain Geology, v. 3, p. 27–31.

Picard, M.D., and High JR., L.R., 1968, Rhythmic alteration in Triassic Chugwater and Brunswick Formations, Wyoming and New Jersey: University of Wyoming Contributions to Geology, v. 2, p. 87–99.

Picard, D.M., Aadland, R., and High JR., L.R., 1969, Correlation and stratigraphy of the Triassic Red Peak and Thaynes Formations, western Wyoming and adjacent Idaho: American Association of Petroleum Geologists Bulletin, v. 53, p. 227–2289.

Pipirngos, G.N., 1968, Correlation and Nomenclature of some Triassic and Jurassic Rocks in south-central Wyoming: Geological Survey Professional paper 594-D, p. 1–29.

Pipiringos, G.N., and O'Sullivan, R.B., 1978, Principal unconformities in Triassic and Jurassic rocks, western interior United States—a preliminary survey: US Geol: Survey Prof. Paper 1035A, p. A, v. 1.

Pollard, D., and Schulz, M., 1994, A model for the potential locations of Triassic evaporite basins driven by paleoclimatic GCM simulations: Global and Planetary Change, v. 9, no. 3-4, p. 233–249.

Preto, N., Kustatscher, E., and Wignall, P. 2010, Triassic climates--State of the art and perspectives: Palaeogeography.

Prochnow, S., Nordt, L., Atchley, S., and Hudec, M., 2006, Multi-proxy paleosol evidence for middle and late Triassic climate trends in eastern Utah: Palaeogeography Palaeoclimatology Palaeoecology, v. 232, no. 1, p. 53–72.

Pruss, S., and Bottjer, D., 2004, Late Early Triassic microbial reefs of the western United States: a description and model for their deposition in the aftermath of the end-Permian mass extinction: Palaeogeography Palaeoclimatology Palaeoecology, v. 211, no. 1-2, p. 127–137.

Pruss, S., Corsetti, F., and Bottjer, D., 2005, The unusual sedimentary rock record of the Early Triassic: A case study from the southwestern United States: Palaeogeography Palaeoclimatology Palaeoecology, v. 222, no. 1-2, p. 33–52.

Pruss, S., Bottjer, D., Corsetti, F., and Baud, A., 2006, A global marine sedimentary response to the end-Permian mass extinction: examples from southern Turkey and the western United States: Earth-Science Reviews, v. 78, no. 3-4, p. 193–206.

Pryor, W.A., 1967, Biogenic directional features on several recent point-bars: Sedimentary Geology, v. 1, p. 235–245.\

Racki, G., 1999, Silica-secreting biota and mass extinctions: survival patterns and processes: Palaeogeography Palaeoclimatology Palaeoecology, v. 154, no. 1, p. 107–132.

Ramezani, J., Hoke, G.D., Fastovsky, D.E., Bowring, S.A., Therrien, F., Dworkin, S.I., Atchley, S.C., and Nordt, L.C., 2011, High-precision U-Pb zircon geochronology of the Late Triassic Chinle Formation, Petrified Forest National Park (Arizona, USA): Temporal constraints on the early evolution of dinosaurs: Geological Society of America Bulletin, v. 123, no. 11-12, p. 2142–2159, doi: 10.1130/B30433.1.

Raup, D. M., and Sepkoski, J. J., Jr. 1982. Mass extinctions in the marine fossil record. Science 215:1501–1503.

Reeside, J.B., Applin, P.L., Colbert, E.H., Gregory, J.T., Hadley, H.D., Kummel, B., Lewis, P.J., Love, J.D., Maldonado-Koerdell, M., Mckee, E.D., Claughlin, D.B., Muller, S.W., Reinemund, J.A, Rogers, J., Sanders, J., Silberling, N.J., And Waage, K., 1957, Correlation Of The Triassic Of North America Exclusive Of Canada: Geological Society Of America Bulletin, V. 68, P. 1451–151.

Retallack, G.J., 1988, Field recognition of paleosols: Geological Society of America Special Paper 216, p. 1–20.

Retallack, G., 1996, Early Triassic therapsid footprints from the Sydney basin, Australia: Alcheringa: An Australasian Journal of Palaeontology, v. 20, no. 4, p. 301–314.

Riding, R., 2000, Microbial carbonates: the geological record of calcified bacterial–algal mats and biofilms: Sedimentology, v. 47 p. 179–214.

Rieppel, O., 1998, Corosaurus alcovensis Case and the phylogenetic interrelationships of Triassic stem-group Sauropterygia: Zoological Journal of the Linnean Society, v. 124, no. 1, p. 1–41.

Rieppel, O. and Reisz, R.R., 1999, The origin and early evolution of turtles: Annual Review of Ecology and Systematics, v. 30, p. 1–22, doi: 10.1146/annurev.ecolsys.30.1.1.

Rieppel, O., And Reisz, R.R., 1999, The Origin And Early Evolution Of Turtles: Annual Review Of Ecology And Systematics,, P. 1–22.

Riggs, N., Ash, S., Barth, A., Gehrels, G., and Wooden, J., 2003, Isotopic age of the Black Forest Bed, Petrified Forest Member, Chinle Formation, Arizona: an example of dating a continental sandstone: Geological Society of America Bulletin, v. 115, no. 11, p. 1315–1323.

Rogers, R.R., Swisher III, C.C., Sereno, P.C., Forster, C.A. and Monetta, A.M., 1993. The lschigualasto tetrapod assemblage (Late Triassic) and $^{40}Ar/^{39}Ar$ calibration of dinosaur origins: Science, v. 260, p. 794–797.

Ronov, A., Khain, V., Balukhovsky, A., and Seslavinsky, K., 1980, Quantitative analysis of Phanerozoic sedimentation: Sedimentary Geology, v. 25, no. 4, p. 311–325.

Rühle v.Lilienstern, H., 1939. Fährtenund Spürenim Chirotheriem-Sandstein von Südthüringen. Fortschritte der Geologie und Paläontologie v. 12, p. 293–387.

Sadler, P.M., 1981, Sediment accumulation rates and the completeness of stratigraphic sections: The Journal of Geology, p. 569–584.

Sahney, S., and Benton, M.J., 2008, Recovery from the most profound mass extinction of all time: Proceedings of the Royal Society B: Biological Sciences, v. 275, no. 1636, p. 759–765.

Schoene, B., Guex, J., Bartolini, A., Schaltegger, U., and Blackburn, T.J., 2010, Correlating the end-Triassic mass extinction and flood basalt volcanism at the 100 ka level: Geology, v. 38, no. 5, p. 387–390, doi: 10.1130/G30683.1.

Sennikov, A.G., 1996, Evolution of the Permian and Triassic tetrapod communities of Eastern Europe: Palaeogeography Palaeoclimatology Palaeoecology, v. 120, p. 331–351.

Sephton, M.A., Amor, K., Franchi, I.A., Wignall, P.B., Newton, R., and Zonneveld, J.-P., 2002, Carbon and nitrogen isotope disturbances and an end-Norian (Late Triassic) extinction event: Geology.

Sereno, P., 1997, The origin and evolution of dinosaurs: Annual Review of Earth and Planetary Sciences, v. 25, p. 435–489.

Sereno, P.C., 1999, The evolution of dinosaurs: Science, v. 284, no. 5423, p. 2137–2147.

Silberling, N.J., and Wallace, R.E., 1969, Stratigraphy of the Star Peak Group (Triassic) and overlying lower Mesozoic rocks, Humboldt Range, Nevada: USGS Professional Paper 592.

Sirna, G., Dalla Vecchia, F.M., Muscio, G., and Piccoli, G., 1994, Catalogue of Paleozoic and Mesozoic vertebrates and vertebrate localities of the Tre Venezie area (North Eastern Italy): Memorie di Scienze Geologiche, v. 46, p. 255–281.

Smith, A. B. 2001. Large-scale heterogeneity of the fossil record: implications for Phanerozoic biodiversity studies. Philos. Trans. R. Soc. Lond. B 356:351–367.

Speed, R.C., 1978, Paleogeographic and plate tectonic evolution of the Early Mesozoic marine province of Western GReat Basin: In Howell, D.G., and McDougall, K.A., eds., Mesozoic paleogeography of the western United States, SEPM - Pacific Coast Paleogeography Symposium 2. p. 253–270.

Stewart, J.H., Poole, F.G., and Wilson, R.F., 1972, Stratigraphy and origin of the Triassic Moenkopi Formation and related strata in the Colorado Plateau region: U.S. Geological Survey professional paper 692.

Stewart, J.H., Poole, F.G., and Wilson, R.F., 1972, Stratigraphy and origin of the Chinle Formation and related Upper Triassic Strata in the Colorado Plateau Region: U.S. Geological Survey professional paper 690,, p. 1–343.

Sloss, L.L., 1976, Areas and volumes of cratonic sediments, western North America and eastern Europe: Geology, v. 4, no. 5, p. 272.

Soil Survey Division Staff, 1999, Soil taxonomy: a basic system for soil classification for making and interpreting soil surveys: U.S. Government Printing Office, Washington, D.C., 831 p.

Solien, M.A., 1979, Conodont biostratigraphy of the Lower Triassic Thaynes Formation, Utah: Journal of Paleontology,, p. 276–306.

Soreghan, G.S., 1992, Preservation and paleoclimatic significance of eolian dust in the Ancestral Rocky Mountains province: Geology, v. 20, p. 1111–1114.

Steiner, M.B., Morales, M., and Shoemaker, E., 1993, Magnetostratigraphic, biostratigraphic, and lithologic correlations in Triassic strata of the western United States: Society of Economic Paleontologists and Mineralogists Special Publications 49, p. 41–57.

Storrs, G.W., 1991, Anatomy and relationships of *Corosaurus alcovensis* (Diapsida: Sauropterygia) and the Triassic Alcova Limestone of Wyoming: Bulletin of the Peabody Museum of Natural History, v. 44, p. 1–151.

Tanner, L., 2010, The Triassic isotope record: Geological Society London Special Publications, v. 334, no. 1, p. 103.

Tanner, L., and Lucas, S.G., 2007, The Moenave Formation: Sedimentologic and stratigraphic context of the Triassic-Jurassic boundary in the Four Corners area, southwestern USA: Palaeogeography Palaeoclimatology Palaeoecology, v. 244, p. 111–125.

Tucker, M., and Benton, M., 1982, Triassic environments, climates and reptile evolution: Palaeogeography Palaeoclimatology Palaeoecology, v. 40, no. 4, p. 361–379.

Turner, B.R., 1978, Trace fossils from the Upper Triassic fluviatile Molteno Formation of the Karoo (Gondwana) Supergroup, Lesotho: Journal of Paleontology, v. 52, p. 959–963.

Twitchett, R., 2006, The palaeoclimatology, palaeoecology and palaeoenvironmental analysis of mass extinction events: Palaeogeography Palaeoclimatology Palaeoecology, v. 232, no. 2-4, p. 190–213, doi: 10.1016/j.palaeo.2005.05.019.

Twitchett, R.J., and Wignall, P.B., 1996, Trace fossils and the aftermath of the Permo-Triassic mass extinction: evidence from northern Italy: Palaeogeography Palaeoclimatology Palaeoecology, v. 124, no. 1-2, p. 137–151, doi: 10.1016/0031-0182(96)00008-9.

Valdiserri, D., and Avanzini, M., 2007, A tetrapod ichnoassociation from the Middle Triassic (Anisian, Pelsonian) of Northern Italy: Ichnos, v. 14, p. 105–116, doi: 10.1080/10420940601010703.

Veevers, J.J., Tewari, R.C., Mishra, H.K., 1996. Aspects of Late Triassic to Early Cretaceous disruption of the Gondwana coalbearing fan of east-central Gondwanaland. In: Dimri, D.B. (Ed.), Ninth International Gondwana Symposium. International Gondwana Symposium, pp. 637– 646.

Veizer, J., 1989, Strontium isotopes in seawater through time: Annual Review of Earth and Planetary Sciences.

Veizer, J., Compston, W. 1976. $^{87}Sr/^{86}Sr$ in Precambrian carbonates as an index of crustal evolution. Geochimica et Cosmochimica Acta, v. 40, p. 905–914.

Visscher H., Brinkhuis H., Dilcher D. L., Elsik W. C., Eshet Y., Looy C. V., Rampino W. R., and Travers A. (1996) The terminal Paleozoic fungal event: Evidence of terrestrial ecosystem destabilization and collapse. Proc. Natl. Acad. Sci. U. S. A. 93, 2155–2158.

Webb, S.K., 1980, Early Triassic tetrapod trackways in the Moenkopi Formation of Southeastern Utah: Geological Society of America Abstracts with Programs, v. 12, p. 308.

Welles, S.P., 1947, Vertebrates from the Upper Moenkopi Formation of Northern Arizona: University of California Bulletin of the Department of Geological Sciences, v. 27, no. 7, p. 241–294.

Wilson, J.A., 2005, Integrating ichnofossil and body fossil records to estimate locomotor and posture and spatiotemporal distribution of early sauropod dinosaurs: a stratocladistic approach: Paleobiology, v. 31, p. 400–423.

Wilson, J.A., Mariscano, C.A., and Smith, R.M.H., 2009, Dynamic locomotor capabilities revealed by early dinosaur trackmakers from southern Africa: PLos ONE, v. 4, e7331, doi: 10.1371/journal.pone.0007331.

Wignall, P.B., and Twitchert, R.J., 2002, Permian-Triassic sedimentology of Jameson Land, East Greenland; incised submarine channels in an anoxic basin, Journal of the Geological Society (London), v. 159, p. 691–703.

Wilkinson, B.H., Opdyke, B.N., and Algeo, T.J., 1991, Time partitioning in cratonic carbonate rocks: Geology, v. 19, no. 11, p. 1093–1096, doi: 10.1130/0091-7613(1991)019<1093:TPICCR>2.3.CO;2.

Woodcock, N.H., 2004, Life span and fate of basins: Geology, v. 32, no. 8, p. 685, doi: 10.1130/G20598.1.

Woody, D.T., 2006, Revised stratigraphy of the lower Chinle Formation (Upper Triassic) of Petrified Forest National Park, Arizona: Museum of Northern Arizona Bulletin, v. 62, p. 17–45.

Worsley, T.R., Nance, D., and Moody, J.B., 1984, Global tectonics and eustasy for the past 2 billion years: Marine Geology, v. 58, no. 3, p. 373–400.

Wyld, S., 1991, Permo-Triassic Tectonism In Volcanic Arc Sequences Of The Western United-States Cordillera And Implications For The Sonoma Orogeny: Tectonics, v. 10, no. 5, p. 1007–1017.

Wyld, S.J., 2000, Triassic evolution of the arc and backarc of northwestern Nevada, and evidence for extensional tectonism: Geological Society of America Special Papers, p. 185–208.

Yin, H., Zhang, K., Tong, J., Yang, Z. & Wu, S. 2001. The global stratotype section and point (GSSP) of the Permian–Triassic boundary. Episodes, 24, 102–114.

Zangerl, R., 1963, Preliminary results of a restudy of Corosaurus alcovensis Case, the only known New World nothosaur: Rocky Mountain Geology, v. 2, no. 2, p. 117.

Zeigler, K., Kelley, S., and Geissman, J., 2008, Revisions to stratigraphic nomenclature of the Upper Triassic Chinle Group in New Mexico: New insights from geologic mapping, sedimentology, and magnetostratigraphic/paleomagnetic data: Rocky Mountain Geology, v. 43, no. 2, p. 121.

Zeigler, K.E., and Geissman, J.W., 2011, Magnetostratigraphy of the Upper Triassic Chinle Group of New Mexico: Implications for regional and global correlations among Upper Triassic sequences: Geosphere, v. 7, no. 3, p. 802–829, doi: 10.1130/GES00628.S1.

Ziegler, A., Eshel, G., Rees, P., Rothfus, T., Rowley, D., and Sunderlin, D., 2003, Tracing the tropics across land and sea: Permian to present: Lethaia, v. 36, no. 3, p. 227–254.

Appendix 2.1

This appendix is a graphical representation of the synthetic columns created for the Triassic Database (TDB). The 35 synthetic columns were created by compiling data for each of the 35 outcrop regions (see Fig. 2.2) and drafting a composite section. Lithologies are represented based on their relative abundance and stratigraphic distribution to best reflect lithologic variability throughout a given lithostratigraphic unit.

If, for instance, four measured sections from the literature are compared for the compilation of a synthetic column and three demonstrate an upper third of the section as entirely mudstone, but the fourth shows a time-equivalent upper third with alternating sandstone and mudstone, the synthetic column will reflect the variability by expressing primarily mudstone with a minority of sandstone (one or two thin sandstone intervals). In this manner lateral variability within a given area is accounted for, while still representing the principal lithology.

This page intentionally left blank

See attached file (Appendix 2.1)

Appendix 2.2

The dominant lithology chart was created by defining the major lithology that contributed to a given lithostratigraphic unit and plotting it across its duration for each of the 35 columns. Time series of single lithologies were calculated to produce the proportional and absolute lithologic distribution plots (Fig. 2.9, and Fig. 2.16).

This page intentionally left blank

See attached file (Appendix 2.2)

Appendix 3.1 – 3.2

These appendices represent the temporal ranges of taxa (Appendix 3.1) and ichnotaxa (Appendix 3.2) that were found in the Paleobiology Database (PaleoDB). Taxa were culled from the PaleoDB by searching for collections from each of the 233 lithostratigraphic units in the Triassic Database. All vertebrate genera represented in each of the 233 lithostratigraphic units include searches for redundant names such as Petrified Forest Member, or Petrified Forest Formation to ensure the greatest faunal representation. Ecology (e.g., trophic level), clade, and geologic attributes were recorded for each instance. Absolute numbers of individual taxa were not recorded since the focus was genus richness not abundance.

This page intentionally left blank

See attached file (Appendix 3.1)

This page intentionally left blank

See attached file (Appendix 3.2)

Appendix 5.1.

Sample	Mass	% Dissolved Carbonate	Rb ppm	Sr ppm	$^{87}Rb/^{86}Sr$	$^{87}Sr/^{86}Sr$	2-SE
AS-2	0.00575	97	0.32	241	0.0038	0.70843	0.00001
AS-3	0.00677	99	0.44	531	0.0024	0.70817	0.00001
AS-4	0.00476	95	0.67	656	0.0030	0.70816	0.00001
AS-5	0.00497	93	0.88	367	0.0069	0.70825	0.00001
AS-6	0.00453	94	0.79	256	0.0089	0.70831	0.00001
AS-7	0.00503	96	0.39	287	0.0039	0.70825	0.00001
AS-10	0.00605	89	1.03	658	0.0045	0.70819	0.00001

Appendix 5.2.

Western United States

Stage	Formation	State	$^{87}Sr/^{86}Sr$	2-SE	Source
?	Alcova Limestone	WY	0.708428	1.0E-05	This study; AS-2
?	Alcova Limestone	WY	0.708172	1.2E-05	This study; AS-3
?	Alcova Limestone	WY	0.708164	1.1E-05	This study; AS-4
?	Alcova Limestone	WY	0.708247	9.0E-06	This study; AS-5
?	Alcova Limestone	WY	0.708309	9.0E-06	This study; AS-6
?	Alcova Limestone	WY	0.708246	1.0E-05	This study; AS-7
?	Alcova Limestone	WY	0.708187	1.0E-05	This study; AS-10
middle Griesbachian	Dinwoody	UT	0.70743		Koepnick et al., 1990
middle Griesbachian	Dinwoody	UT	0.7075		Koepnick et al., 1990
lower Smithian	Thaynes	ID	0.70778		Koepnick et al., 1990
lower Smithian	Thaynes	ID	0.70792		Koepnick et al., 1990
lower Smithian	Thaynes	NV	0.70788		Marenco et al., 2008
Spathian	Virgin Limestone	NV	0.70813		Marenco et al., 2008
Spathian	Virgin Limestone	NV	0.70816		Marenco et al., 2008
Spathian	Virgin Limestone	NV	0.70806		Marenco et al., 2008
Spathian	Virgin Limestone	NV	0.70804		Marenco et al., 2008
Spathian	Virgin Limestone	NV	0.70823		Marenco et al., 2008
Spathian	Virgin Limestone	NV	0.70821		Marenco et al., 2008
Spathian	Virgin Limestone	NV	0.7082		Marenco et al., 2008

Western United States

Stage	Formation	State	$^{87}Sr/^{86}Sr$	2-SE	Source
upper Spathian	Thaynes	ID	0.70835		Koepnick et al., 1990
Spathian	Virgin Limestone	NV	0.70814		Marenco et al., 2008
Spathian	Virgin Limestone	NV	0.70822		Marenco et al., 2008

Europe

Stage	Formation	State	$^{87}Sr/^{86}Sr$	2-SE	Source
Griesbachian	Europe		0.707354	1.0E-05	Korte et al., 2003
Griesbachian	Europe		0.70735	9.0E-06	Korte et al., 2003
Griesbachian	Europe		0.707485	8.0E-06	Korte et al., 2003
Griesbachian	Europe		0.707419	7.0E-06	Korte et al., 2003
Griesbachian	Europe		0.70727	7.0E-06	Korte et al., 2003
Dienerian	Europe		0.707463	7.0E-06	Korte et al., 2003
Dienerian	Europe		0.707478	1.5E-05	Korte et al., 2003
Dienerian	Europe		0.707679	1.0E-05	Korte et al., 2003
Smithian	Europe		0.707876	1.0E-05	Korte et al., 2003
Spathian	Europe		0.70816	8.0E-06	Korte et al., 2003
Spathian	Europe		0.708154	8.0E-06	Korte et al., 2003
Spathian	Europe		0.708186	1.1E-05	Korte et al., 2003
Spathian	Europe		0.708172	8.0E-06	Korte et al., 2003

Europe

Stage	Formation	State	$^{87}Sr/^{86}Sr$	2-SE	Source
Spathian	Europe		0.708178	8.0E-06	Korte et al., 2003
Spathian	Europe		0.708166	9.0E-06	Korte et al., 2003
Spathian	Europe		0.708219	1.4E-05	Korte et al., 2003
Spathian	Europe		0.708127	9.0E-06	Korte et al., 2003
Spathian	Europe		0.70814	9.0E-06	Korte et al., 2003
Spathian	Europe		0.708124	8.0E-06	Korte et al., 2003
Anisian	Europe		0.708155	8.0E-06	Korte et al., 2003
Anisian	Europe		0.708164	1.0E-05	Korte et al., 2003
Anisian	Europe		0.708024	8.0E-06	Korte et al., 2003
Anisian	Europe		0.707859	7.0E-06	Korte et al., 2003
Anisian	Europe		0.707849	6.0E-06	Korte et al., 2003
Anisian	Europe		0.708027	8.0E-06	Korte et al., 2003
Anisian	Europe		0.707846	8.0E-06	Korte et al., 2003
Anisian	Europe		0.707812	8.0E-06	Korte et al., 2003
Anisian	Europe		0.707841	8.0E-06	Korte et al., 2003